

Essays on the Scenario-based Measurement of Financial Risks

Dissertation
zur Erlangung des Grades eines Doktors der
wirtschaftlichen Staatswissenschaften
(Dr. rer. pol.)
des Fachbereichs Rechts- und Wirtschaftswissenschaften

der Johannes Gutenberg-Universität Mainz
vorgelegt von
Philipp Aigner, M.Sc.

in Mainz

im Jahre 2023

Erstgutachter: Prof. Dr. Andrej Gill
Zweitgutachter: Prof. Dr. Sebastian Schlütter
Drittgutachter: Prof. Dr. Helmut Gründl
Tag der mündlichen Prüfung: 7. Juli 2023

List of original Working Papers

- 1) Philipp Aigner*, Prof. Dr. Sebastian Schlütter[†]:
“Enhancing Gradient Capital Allocation with Orthogonal Convexity Scenarios”
- 2) Philipp Aigner* :
“Identifying Scenarios for the Own Risk and Solvency Assessment of Insurance Companies”
- 3) Philipp Aigner*, M.Sc., Prof. Dr. Sebastian Schlütter[†]:
“Scenarios of Systemic Risk”

* Mainz University of Applied Sciences, School of Business, Lucy-Hillebrand-Str. 2, 55128 Mainz, Germany; email: philipp.aigner@hs-mainz.de.

[†] Mainz University of Applied Sciences, School of Business, Lucy-Hillebrand-Str. 2, 55128 Mainz, Germany; Fellow of the International Center for Insurance Regulation, Goethe University Frankfurt; email: sebastian.schluetter@hs-mainz.de.

Contents

	Page
Summary	1
1 Enhancing Gradient Capital Allocation with Orthogonal Convexity Scenarios	8
1.1 Introduction	9
1.2 Motivating example: RORAC maximization	12
1.3 Targets of a scenario-based risk measurement	14
1.4 Existing approaches	16
1.5 Orthogonal convexity scenarios (OCS)	18
1.6 Applications	24
1.7 Conclusion	32
1.8 Appendix	34
References	42
2 Identifying Scenarios for the Own Risk and Solvency Assessment of Insurance Companies	46
2.1 Introduction	47
2.2 Orthogonal convexity scenarios for the ORSA	50
2.3 Calibration of ORSA scenarios for market risk	53
2.4 Results	64
2.5 Conclusion	69
2.6 Appendix	70
References	78
3 Scenarios of systemic risk	82
3.1 Introduction	83

3.2	Measuring systemic risk	85
3.3	Orthogonal convexity scenarios (OCS)	87
3.4	Empirical calibration of OCS for systemic risk	91
3.5	Conclusion	101
3.6	Appendix	102
	References	110
	Conclusion	112
	References	CXXI

List of Figures

	Page
1. Orthogonal convexity scenarios of portfolio risk	8
1.1 Dependence structure of the exemplary portfolio	25
1.2 Ellipsoids spanned by PCA- and OCS	28
1.3 Contribution analysis	29
1.4 Risk limits	32
1.5 Asset selection	40
2. Identifying Scenarios for the Own Risk and Solvency Assessment of Insurance Companies	46
2.1 Module structure of the Solvency II regulation	57
2.2 Changing SCRs resulting from portfolio shifts	67
2.3 Levelplots of the relative measurement errors	68
2.4 Changing SCRs based on the alternative portfolio set-up	77
3. Scenarios of systemic risk	82
3.1 Changing sensitivities	99
3.2 Density function of $Z(u)$	108

List of Tables

	Page
1. Orthogonal convexity scenarios of portfolio risk	8
1.1 OCS and PCA-scenarios	27
1.2 Evaluation of new portfolios	27
2. Identifying Scenarios for the Own Risk and Solvency Assessment of Insurance Companies	46
2.1 Exemplary bond investments	62
2.2 Exemplary stock investments	63
2.3 Correlation matrix of the investments considered and the interest rate . .	63
2.4 SCRs resulting from f^{SF} and f^{true}	64
2.5 Euler allocations of the two different approaches	65
2.6 OCS for the exemplary portfolio	65
2.7 Risk-free interest rates from August 2021	72
2.8 Stress parameters for spread risk of unrated bonds	72
2.9 Stress parameters for spread risk of rated bonds	73
2.10 Alternative bond investments for robustness check	75
2.11 Alternative stock investments for robustness check	75
2.12 Alternative correlation matrix of investments for robustness check	76
2.13 Parameters for hazard rate processes provided by the literature	76
2.14 OCS for the alternative portfolio composition	77
3. Scenarios of systemic risk	82
3.1 Summary of institutions inspected	94
3.2 Resulting orthogonal convexity scenarios	97

3.3	Systemic risk for changing capitalizations	98
3.4	Return scenarios from an investor's perspective	100
3.5	Strategies in the exemplary set-up	104

Summary

“The advantage of knowing about risks is that we can change our behavior to avoid them.”

(Robert F. Engle, Risk and volatility: Econometric models and financial practice, Noble Lecture, 2003)

In the processing of the financial crisis of 2007/2008 it became clear to both, practitioners and researchers, that enterprise risk management (ERM), as it had been applied until then, was flawed, vulnerable and allowed for excessive risk taking.¹ The questions arose as to how risks can be measured reliably and how it can be ensured that the results of ERM are efficiently integrated into the steering process of financial institutions. In the aftermath, new, more consistent and prudential regulatory frameworks have been set up for financial institutions, such as Basel III for banks and Solvency II for insurance companies in the European Union. These provide guidance for an adjusted risk management procedure and can be seen as a “major step ahead”, cf. Doff (2016). However, there still remains space for improvement in several aspects of, two of which this work addresses: the lack of transparency of risk measurement methodologies and the lack of reliability of regulatory measurement approaches.

Firstly, the lack of transparency of complex risk measurement methodologies has been identified as one of the central disadvantages of risk management prior to the financial crisis, cf. for instance Stulz (2008). Stulz in particular sees “providing the board and management with timely information that enables them to assess the consequences of retaining or discarding risks” as one of the central tasks of risk management. Similarly, Aven (2016) identifies the description and presentation of the results “in a way that is useful to decision makers and that clearly presents the assumptions made and their justification in terms of the knowledge on which the assessment is based” as one of the central issues of risk measurement and management. If these requirements for a company’s risk management are not fulfilled, the results cannot be adequately incorporated into a financial institution’s decision-making process. This leads then – in the worst case – to inappropriate risk steering. Although the new regulatory expectations resulting from the

¹Cf. for instance Aebi et al. (2012), Eling and Schmeiser (2010) or Huber and Scheytt (2013) among many others.

financial crisis provide some guidance in that sense, the lack of transparency is still a key challenge for a company's risk management practices today, cf. for instance Wilson (2015, p. 599).

Secondly, the lack of reliability of regulatory approaches to risk measurement, such as the Solvency II standard formula, poses a crucial challenge to tackle. A general criticism of such standardized approaches has been formulated by Scherer and Stahl (2021) who state that they "lack sound economic and mathematical reasoning". On the one hand, this is a valid statement, since there is a lot of evidence in the literature that a standardized approach may provide adverse steering incentives.² On the other hand, regulatory requirements have to address a broad audience. Large companies exposed to the supervisory authorities would theoretically have the capacities to set up a risk measurement environment that evaluates risk more precisely and firm-specificly than the regulatory approaches. However, small or medium-sized companies may lack these capacities but are nevertheless able to conduct their risk measurement in a reasonable manner based on the regulatory suggestions. From that point of view, the regulatory approaches have a certain *raison d'être* and it seems reasonable to adjust the risk measurement instead, bringing it in line with a complex measurement in a feasible manner.

More generally speaking, it is standard in risk management to measure risk based on a single number, resulting for example from regulatory requirements, internal models or risk measures, such as the Value-at-Risk or the Tail-Value-at-Risk. This number has a great impact on steering decisions within a company and is influenced, for instance, by the segment volumes within a company or the asset volumes in a portfolio optimization context. These volumes are now the adjustment screws for the decision makers to avoid excessive risk taking or to optimize the risk-return profile of the company. However, for effective decision making, it is necessary to know beforehand how the overall risk changes when the volumes change. Thus, there is a functional relationship between the volumes and the risk which we want to evaluate later on.

To address the two problems mentioned before, stress scenarios have been increasingly focused upon and are nowadays expected by regulatory authorities as part of the risk management, cf. for instance EIOPA (2015) and BaFin (2017). A broad strand of literature in the stress scenario context deals with the identification of stochastic scenarios,

²Cf. for instance Becker and Ivashina (2015), Chen et al. (2019), Fischer and Schlütter (2015), Braun et al. (2017) or Pfeifer and Strassburger (2008).

stressing the underlying distribution of the risk vector which comprises single risky positions, to be evaluated.³ These approaches can provide a reasonable evaluation of a company's current risk situation and are therefore quite relevant. However, they are again complicated to communicate to a financial institution's board due to their theoretical complexity. Therefore, they only allow a tackling of the second problem mentioned. Another suggestion is to derive stress scenarios by decomposing the multivariate risk distribution of the evaluated risk vector. This then results in deterministic stress scenarios, the outcomes of which can easily be aggregated towards the overall portfolio risk. There is a strand of literature in research dealing with capital allocations providing such a decomposition of risk vectors.⁴ One of the well-studied methodologies in that sense is the gradient capital allocation, also known as the Euler-allocation, cf. Tasche (2008). Precisely speaking, the gradient capital allocation points out the marginal impact of segment or asset volumes on diversified capital needs. It thus shows which segments or assets to marginally expand or reduce in order to achieve an optimal risk-return profile, cf. Tasche (2008). However, the informative value of capital allocation methods is limited when considering non-marginal portfolio changes. This is because risk diversification is typically not linear, but rather exhibits curvatures. Due to the fact that only a single scenario is derived, capital allocations provide a linear function depending on risk volumes such that this curvature cannot be captured. For example, the risks of a fund's investments into a new asset category may be well diversified with other risks as long as the investments are of small volume; after expanding investments into the new category, these risks can shape the bank's overall risk profile. Another widely-employed approach to the definition of stress scenarios is the Principal Component Analysis (PCA), cf. Hull (2018, pp.488 ff.). It decomposes a given risk distribution into multiple scenarios which are orthogonal in the sense of the Pearson correlation. By selecting multiple scenarios, the curvature in the functional relationship can theoretically be captured. However, the PCA assumes a multivariate elliptical distributed risk vector, imposing a severe and in practice often not fulfilled restriction.

This work now provides a suggestion for how to determine so-called "orthogonal convexity scenarios" (OCS). We will show that the OCS allow to address both aforementioned

³Cf. for instance Pesenti et al. (2019), Makam et al. (2021), Packham and Woebeking (2019) or Breuer and Csiszár (2013a).

⁴Cf. Guo et al. (2021) for a detailed overview of the different methods.

problems in the deterministic sense. We will thereby obtain a flexible and reliable risk measurement tool that is also easy to communicate.

Chapter 1 first develops the necessary theory, introducing the OCS technically. Generally, the scenarios are based on the so-called “hybrid approach” for risk measurement, cf. Rosenberg and Schuermann (2006), which allows univariate risk distributions to be heavy-tailed and skewed. In a second step, univariate risks are aggregated using a relatively simple square-root formula. However, the hybrid approach is generally only valid for elliptical distributions. In particular, we base the scenarios on the hybrid approach in connection with so-called *sensitivity-implied tail correlation matrices* provided by Paulusch and Schlütter (2022). The authors show that the hybrid approach thereby meets first and second-order sensitivities in line with a pre-specified “true” risk measurement. By basing the determination of the OCS on Paulusch and Schlütter (2022), we can ensure that the resulting scenario-based risk measurement has the same properties to meet first and second-order sensitivities of the underlying “true” risk. Notably, the aforementioned gradient capital allocation only meets the first-order sensitivities due to its linearity resulting from the single scenario situation. However, examples in Gründl and Schmeiser (2007, pp. 208 -314) highlight that adding new contracts to an insurance portfolio may lead to errors in pricing of insurance contracts when they are based on the gradient capital allocation due to changing portfolio structures. The main challenge is that changing diversification effects can not be captured.⁵ To overcome this problem, it has already been suggested by Gouriéroux et al. (2000) to also consider second-order derivatives of the Value-at-Risk or a risk measure in general. However, to employ such a methodology, the user has to collect second order sensitivities for all portfolio combinations in terms of the Hessian matrix. These can become difficult to interpret and therefore does not reasonably allow the communication of the current risk profile to stakeholders. We show that our OCS allow the depiction of second-order sensitivities in such a simple manner that they can be used to communicate the risk profile and its potential changes. We find that the suggested approach allows for a reasonable approximation of the true risk in the sense of a second-order polynomial in the neighborhood of an actual portfolio, allowing the evaluation of marginal and even non-marginal portfolio changes that may be considered. Notably, the approach makes no distributional assumptions, whereby tail-

⁵Similar results in the context of portfolio optimization are provided by Buch et al. (2011).

dependencies of the risk drivers can be depicted and – by including several scenarios – changing diversification effects are reflected. Chapter 1 further provides several applications of OCS in terms of risk contributions, risk communication and risk limiting.

Overall, our approach, based on deterministic scenarios, provides the risk management department of a financial institution with a methodology to communicate not only the current risk situation to the board in a simple manner, but also provides a foundation for steering decisions. Therefore, we are able to tackle the lack of transparency of risk measurement results without losing information.

Chapter 2 employs the scenarios developed in Chapter 1 to tackle the regulatory requirements of the “Own Risk and Solvency Assessment” (ORSA) under Solvency II. Therein, the management is expected to assess whether its risk profile deviates from the assumptions underlying the Solvency Capital Requirements (SCR) calculations, cf. EIOPA (2015), Guidelines 2 & 12. More precisely, BaFin (2016) expects insurers to “take into account risks that are not or not adequately included in the standard formula” and “must develop a suitable assessment procedure for them”. To develop such a methodology, the ORSA, Guidelines 4 & 7, suggest employing (reverse) scenario analyses and stress testing, but leave the question open how to identify these.⁶ Doff (2016) highlights that stress testing makes it possible to “include specific risks that are absent from the current Solvency II framework”. To identify such missing risks and at the same time to adjust the risk measurement, we derive orthogonal convexity scenarios. To evaluate the proposition, a partial internal model (IM) in line with Gatzert and Martin (2012) and Eckert et al. (2016) is set up to represent the true market risk resulting from a portfolio comprising bond and stock investments. Its outcome is denoted by f^{IM} . Additionally, the risk is measured in line with the standard formula (SF) of Solvency II for the market risk sub-module, the outcome of which is then denoted by f^{SF} . We find that fitting the internal model for recent interest rate and bond data, leads to a severe gap between the results based on f^{IM} and f^{SF} . We show that this gap can be directly approximated based on the OCS. In particular, we find that government bonds, which are considered to be spread risk free under Solvency II, have to be precisely included in the measurement process. Our observations here are in line with Gatzert and Martin (2012), who highlight exactly this problem. Again, due to only weak assumptions made, the approach allows for

⁶Cf. EIOPA (2015).

a widely applicable and at the same time simple representation of this gap. Furthermore, we show that rewriting the approximation outcome as

$$f^{\text{SF}}(u) + g(u) \approx f^{\text{IM}}(u)$$

with u reflecting asset volumes, allows for an extension of the standard formula that meets the true risk in the sense of first- and second-order sensitivities. Therein, g represents the approximation of $f^{\text{IM}}(u) - f^{\text{SF}}(u)$ based on the OCS. Overall Chapter 2 contributes to the literature in three ways: firstly, we can validate the shortcomings of standardized approaches. Secondly, a practical idea of how to address the ORSA requirements for stress scenarios is presented. Thirdly, it is empirically evaluated as to how meaningful scenarios for an exemplary company may look. The last part may also provide the regulator with a starting point for additional actions: by identifying the OCS-based function g for a representative insurer, we also obtain representative scenarios that could be provided to an insurer to then extend its risk measurement and thereby adjust the standard formula in a reasonable way.

Chapter 3 embeds the OCS methodology in the context of systemic risk with the aim of highlighting how the scenarios can improve the risk steering within a specific context. Systemic risk is a major threat to modern economies and societies making it necessary for a regulator to address these risks. A strand of literature, therefore, deals with an appropriate definition of capital requirements. To this end, Acharya et al. (2017) have lately suggested a tax policy for financial institutions. Their approach is based on the so-called “Systemic Expected Shortfall” (SES) measuring the marginal contributions of companies to the overall systemic risk. It is to be noted that the approach corresponds to the gradient capital allocation from the enterprise risk management literature, cf. again Tasche (2008). As previously mentioned, the gradient capital allocation faces the problem that only marginal changes – in context of the systemic risk – in volumes can be considered. In this sense, the OCS provide an extension to the approach of Acharya et al., since the first OCS can be chosen in such a way that it directly coincides with the gradient capital allocation and therefore with the SES. In the enterprise risk management context, Buch et al. (2011) suggest employing second-order derivatives with respect to segment volumes in order to extend the gradient capital allocation. Unfortunately, when the number of companies to be considered for the determination of systemic risk becomes

too high, the Hessian matrix reflecting second-order sensitivities becomes difficult to fit, cf. for instance Gourieroux et al. (2000). OCS, by considering second-order sensitivities, provide a reasonable starting point in order to avoid miss-evaluations and distorted steering incentives. In this chapter, we use publicly available data of “systemically relevant institutions”, indicated by the Financial Stability Board (FSB) annually. We find empirical evidence that the SES along with OCS indeed allows for a more robust evaluation of contributions of individual firms to systemic risk. In particular, such a combination allows the quick evaluation of systemic risk when volumes of the financial institutions change. Furthermore, our empirical analysis provides evidence that insurance companies, which have not been designated as systemically relevant by the FSB, indeed play an important role.

Chapter 1

Enhancing Gradient Capital Allocation with Orthogonal Convexity Scenarios^{*}

Abstract

Gradient capital allocation, also known as Euler allocation, is a technique used to redistribute diversified capital requirements among different segments of a portfolio. The method is commonly employed to identify dominant risks, assessing the risk-adjusted profitability of segments, and establishing for limit systems. However, capital allocation can be misleading in all these applications because it only accounts for the current portfolio composition and ignores how diversification effects may change with a portfolio restructuring. This paper proposes enhancing the gradient capital allocation by adding "orthogonal convexity scenarios" (OCS). OCS identify risk concentrations that potentially drive portfolio risk and become relevant after restructuring. OCS have strong ties with principal component analysis (PCA), but they are a more general concept and compatible with common empirical patterns of risk drivers being fat-tailed and increasingly dependent in market downturns. We illustrate possible applications of OCS in terms of risk communication and risk limits.

JEL classification: G28, G32, D62, H23.

Keywords: Risk capital allocation, Scenario analysis, Risk communication, Risk limiting

^{*}Earlier versions of this paper were presented at the CEQURA 2020, the annual meeting of the DVfVW 2021, the International Congress of Insurance: Mathematics and Economics 2021, the ARIA annual meeting 2021 and the annual meeting of the German Finance Association 2021.

1.1 Introduction

Risk diversification within an investment portfolio or multi-segment firm can help to reduce the portfolio's potential loss. Capital needs for the portfolio, e.g. on the basis of Value-at-Risk or Expected Shortfall, are therefore typically lower for the portfolio than the sum of capital needs for the portfolio segments stand-alone. The gradient (synonymous Euler) capital allocation mechanism distributes the diversified capital requirement back to portfolio segments. It is thus a relatively simple tool to inform stakeholders which segments are dominant risk drivers when accounting for risk diversification in the portfolio. Precisely speaking, the gradient capital allocation points out the marginal impact of segment volumes on diversified capital needs. Therefore, it enables drawing conclusions about which segments to marginally expand or reduce to achieve an optimal risk-return profile (cf. Tasche, 2008).¹

The informative value of gradient capital allocation is limited, however, when realistically considering non-marginal portfolio changes. In fact, risk diversification is typically not linear, but rather exhibits curvatures. For example, risks of a fund's investments into a new asset category may be well diversified with other risks as long as the investments are of small volume. Yet, after expanding investments into the new category, these risks could substantially shape the bank's overall risk profile. Examples in Gründl and Schmeiser (2007, pp. 308-314) highlight errors in pricing of insurance contracts based on capital allocation when new contracts are added to an existing portfolio and hence the structure of the portfolio changes. Similarly, Buch et al. (2011) show that a control problem for portfolio optimization can fail when only relying on first-order derivatives; to reach the optimum, the authors propose a correction term that includes second-order derivatives. Gouriéroux et al. (2000) identify an efficient stock portfolio—with risk being measured by Value-at-Risk instead of the variance—and to this end employ first and second-order derivatives of Value-at-Risk.

Whereas second-order derivatives could enhance the accuracy of forecasting the effects of portfolio restructuring on capital needs, they convey a more elusive information structure than the gradient capital allocation. Technically, one has to collect second-order

¹Recently, there has been growing interest in meaningful risk decomposition in line with gradient-based capital allocation. For this purpose, Schilling et al. (2020) propose a martingale representation theorem (MRT) decomposition to decompose the dynamic risks of a company into individual components.

derivatives with respect to all combinations of portfolio segments in a Hessian matrix. Especially for situations with many portfolio segments, such a Hessian matrix is difficult to interpret. Therefore, neither the gradient capital allocation nor the Hessian matrix provide a straightforward means to communicate to decision makers how the risk profile of a portfolio is affected by restructuring. While it may be possible to calculate the exact capital requirement of a new portfolio by re-running the risk model, as proposed by Gründl and Schmeiser (2007), the challenge remains how decision-makers can reach an insightful understanding of the risk situation beforehand in order to identify promising portfolio changes.

This paper regards the gradient capital allocation as a first scenario and shows that a small set of further deterministic scenarios may approximate the original risk measurement including its most relevant curvatures.² Our scenarios decompose the multivariate risk distribution similarly to a principal component analysis (PCA). Whereas the components of the traditional PCA are orthogonal in terms of Pearson correlations, we define orthogonality based on the marginal contribution of portfolio components on diversified capital. Our method builds on the “hybrid approach” of risk measurement introduced by Rosenberg and Schuermann (2006). The hybrid approach allows univariate risk distributions to be heavy-tailed and skewed, and aggregates univariate risk measurements using a square-root formula. Whereas the square-root formula in connection with the Pearson correlation matrix can aggregate risks accurately only in case of multivariate elliptical distributions, Paulusch and Schlütter (2022) introduce the so-called “sensitivity-implied tail correlation matrix”. With the latter matrix, the hybrid approach accurately reflects first and second-order sensitivities of an original “true” risk measurement irrespective of an elliptical distribution assumption. Using this set-up, we translate the original risk measurement into a measurement based on “orthogonal convexity scenarios” (OCS). The OCS-based risk measurement reflects the original risk measurement in terms of (i) all first-order derivatives (i.e. the gradient capital allocation) and (ii) second-order derivatives with respect to portfolio changes in a certain subspace.

We explain several applications of our proposed OCS approach to outline its advantages compared to traditional methods. The stochastic distributions of the segments’ profits

²In this sense, our target differs from that of articles such as Breuer and Csiszár (2013), who identify stress scenarios of the input factors of risk models, for example to assess the model risk relating to changes in these factors.

or losses used include skewed and heavy-tailed distributions which are partly connected with a Gumbel copula modeling increased tail dependencies. Portfolio risk is measured by the 99% Value-at-Risk of unexpected losses.

Our example substantiates that convexity of portfolio risk has to be evaluated from a holistic perspective. Considering a stylized financial institution with three business segments, the traditional gradient allocation (i.e. our first OCS) misses the true Value-at-Risk especially when the volumes of segments 1 and 2 move in the same direction (e.g. both are increased) but the volume of segment 3 moves in the opposite direction (is reduced). In terms of stochastic distributions, this is because segments 1 and 2 exhibit an increased tail dependence; segment 3 is well diversified in the initial portfolio, but it includes heavy-tailed risks that could become dominant if the segment is overproportionally expanded. Accordingly, our second OCS assigns segments 1 and 2 values of the same sign, but segment 3 a value of the opposite sign. As for the gradient allocation, the values of all OCS can be regarded as a meaningful realization of the multivariate distribution of segment risks.

A first application of OCS is therefore to support the communication of risk concentrations and diversification effects between risk modelers on the one hand and decision makers and other stakeholders on the other. In fact, this communication has been regarded in the literature as both challenging and essential to establishing effective and value-adding Enterprise Risk Management.³ While the gradient capital allocation is a relatively simple tool to communicate dominant risk drivers and natural hedging effects in the initial portfolio, our additional OCS can provide a more solid understanding, since they account for changes in risk diversification following portfolio changes which are particularly impactful for the risk diversification pattern.

Secondly, OCS can support the graphical visualization of portfolio risk in order to provide another tool for risk communication or to serve as a starting point for validating the risk model. In a plot of multivariate realizations of the segment's profits or losses, OCS generally lie on the surface of an ellipsoid. The orientation of this ellipsoid reflects risk contributions in the initial portfolio (i.e. the gradient allocation), and its width reflects convexity of portfolio risk. In the special case of a multivariate elliptical distribution, the

³Communication gaps between risk modelers and decision makers have been identified as a trigger of the 2007-2008 financial crisis, cf. (Stulz, 2008, p. 45) and Eling and Schmeiser (2010, p. 16), and are still considered as a central challenge in Enterprise Risk Management, cf. Wilson (2015, p. 599), Aven (2016, p. 10).

orientation of the ellipsoid coincides with the OLS regression function when regressing a segment's profits on the entire portfolio's profits; convexity of portfolio risk depends on the standard deviation of the regression's residuals.

Thirdly, the gradient capital allocation can be applied as a basis for breaking down a portfolio risk limit to portfolio segments.⁴ In this sense, segments receiving higher amounts from the gradient allocation have a higher impact on the overall portfolio risk and should therefore be more strictly limited and monitored. However, the effectiveness of the limit system in this set-up is only ensured as long as the gradient allocation correctly reflects the risk structure of the portfolio, i.e. the composition of the portfolio may not change too much. OCS can help integrate the latter condition directly into the risk limit system. For this purpose, we propose risk limits of first and second order: while first-order limits are defined with the condition of the portfolio's risk structure remaining within certain constraints, second-order limits monitor whether this condition is met. We demonstrate that second-order limits are tight for segments that exert a strong convex impact on diversified capital and are hence likely to become relevant risk drivers; segments with a slight convex impact, in turn, receive a loose limit.

The remainder of this article is structured as follows. Section 1.2 provides a suggestive example concerning a financial firm's RORAC outlining the limitation of the gradient capital allocation and how OCS can address it. Section 1.3 provides the general set-up and defines quality criteria of a scenario-based risk measurement. Section 1.4 defines the gradient scenario and identifies its shortcomings in terms of the defined quality criteria. PCA-scenarios are then presented and discussed. Section 1.5 defines OCS, presents their structural relationship with the gradient scenario and with PCA-scenarios, and shows how they make the scenario-based risk measurement suitable in terms of the quality criteria. Section 1.6 outlines possible applications of OCS. Section 1.7 concludes.

1.2 Motivating example: RORAC maximization

Let us consider a financial institution with three business segments. The segments can deliver random profits or losses.⁵ The firm's overall potential losses are measured by the 99% Value-at-Risk of 100 monetary units. The gradient capital allocation splits the Value-at-Risk to the three segments with values $30.8 + 45.1 + 24.1 = 100$. Suppose the

⁴Cf. Jorion (2006), Buch et al. (2011), Erel et al. (2015).

⁵Details about the distribution assumptions are presented later in section 1.6.1.

segments' expected profits are $1.4+2.2+1.4 = 5$. Therefore, the Return on Risk-Adjusted Capital (RORAC) of the entire firm is $5/100=5\%$, and based on the gradient allocation, the segments' RORACs are $1.4/30.8=4.55\%$, $2.2/45.1=4.87\%$, and $1.4/24.1=5.81\%$.

According to Tasche (2008, p. 428 f.), the gradient allocation is "RORAC compatible". Hence, given that the RORACs of segments 1 and 2 (segment 3) are smaller (larger) than the RORAC of the entire firm, the firm's RORAC increases when segments 1 and 2 are slightly reduced and segment 3 is slightly expanded. However, analogous to what Buch et al. (2011, p. 3006) point out for their example, it is unclear to what extent the segments should change.

Suppose segments 1 and 2 each reduce their businesses by 25% and segment 3 expands by 50%. If the segments' risk contributions in the new portfolio were similar to those in the initial portfolio, then the gradient allocation could estimate the new Value-at-Risk in terms of $0.75 \cdot 30.8 + 0.75 \cdot 45.1 + 1.5 \cdot 24.1 = 93.1$. The new RORAC was therefore $(0.75 \cdot 1.4 + 0.75 \cdot 2.2 + 1.5 \cdot 1.4)/93.1 = 4.8/93.1 = 5.2\%$. However, risks of segment 3 are much more dominant in the new portfolio and the segment's contribution is severely underestimated by the given gradient allocation. Recognizing the distribution assumptions in the example, the true Value-at-Risk of the new portfolio is 101.9, and the new RORAC is $4.8/101.9 = 4.7\%$, thus lower than for the initial portfolio.

We now describe the initial portfolio's risk structure using the gradient allocation and one additional orthogonal convexity scenario (OCS). In the present example, the next OCS assigns the values -19.0 , -33.1 and 52.1 to the three segments. It thus points out that losses in segment 3 could occur at the same time as gains in segments 1 and 2 (or the other way around). The Value-at-Risk for the new portfolio can be estimated by the root sum of squares with the two scenarios, i.e.

$$\begin{aligned} & \sqrt{(0.75 \cdot 30.8 + 0.75 \cdot 45.1 + 1.5 \cdot 24.1)^2 + (0.75 \cdot (-19.0) + 0.75 \cdot (-33.1) + 1.5 \cdot 52.1)^2} \\ & = \sqrt{93.1^2 + 39.1^2} = 100.9, \end{aligned}$$

which is much closer to the new portfolio's true Value-at-Risk (101.9) than the estimate with only the gradient allocation (93.1). OCS thus provide in simple terms a decision-making basis for decision makers. Since OCS go beyond the purely marginal informativeness of the gradient allocation, they prevent the company from missteering.

1.3 Targets of a scenario-based risk measurement

The technical basis of our considerations is a mapping from a vector $u = (u_1, \dots, u_n)^T \in \mathbb{R}^n$, with $n \in \mathbb{N}$, to a real-valued risk measurement,

$$f : U \rightarrow \mathbb{R} \tag{1.1}$$

with $U \subseteq \mathbb{R}^n$ being open and convex. Function $f(u)$ represents the firm's target value and will be referred to as the *original risk measurement* going forward. The vector u defines the composition of the firm's portfolio, U is the set of admissible portfolios and $u_{\text{initial}} \in U$ is the firm's initial portfolio. The technical assumption throughout our paper is

Assumption (A): $f(u)$, as defined in (1.1), is positive homogeneous of degree one, i.e. for all $\lambda > 0$ we have $f(\lambda \cdot u) = \lambda \cdot f(u)$. Moreover, $f(u_{\text{initial}}) > 0$ and $f(u)$ is twice continuously differentiable at $u_{\text{initial}} \in U$.

A classical example for specifying $f(u)$ considers an n -dimensional portfolio with vector u containing exposures to risk factors.⁶ Let the random vector $\mathbf{X} = (X_1, \dots, X_n)^T$ model the losses (or gains in case of negative values) of the portfolio's n positions with finite expectations. Hence,

$$u^T \mathbf{X} = \sum_{i=1}^n u_i X_i$$

is the loss (or gain) of the portfolio. Let ϱ be a law-invariant, positive homogeneous and translation-invariant risk measure.⁷ The original risk measurement can then be defined as the risk measurement of unexpected portfolio losses,

$$f_{\text{stoch}} : U \rightarrow \mathbb{R}, u \mapsto \varrho(u^T \mathbf{X}) - \mathbb{E}(u^T \mathbf{X}) \tag{1.2}$$

The differentiability of $f_{\text{stoch}}(u)$ depends on the risk measure and the multivariate distribution of \mathbf{X} . It is discussed, for instance, in Gouiroux et al. (2000), Tasche (2008) and Hong and Liu (2009).

There are several further examples of $f(u)$ which comply with *Assumption (A)*. For example, $f(u)$ can be a deterministic risk measurement in the sense of the hybrid approach

⁶This specification is consistent with, for example, Rockafellar et al. (2000), Zanjani (2002), Tasche (2008).

⁷McNeil et al. (2015, p. 275 ff.) summarize desirable properties of risk measures.

of Rosenberg and Schuermann (2006).⁸ The hybrid approach is employed in some regulatory capital requirement frameworks, such as the Solvency II standard formula for insurance regulation in the European Union. Moreover, Assumption (A) is consistent with the risk measurement based on the contingent claims approach in Myers and Read (2001) and Erel et al. (2015),⁹

Our target is to approximate $f(u)$ using a measurement based on deterministic scenarios $x \in \mathbb{R}^n$. We do not necessarily restrict ourselves to a single scenario, but allow for $m \in \{1, \dots, n\}$ scenarios, x_1, \dots, x_m . Function $g_m(u)$ provides an approximation of $f(u)$ based on m scenarios:

$$g_m : \mathbb{R}^n \rightarrow \mathbb{R}, u \mapsto \sqrt{\sum_{j=1}^m (x_j^\top u)^2} \quad (1.3)$$

In terms of the stochastic approach in (1.2), the scenarios x_1, \dots, x_m can be viewed as realizations of the random vector \mathbf{X} .¹⁰ For each scenario x_j , $u^\top x_j$ is the portfolio loss (or gain) conditioned on scenario x_j having been realized.

In case of $m = 1$ scenario, $g_m(u)$ simplifies to $|x_1^\top u|$. For $m > 1$, the root sum of squares in (3.10) is analogous to risk aggregation for elliptical distributions and thus consistent with a risk measurement based on a Principal Component Analysis (PCA), as we will discuss later in section 1.4.2. In other words, the risk aggregation in (3.10) coincides with the hybrid approach of Rosenberg and Schuermann (2006), with the correlation matrix being an identity matrix.

Going forward, we investigate to what extent $g_m(u)$ is in line with the original risk measurement $f(u)$. Specifically, we study whether $g_m(u)$ may serve as a local approximation of $f(u)$ at an initial portfolio u_{initial} . To this end, we will assess $g_m(u)$ based on the following “quality criteria” (QC):

(QC1) Reflect the risk of the initial portfolio:

For the initial portfolio $u_{\text{initial}} \in U$, we have $g_m(u_{\text{initial}}) = f(u_{\text{initial}})$.

(QC2) Reflect first-order sensitivities:

Let $V_1 \subseteq \mathbb{R}^n$ be a space of possible portfolio changes. Starting from $u_{\text{initial}} \in U$, $g_m(u)$ accurately reflects the change in portfolio risk due to a marginal exposure

⁸Paulusch (2017) deals with homogeneity of risk measurement in the sense of the hybrid approach.

⁹For details about the homogeneity assumption in connection with the Default Put Option, cf. Mildenhall (2004).

¹⁰This notion of a scenario is consistent with McNeil and Smith (2012).

change in the direction of $v \in V_1$, i.e.

$$\frac{\partial}{\partial h} g_m(u_{\text{initial}} + h \cdot v) \Big|_{h=0} = \frac{\partial}{\partial h} f(u_{\text{initial}} + h \cdot v) \Big|_{h=0} \text{ for all } v \in V_1$$

(QC3) Reflect second-order sensitivities:

Let $V_2 \subseteq V_1$ be a space of possible portfolio changes. Starting from $u_{\text{initial}} \in U$, $g_m(u)$ accurately reflects second-order derivatives of portfolio risk with respect to exposure changes in the directions of $v_1, v_2 \in V_2$, i.e.

$$\begin{aligned} & \frac{\partial^2}{\partial h_1 \partial h_2} g_m(u_{\text{initial}} + h_1 \cdot v_1 + h_2 \cdot v_2) \Big|_{h_1=h_2=0} = \\ & = \frac{\partial^2}{\partial h_1 \partial h_2} f(u_{\text{initial}} + h_1 \cdot v_1 + h_2 \cdot v_2) \Big|_{h_1=h_2=0} \end{aligned}$$

for all $v_1, v_2 \in V_2$

If the scenario-based risk measurement $g_m(u)$ satisfies (QC2) with $V_1 = \mathbb{R}^n$, then the scenario-based risk measurement provides “correct” marginal steering signals in the sense of Tasche (2008), as they are in line with those of the true risk measurement. Technically, (QC2) implies that the gradient capital allocation based on $g_m(u)$ coincides with the one based on $f(u)$, i.e.

$$g_m(u_{\text{initial}}) = \sum_{i=1}^n u_i \cdot \frac{\partial}{\partial u_i} g_m(u) \Big|_{u_{\text{initial}}} = \sum_{i=1}^n u_i \cdot \frac{\partial}{\partial u_i} f(u) \Big|_{u_{\text{initial}}} = f(u_{\text{initial}}) \quad (1.4)$$

Apparently, Eq. (1.4) shows that (QC1) holds as a side effect. In turn, criterion (QC3) points out that $g_m(u)$ reflects (at least in part) the curvature of $f(u)$. (QC3) therefore aims for overcoming limitations of the gradient capital allocation, as identified for example by Buch et al. (2011).

1.4 Existing approaches

1.4.1 The gradient scenario

The gradient capital allocation principle defines an n -dimensional vector which we call the “gradient scenario” and use as a starting point of our analysis. We define

$$x^{\text{grad}} := \nabla_u f(u) \Big|_{u=u_{\text{initial}}} \quad (1.5)$$

In connection with definition (1.2) and the risk measure VaR, assuming a situation where VaR is coherent, the gradient scenario coincides with the so-called “Least Solvent Likely Event” (LSLE) suggested by McNeil and Smith (2012).¹¹ Proposition 1.1 states that x^{grad} is the only scenario which provides a local linear approximation of $f(u)$, and it is unique in this sense.

Proposition 1.1. Consider $m = 1$ with the gradient scenario defined in (3.8). Then, $g_m(u)$ fulfills criteria (QC1) and (QC2) with $V_1 = \mathbb{R}^n$.

1.4.2 Principal component analysis (PCA)

PCA identifies important patterns of a multivariate distribution and thus allows for defining multiple scenarios. Consider the original risk measurement $f(u) = f_{\text{stoch}}(u)$ from (1.2). Let Σ denote the covariance matrix of \mathbf{X} , and let the vectors $w_i \in \mathbb{R}^n$, $i = 1, \dots, n$, denote the eigenvectors of Σ . Then the random variables $w_i^T \cdot \mathbf{X}$ and $w_j^T \cdot \mathbf{X}$, $i \neq j$, are pairwise uncorrelated, since

$$\text{cov}(w_i^T \cdot \mathbf{X}, w_j^T \cdot \mathbf{X}) = w_i^T \cdot \Sigma \cdot w_j = 0 \quad (1.6)$$

Moreover, scenarios can be defined as

$$x_j^{\text{PCA}} := \frac{\Sigma \cdot w_j}{\sqrt{w_j^T \Sigma w_j}} \cdot z \quad (1.7)$$

with $j = 1, \dots, n$ and some factor $z > 0$. For two special cases, Eq. (1.7) allows for a proper scenario-based risk measurement, as Proposition 1.2 points out.

Proposition 1.2. Assume that the original risk measurement is defined by $f(u) = f_{\text{stoch}}(u)$ from (1.2) and that the covariance matrix Σ of the random vector \mathbf{X} exists. For $m \in \{1, \dots, n\}$, let $w_1, \dots, w_m \in \mathbb{R}^n$, denote the eigenvectors of Σ relating to its positive eigenvalues sorted in descending order. Suppose that one of the following conditions holds:

- a. Risk measure ϱ is the standard deviation. In Eq. (1.7), z is set to 1.
- b. \mathbf{X} follows an elliptical distribution with the risk measure ϱ being proportional to the standard deviation by factor $z > 0$.¹²

¹¹The coincidence is proven by McNeil and Smith (2012) in Corollary 4.4.

¹²For elliptical distributions, the condition of proportionality is satisfied, e.g. for Value-at-Risk and Expected Shortfall. For example, when \mathbf{X} follows a multivariate normal distribution and the risk measure is the Value-at-Risk with confidence level ζ , then the factor z is the ζ -percentile of the standard normal distribution.

Define function $g_m(u)$ according to (3.10) in connection with the scenarios in Eq. (1.7). For $u \in \text{span}\{w_1, \dots, w_m\}$, we have $g_m(u) = f(u)$. Moreover, if $u_{\text{initial}} \in \text{span}\{w_1, \dots, w_m\}$, $g_m(u)$ satisfies (QC1), (QC2) with $V_1 = \mathbb{R}^n$ and (QC3) with $V_2 = \text{span}\{w_1, \dots, w_m\}$.

Hence, irrespective of the number of PCA-scenarios used, these scenarios reflect the true risk measurement in terms of the gradient allocation with respect to all risks and, to a limited extent, in terms of convexity if the conditions of Proposition 1.2 are fulfilled and if $u_{\text{initial}} \in \text{span}\{w_1, \dots, w_m\}$.

The conditions in Proposition 1.2 are, however, quite restrictive. For downside risk measures, such as Value-at-Risk and Expected Shortfall, \mathbf{X} must include neither skewed marginal distributions nor increased tail dependencies. As an example, PCA has been considered as a useful tool for measuring interest rate risks of a bond portfolio in “normal times”.¹³ In a low-yield environment, however, lower bounds for interest rates may become more relevant (cf. Christensen and Rudebusch, 2015), suggesting that interest rates follow a skewed distribution and implying that PCA-scenarios can not properly reflect the Value-at-Risk (cf. Schlütter, 2021).

1.5 Orthogonal convexity scenarios (OCS)

1.5.1 Defining OCS

To derive a scenario-based risk measurement with useful results for non-elliptical distributions, we replace the covariance matrix with a more general measure for stochastic dependencies. Paulusch and Schlütter (2022) demonstrate that a risk measurement $f(u)$ fulfilling assumption (A) can be approximated by a deterministic function which has the structure of the hybrid approach of Rosenberg and Schuermann (2006). Specifically, the second-order Taylor polynomial of $f^2(u)$ at u_{initial} can be presented using a matrix function

$$P_{f^2}(u) = 0.5u^T H u \quad (1.8)$$

with H being the Hessian matrix of $f^2(u)$ evaluated at $u = u_{\text{initial}}$.¹⁴ Taking the square-root on both sides of (1.8) provides a local approximation of $f(u)$:

$$g_{\text{Taylor}}(u) = \sqrt{P_{f^2}(u)} = \sqrt{0.5u^T H u} \quad (1.9)$$

¹³Cf. Frye (1997), Golub and Tilman (1997) and Hull (2018, pp. 204 ff.).

¹⁴Cf. Paulusch and Schlütter (2022), Theorem 1.

$g_{\text{Taylor}}(u)$ reflects $f(u)$ at u_{initial} up to second-order derivatives.

Recall that the PCA builds on vectors w_i implying that the random variables $w_i^T \cdot \mathbf{X}$ and $w_j^T \cdot \mathbf{X}$ are pairwise uncorrelated, cf. line (1.6). In our proposed approach, we identify vectors w_1, \dots, w_m that are pairwise orthogonal in a context that allows for useful scenarios as a basis of $g_m(u)$. Mathematically, orthogonality is defined in connection with a symmetric bilinear form $\langle \cdot, \cdot \rangle$ and two vectors w_i, w_j are called orthogonal if $\langle w_i, w_j \rangle = 0$. Lemma 1.1 introduces the symmetric bilinear form that we use later on.

Lemma 1.1. *Let assumption (A) be fulfilled and let H denote the Hessian matrix of $f^2(u)$ evaluated at $u_{\text{initial}} \in U$. Then*

$$\begin{aligned} \langle w_i, w_j \rangle_H &:= \frac{\partial^2}{\partial h_i \partial h_j} f^2(u_{\text{initial}} + h_i w_i + h_j w_j) \Big|_{h_i=h_j=0} \\ &= w_i^T H w_j \end{aligned} \quad (1.10)$$

defines a symmetric bilinear form on $U \times U$.

The basic idea behind the orthogonal convexity scenarios is to select linear independent vectors $w_1, \dots, w_m \in \mathbb{R}^n$ which span a subspace $V \subseteq \mathbb{R}^n$ with $u_{\text{initial}} \in V$. The vectors w_1, \dots, w_m should be pairwise orthogonal in the sense of $\langle \cdot, \cdot \rangle_H$ and satisfy $\langle w_i, w_i \rangle_H > 0$ for all $i = 1, \dots, m$. Then, any $u \in V$ can be represented as¹⁵

$$u = \sum_{j=1}^m \frac{\langle w_j, u \rangle_H}{\langle w_j, w_j \rangle_H} \cdot w_j \quad (1.11)$$

Let

$$\tilde{u}_j = \frac{\langle w_j, u \rangle_H}{\langle w_j, w_j \rangle_H} \cdot w_j \text{ for } j = 1, \dots, m \quad (1.12)$$

Then we have

$$\begin{aligned} u^T H u &= (\tilde{u}_1 + \dots + \tilde{u}_m)^T H (\tilde{u}_1 + \dots + \tilde{u}_m) \\ &= \tilde{u}_1^T H \tilde{u}_1 + \dots + \tilde{u}_m^T H \tilde{u}_m \end{aligned} \quad (1.13)$$

where the last equation follows from the pairwise orthogonality of the w_j (which implies pairwise orthogonality of the \tilde{u}_j). Lemma 1.2 defines vectors x_j^{OCS} , which we call *orthogonal convexity scenarios* (OCS).

¹⁵Cf. for example Clay et al. (2015, p. 341), Theorem 5.

Lemma 1.2. *Let the assumptions of Lemma 1.1 be fulfilled. For $m \in \{1, \dots, n\}$, assume that $w_1, \dots, w_m \in \mathbb{R}^n$ are pairwise orthogonal in the sense of $\langle \cdot, \cdot \rangle_H$ and satisfy $\langle w_i, w_i \rangle_H > 0$ for all $i = 1, \dots, m$. For all $j \in \{1, \dots, m\}$, define*

$$x_j^{OCS} := \frac{Hw_j}{\sqrt{2w_j^T Hw_j}} \quad (1.14)$$

Then

$$\left((x_j^{OCS})^T u \right)^2 = 0.5 \tilde{u}_j^T H \tilde{u}_j \quad (1.15)$$

with \tilde{u}_j being defined as in line (1.12) based on w_j and u .

According to Eq. (1.14), each OCS is determined based on an underlying portfolio vector w_j . Condition $\langle w_i, w_i \rangle_H > 0$ means that $f(u)$ is locally at u_{initial} strictly convex with respect to changes in direction w_i . The assumption is satisfied, for example, if $f(u)$ is specified by Eq. (1.2) with a risk measure that satisfies the *convexity axiom*.

Based on Lemma 1.2 we can derive the OCS-based risk measurement of portfolio $u \in V$. To this end, entering Eq. (1.15) into Eq. (1.13) implies

$$g_m^2(u) = \sum_{j=1}^m \left((x_j^{OCS})^T u \right)^2 = 0.5 \sum_{j=1}^m \tilde{u}_j^T H \tilde{u}_j \stackrel{(1.13)}{=} 0.5 u^T H u \stackrel{(1.8)}{=} P_{f_2}(u) \quad (1.16)$$

Taking the square-root on both sides of Eq. (1.16) implies that $g_m(u)$ in connection with the OCS from Eq. (1.14) approximates the true risk measurement $f(u)$ in the sense of a second-order Taylor approximation at $u = u_{\text{initial}}$. Theorem 1.1 outlines this result.

Theorem 1.1. *Let the assumptions of Lemma 1.2 be fulfilled and assume that $u_{\text{initial}} \in \text{span}\{w_1, \dots, w_m\}$. Then $g_m(u)$ as defined in line (3.10) in connection with the scenarios x_j^{OCS} defined in Eq. (1.14), for $j = 1, \dots, m$, fulfills (QC1), (QC2) with $V_1 = \mathbb{R}^n$ and (QC3) with $V_2 = \text{span}\{w_1, \dots, w_m\}$. For $u \in \text{span}\{w_1, \dots, w_m\}$, we have $g_m(u) = g_{\text{Taylor}}(u)$.*

The statements of Theorem 1.1 are analogous to those of Proposition 1.2. Hence, OCS allow a generalization of the PCA-based risk measurement with respect to skewed distributions and increased tail dependencies.

The condition $u_{\text{initial}} \in \text{span}\{w_1, \dots, w_m\}$ can be ensured by setting $w_1 = u_{\text{initial}}$. Corollary 1.1 shows that the corresponding first OCS then coincides with the gradient scenario defined in Eq. (3.8).

Corollary 1.1. *Let the assumptions of Lemma 1.1 be fulfilled and $w_1 = u_{initial}$. Then we have*

$$x_1^{OCS} = x^{grad}$$

with x_1^{OCS} being defined as in Eq. (1.14) and x^{grad} as in Eq. (3.8).

Therefore, OCS can consistently extend the concept of the gradient scenario as introduced in Section 3.1: in addition to the gradient scenario, portfolio risk is communicated with the scenarios $x_2^{OCS}, \dots, x_m^{OCS}$. Based on these scenarios, $g_m(u)$ not only accurately reflects marginal portfolio changes (as it does based on the single gradient scenario), but also reflects how diversification effects alter when the portfolio is changed in directions within the subspace V_2 .

The selection of the OCS, i.e. the selection of the vectors w_1, \dots, w_m , determines the space V_2 for which the scenario-based risk measurement $g_m(u)$ meets the curvature of $f(u)$ in the sense of (QC3), cf. Theorem 1.1. The selection should therefore be made against the background of practical considerations, such that V_2 contains conceivable portfolio changes in light of restrictions of the firm's overall strategy, regulation, etc.

Section 1.5.2 provides guidance on the selection of OCS in the general case. Afterwards, section 1.5.3 explains the selection for an analysis in which the addition of a particular portfolio segment is of interest.

1.5.2 Selecting OCS

This section proposes an iterative approach to select the most meaningful OCS. In this regard, we aim to minimize the approximation error and note that the approximation error for any portfolio $u \in U$ can be decomposed into two parts:

$$f(u) - g_m(u) = \underbrace{f(u) - g_{\text{Taylor}}(u)}_{\text{Error part 1}} + \underbrace{g_{\text{Taylor}}(u) - g_m(u)}_{\text{Error part 2}} \quad (1.17)$$

Only the error part 2 depends on the employed scenarios. For $m = n$ OCS being used, error part 2 is zero for all portfolios u . To select a further scenario, we therefore focus on the error part 2.

Suppose that m vectors w_1, \dots, w_m have been selected in line with the assumptions of Lemma 1.2 and with $u_{initial} \in \text{span}\{w_1, \dots, w_m\}$. Based on these vectors, scenarios have

been determined with Eq. (1.14). With Eq. (1.11), we can write any $u \in U$ as

$$u = \underbrace{\sum_{j=1}^m \frac{\langle w_j, u \rangle_H}{\langle w_j, w_j \rangle_H} \cdot w_j}_{=: \tilde{u}} + u_{\text{remainder}} \quad (1.18)$$

Given that $\langle u_{\text{remainder}}, w_i \rangle_H = 0$ for all $i = 1, \dots, m$, we focus on the subset of vectors that are orthogonal to w_1, \dots, w_m ,

$$U_{\perp} = \{u \in \mathbb{R}^n \text{ such that } \langle u, w_i \rangle_H = 0 \text{ for all } i = 1, \dots, m\}, \quad (1.19)$$

Starting from an arbitrary portfolio $\tilde{u} \in \text{span}\{w_1, \dots, w_m\}$, we identify vector $w_{m+1} \in U_{\perp}$ with the largest error type 2, i.e.

$$w_{m+1} = \operatorname{argmax}\{g_{\text{Taylor}}(\tilde{u} + w) - g_m(\tilde{u} + w) \text{ with } w \in U_{\perp} \text{ and } \|w\|_2 = 1\} \quad (1.20)$$

Appendix 1.8.2 shows that the searched vector w_{m+1} does not depend on $\tilde{u} \in \text{span}\{w_1, \dots, w_m\}$, and can be rewritten as

$$\operatorname{argmax}\{g_{\text{Taylor}}(w) \text{ with } w \in U_{\perp} \text{ and } \|w\|_2 = 1\} \quad (1.21)$$

Moreover, the Appendix shows that w_{m+1} can be identified as the solution of an eigenvalue problem provided that H is positive semidefinite. Adding a further scenario based on w_{m+1} in connection with Eq. (1.14) ensures that the error type 2 is eliminated in the identified direction, i.e. $g_{m+1}(\tilde{u} + w_{m+1}) = g_{\text{Taylor}}(\tilde{u} + w_{m+1})$.

1.5.3 OCS on the surface of an ellipsoid

As a starting point for risk visualizations, Corollary 1.2 shows that the scenarios defined by Eq. (1.14) are on the surface of an ellipsoid. For $n = 2$ or $n = 3$, the ellipsoid can be added into a scatter plot of realizations of the random vector X .

Corollary 1.2. *Let the assumptions of Lemma 1.2 be fulfilled and assume that H is invertible. Then, all scenarios x_j^{OCS} as defined by Eq. (1.14) are on the surface of the ellipsoid*

$$\{v \in \mathbb{R}^n \mid v^{\text{T}} H^{-1} v \leq 0.5\} \quad (1.22)$$

As an example for a situation which allows a two-dimensional visualization, we analyze the situation of adding a particular asset to a preexisting portfolio. Formally, we consider $n = 2$ risks with X_1 reflecting the risks of the preexisting portfolio, X_2 the risks of the asset

of interest and $u_{\text{initial}} = (1, 0)^T$. For this “contribution analysis”, Corollary 1.3 derives two OCS which inform about the first and second-order sensitivity of the portfolio’s aggregate risk with respect to adding X_2 .

Corollary 1.3. *Let the assumptions of Lemma 1.2 be fulfilled with $n = 2$ and $u_{\text{initial}} = (1, 0)^T$, and let h_{ij} denote the entries of H . We set $w_1 = u_{\text{initial}}$, $w_2 = (-h_{12}/h_{11}, 1)^T$ and determine x_1^{OCS} and x_2^{OCS} by Eq. (1.14). Let x_{ij}^{OCS} denote entry j of vector x_i^{OCS} . We have $x_{21}^{\text{OCS}} = 0$ and the function value, gradient and Hessian matrix are given by*

$$\begin{aligned} f(u_{\text{initial}}) &= x_{11}^{\text{OCS}} \\ \nabla_u f(u_{\text{initial}}) &= x_1^{\text{OCS}} \\ H_f(u_{\text{initial}}) &= \begin{pmatrix} 0 & 0 \\ 0 & \frac{(x_{22}^{\text{OCS}})^2}{x_{11}^{\text{OCS}}} \end{pmatrix} \end{aligned}$$

Based on the two OCS defined in Corollary 1.3, the ellipsoid from line (1.22) can be added into a two-dimensional scatter plot of realizations of X_1 and X_2 . We will call the ellipsoid in this context the “contribution ellipsoid”. It allows us to link the marginal impact and the convexity of adding X_2 for the aggregate portfolio risk with the scatter plot.

1.5.4 Example: Multivariate elliptical distribution

For the case of X following a multivariate elliptical distribution, some of our results about OCS can be linked to well-known concepts.

Proposition 1.3. Let the assumptions of Proposition 1.2 be fulfilled. We have

- a. $H = 2z^2\Sigma$
- b. For given w_1, \dots, w_m , we have $x_j^{\text{OCS}} = x_j^{\text{PCA}}$ as defined in Eq. (1.14) and (1.7).
- c. Vectors w_1, \dots, w_m being the eigenvectors of Σ corresponding to positive eigenvalues in descending order satisfy the selection approach in section 1.5.2.
- d. For $z = 1$, the ellipsoid defined in line (1.22) coincides with the ellipsoid of concentration introduced by Darmois (1945), which is defined as¹⁶

$$\{v \in \mathbb{R}^n : v^T \Sigma^{-1} v \leq 1\} \tag{1.23}$$

¹⁶This definition is used by Nordström (1991, p. 397).

e. Let $w_1 = u_{\text{initial}}$. Then each entry j of x_1^{OCS} satisfies

$$x_{1j}^{\text{OCS}} = \beta_j \cdot f(u_{\text{initial}})$$

with

$$\beta_j = \frac{\text{cov}(X_j, \mathbf{X}^T \cdot u_{\text{initial}})}{\text{var}(\mathbf{X}^T \cdot u_{\text{initial}})}$$

Assertion b. means that OCS scenarios coincide with PCA-scenarios when the conditions of Proposition 1.3 are fulfilled and the vectors w_1, \dots, w_m are the eigenvectors of Σ . According to assertion d., the ellipsoid in line (1.22) is a stretched version from the ellipsoid of Darmois (1945) if $z > 1$. It is also a shifted and stretched or compressed version of the ellipsoid of concentration proposed by Cramér (1946).¹⁷

Assertion e. points out that the first OCS (i.e. the gradient capital allocation) relates to the Capital Asset Pricing Model (CAPM) of Sharpe (1964), Lintner (1965) and Mossin (1966). For multivariate normal distributions, this relation was already shown by Panjer (2002), who refers to the β_j as “internal betas”. Starting from this notion, convexity of portfolio risk is driven by the residuals of an (internal) CAPM-like regression of the profits of each portfolio segment on the total portfolio’s profits. Higher OCS point out which group of segments exhibit volatile and highly correlated residuals. We follow up on this analogy in Appendix 1.8.3.

1.6 Applications

1.6.1 Analyzing a portfolio of business segments

We consider a financial institution with three segments as in section 1.2. The random vector $X = (X_1, X_2, X_3)^T$ models the segments’ losses (positive realizations) or gains (negative realizations). The vector $u \in \mathbb{R}^3$ reflects the sizes of segments, with the initial portfolio being characterized by $u_{\text{initial}} = (1, 1, 1)^T$. The distributions of X_2 and X_3 are right-skewed (lognormal and Gamma), while X_1 is normally distributed. The stochastic dependencies of X_1 and X_2 are modeled by a Gumbel copula with a parameter $\Theta = 2$ which models increased tail dependencies. The dependency of $X_1 + X_2$ and X_3 is modeled by a Gaussian copula with correlation parameter $\rho = 0$. The true risk measurement $f(u)$ is defined by Eq. (1.2) in connection with the 99% Value-at-Risk, and we have

¹⁷The statement follows immediately with the definition in Nordström (1991, p. 397).

$f(u_{\text{initial}}) = 100$. Figure 1.1 summarizes the distribution assumptions and presents the univariate risks and the gradient scenario. The gradient scenario points out that segment 2 is currently the most dominant risk in the portfolio.

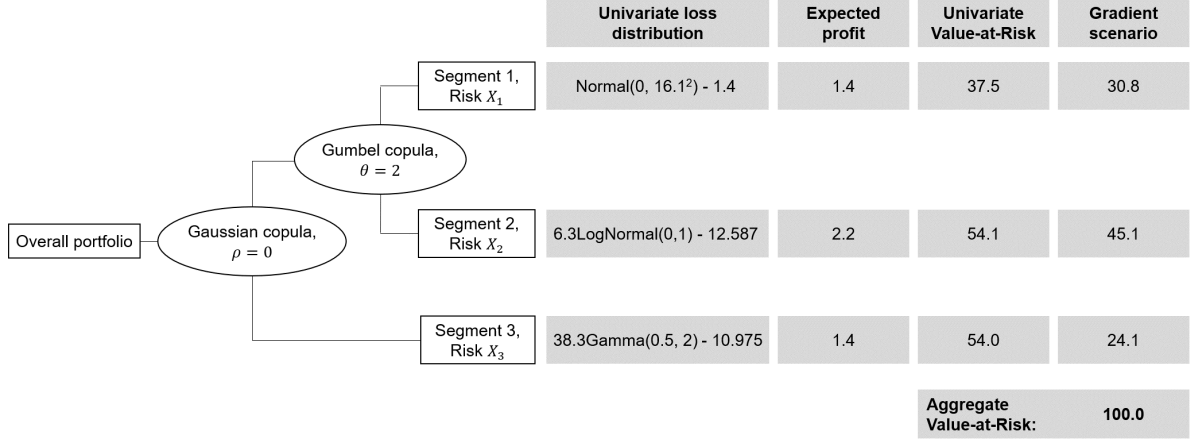


Figure 1.1 Distribution assumptions of the numerical example with three risks, X_1 , X_2 and X_3 . Column “Expected profit” shows the expectation of each random variable multiplied with -1 (since positive realizations reflect losses and negative reflect gains); column “Univariate Value-at-Risk” depicts $VaR_{0.99}(X_i) - E(X_i)$; the gradient scenario in the last column is determined as $\nabla_u f(u) |_{u=u_{\text{initial}}}$.

Table 1.1 presents the OCS and PCA-scenarios.¹⁸ The first OCS is selected as the gradient scenario and thus replicates the last column of Figure 1.1. The last row of Table 1.1 the relative error between $g_m(u)$ and $g_{\text{Taylor}}(u)$,

$$\text{Max. error part 2} = \frac{|g_{\text{Taylor}}(u_{m+1}) - g_m(u_{m+1})|}{g_{\text{Taylor}}(u_{m+1})}, \quad (1.24)$$

with portfolio u_{m+1} being selected as in Eq. (1.21).

For a risk measurement based solely on the gradient scenario, we identify portfolio $u_2 = (0.71, 0.49, 1.81)^T$ which is falsely assessed with $x^{\text{grad}} \cdot u_2 = 87.2$. In fact, diversification effects decrease in u_2 , and the true risk hence amounts to $f(u_2) = 107.0$. The Taylor approximation is $g_{\text{Taylor}}(u_2) = 108.7$, and we thus calculate

$$\text{Max. error part 2} = \frac{|108.7 - 87.2|}{108.7} = 19.6\% \quad (1.25)$$

The second OCS is determined by incorporating $w_2 = u_2$ into Eq. (1.14). In this OCS,

¹⁸To select the OCS, we have set $w_1 = u_{\text{initial}}$. Weightvectors w_2 and w_3 have been selected, successively minimizing the error between the stochastic risk measurement $f(u)$ and the approximation $g_m(u)$ as outlined in Appendix 1.8.2. PCA-scenarios have been determined according to Eq. (1.7). The calculations are based on Monte Carlo simulations of $(X_1, X_2, X_3)^T$ with 1,000,000 simulation paths.

a loss in segment 3 is accompanied by gains in the first two segments. Hence, it states that portfolio risk increases when segment 3 is expanded and the first two segments are reduced. Such a portfolio restructuring would reduce favorable diversification effects between $X_1 + X_2$ on the one hand and X_3 on the other hand. The loss potential of segment 3, modeled by the right-skewed Gamma distribution, would therefore become a more relevant driver of the portfolio's tail risk.

In the third OCS, a loss in segment 1 is accompanied by a gain in segment 2 (and a small gain in segment 3). This scenario points out that an expansion of segment 1 with a reduction of segment 2 (or the other way around) would reduce favorable diversification effects between these two segments.

The left part of Table 1.2 shows how the OCS-based risk measurement evaluates non-marginal segment expansions. For segment 2, an expansion can be well estimated by the gradient scenario (with an error of -2.0%), given that segment 2 is already the dominant risk driver and expanding this segment does not materially impact diversification effects. Using a second OCS makes a small contribution and allows a reduction of the error to 0.5%. Segment 3 is not the dominant risk driver in the initial portfolio, and hence its expansion has a more convex influence on the aggregate risk. Therefore, the gradient scenario causes a relatively large error of -8.6%, and the second OCS helps to reduce the error to -0.9%.

The PCA-scenarios in the right part of Table 1.1—from a qualitative point of view—describe the risk situation similarly to the OCS. In the first and second PCA-scenario, losses occur in the first two segments simultaneously or in the third segment respectively. The third PCA-scenario is similar to the third OCS. Using all three PCA-scenarios, the scenario-based risk measurement of the initial portfolio, i.e. $g_3^{\text{PCA}}(u_{\text{initial}})$, is very close to 100 and hence almost correct. However, the PCA-scenarios do not point out that segment 2 is currently the dominant risk driver. Therefore, $g_3(u)$ substantially understates the sensitivity of the aggregate portfolio risk with respect to the size of segment 2:

$$\frac{\partial}{\partial u_2} g_3^{\text{PCA}}(u_{\text{initial}}) = 30.2 < 45.1 = \frac{\partial}{\partial u_2} f(u_{\text{initial}}) \quad (1.26)$$

Therefore, the PCA-based risk measurement leads to substantial misevaluations for portfolios in an environment of u_{initial} , as shown in the last row of Table 1.1. Specifically, the right part of Table 1.2 points out that a non-marginal expansion of segment 2 is measured

Segment i	OCS			PCA		
	x_{1i} (Gradient)	x_{2i} (2nd OCS)	x_{3i} (3rd OCS)	x_{1i}	x_{2i}	x_{3i}
1	30.8	-18.9	12.7	47.5	-3.8	9.9
2	45.1	-33.2	-10.6	35.6	-5.2	-13.1
3	24.1	52.1	-2.1	6.9	52.8	-0.6
Max. error part 2	19.6%	1.6%	0.0%	42.0%	18.9%	17.6%

Table 1.1 OCS and PCA-scenarios for the example from section 1.6.1. The last row shows the maximal error part 2 as defined in Eq. (1.24).

u_{new}	$f(u_{\text{new}})$	$g_m^{\text{OCS}}(u_{\text{new}})$			$g_m^{\text{PCA}}(u_{\text{new}})$		
		$m = 1$	$m = 2$	$m = 3$	$m = 1$	$m = 2$	$m = 3$
$(1, 2, 1)^{\text{T}}$	148.1	145.1 (-2.0%)	148.9 (0.5%)	149.3 (0.8%)	125.7 (-15.1%)	131.5 (-11.2%)	132.6 (-10.5%)
$(1, 1, 2)^{\text{T}}$	135.8	124.1 (-8.6%)	134.6 (-0.9%)	134.6 (-0.9%)	97.0 (-28.6%)	136.9 (0.8%)	136.9 (0.8%)

Table 1.2 We consider two potential new portfolios, $u_{\text{new}} = (1, 2, 1)^{\text{T}}$ and $u_{\text{new}} = (1, 1, 2)^{\text{T}}$, i.e. expansions of segment 2 or segment 3. Column $f(u_{\text{new}})$ depicts the true risk measurements, i.e. the 99% Value-at-Risk of unexpected losses for the new portfolio. Columns under $g_m^{\text{OCS}}(u_{\text{new}})$ provide the risk measurement based on $m = 1, 2$ or 3 OCS. Columns under $g_m^{\text{PCA}}(u_{\text{new}})$ provide the risk measurement based on PCA-scenarios. The lower lines provide relative errors between scenario-based and true risk measurement (i.e. errors part 1 and 2 from Eq. (1.17) in total). Errors beyond 5% (10%) are highlighted in (dark) grey.

based on PCA-scenarios with an error of -10.5% even if all three PCA scenarios are used.

1.6.2 Risk visualization

Figure 1.2 presents the ellipsoid as defined in (1.22) in a scatter plot of 50,000 realizations of the random vector $(X_1, X_2, X_3)^{\text{T}}$. Realizations with an aggregate loss above the 99% Value-at-Risk, i.e. $x_1 + x_2 + x_3 > f(u_{\text{initial}}) = 100$, are colored in red; the others are colored in gray. The black plane satisfies $x_1 + x_2 + x_3 = 100$ and thus separates the red and gray realizations. We call this plane the VaR-plane, since it marks realizations with an aggregate loss that equals the portfolio's Value-at-Risk. The blue line reflects the gradient scenario, the two green lines reflect the other two OCS.

The plot on the left-hand side of Figure 1.2 shows that the ellipse is wide in the direction of the second OCS, pointing out that the risks of segment 3 are currently well diversified with those of segments 1 and 2 for realizations that are close to the VaR-plane, and that risks of segment 3 could become more dominant if this segment were to be expanded.

The plot on the right-hand side shows that the ellipse is narrow from the perspective of the x_1 - x_2 plane: given that risks of segments 1 and 2 are highly correlated along the VaR-plane, an exchange of these risks would hardly impact the aggregate Value-at-Risk. We next continue the example with a contribution analysis, as described in section 1.5.3.

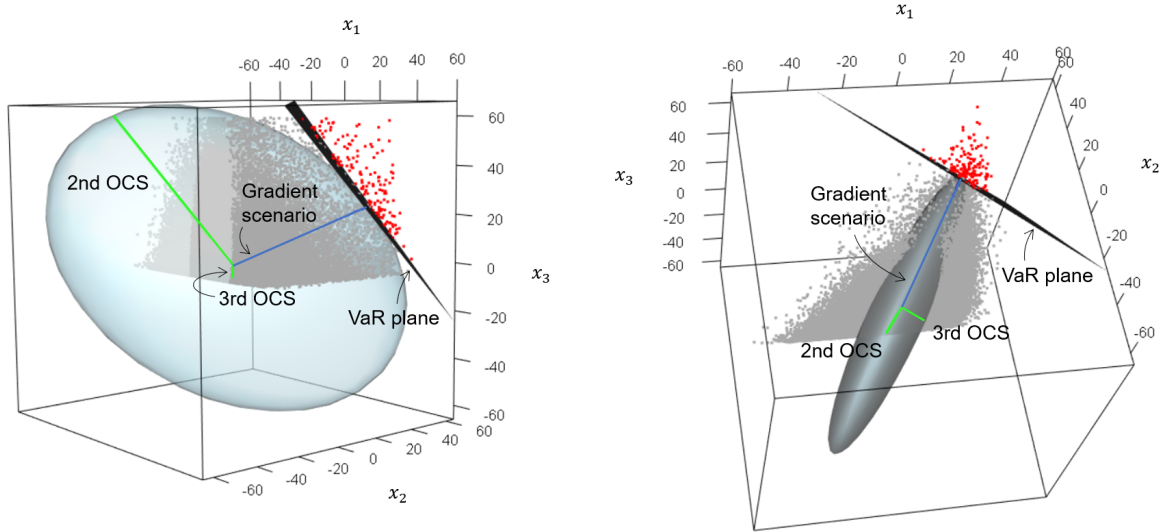


Figure 1.2 The 3d plots show 50,000 realizations of $(X_1, X_2, X_3)^T$ and the ellipsoid from (1.22) from two perspectives. The blue line depicts the gradient scenario; the green lines depict the second and third OCS.

The construction of Figure 1.3 is analogous to Figure 1.5. The upper part of Figure 1.3 investigates an expansion of segment 2. In light of section 1.5.3, we consider $X_1 + X_2 + X_3$ as the risks of the pre-existing portfolio and X_2 as risks which are to be added. The left-hand side of Figure 1.3 presents the contribution ellipsoid in a scatter plot of realizations of portfolio returns, $X_1 + X_2 + X_3$, vs. realizations of X_2, X_3 . On the right-hand side, the blue curve depicts function

$$\tilde{f}(h) = \varrho(X_1 + X_2 + X_3 + h \cdot X_i)$$

for $i = 2, 3$; the red line depicts a first-order approximation of it based on the gradient scenario, i.e. $\tilde{g}_1(h)$ as in Eq. (3.10). The y-coordinate of the respective gradient scenario \tilde{x}_1^{OCS} on the left-hand side coincides with the increase of the red line from $h = 0$ to 1 as stated in Corollary 1.3. The green curve on the right-hand side depicts $\tilde{g}_2(h)$ and hence additionally includes x_2^{OCS} in the approximation of $\tilde{f}(h)$. The y-coordinate of the second OCS, \tilde{x}_2^{OCS} , directly relates to the convexity of $\tilde{f}(h)$, as also stated in Corollary 1.3.

Comparing contribution ellipsoids in the upper and lower parts of Figure 1.3 exhibits two differences of the segments. Firstly, due to the larger y-coordinate of \tilde{x}_1^{OCS} , the ellipsoid of segment 2 is directed upwards more strongly than for segment 3, pointing out that X_2 is connected more strongly to tail risks of the portfolio than X_3 . Secondly, because of the larger y-coordinate of \tilde{x}_1^{OCS} , the contribution ellipsoid of segment 3 is wider than the one for segment 2. Consequently, a non-marginal extension of segment 3 can make X_3 a dominant risk in the portfolio, and $\tilde{f}(h)$ is hence more curved for segment 3 than for segment 2.

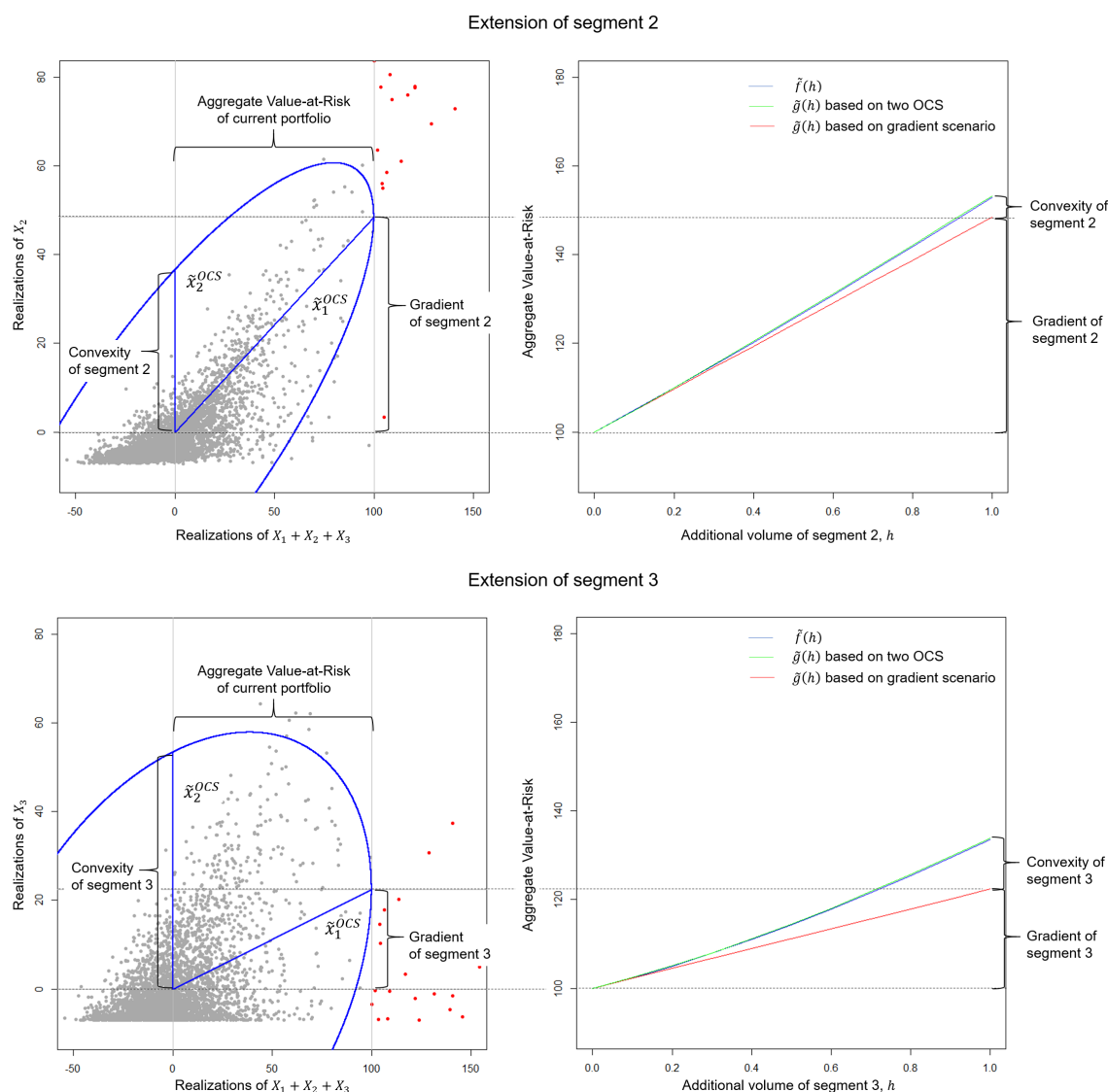


Figure 1.3 Left hand-side: scatter plot of X_2 (bottom part) and X_3 (lower part) vs. $X_1 + X_2 + X_3$ with contribution ellipsoids and OCS. Right part: Aggregate Value-at-Risk according to true risk measurement (blue curve), gradient scenario (red line) and first two OCS (green curve).

1.6.3 Risk limiting

In their “Principles for An Effective Risk Appetite Framework”, the Financial Stability Board (2013, p. 6. f.) requires financial institutions to install risk limits in order to allocate their aggregate risk appetite to lower levels such as business segments or risk categories. In this sense, the gradient capital allocation could be a starting point for risk limits, as it points out how much a marginal expansion of segments affects the company’s risk. If several segments change their volumes adversely, the composition of diversification effects changes, and hence the segments’ contributions to the company’s overall risk alter. Therefore, the initially defined risk limits may become ineffective. Buch et al. (2011, p. 3005) propose limits that build on the gradient capital allocation per business segment. To ensure that the aggregate limit is not breached, the authors include a parameter Λ , which is an upper bound for the largest eigenvalue of the Hessian matrix of $f(u)$ on the set of portfolios U . A drawback of their approach is that Λ does not recognize that convexity may vary across segments, i.e. that volume changes in some segments may change the risk profile of the portfolio more immediately than others. We now outline an approach that overcomes this drawback.

Suppose the firm from section 1.6.1 holds enough equity capital to increase the aggregate Value-at-Risk from 100 to 120. OCS allow for a natural starting point to define risk limits in two stages: a first-order limit is based on the gradient scenario controlling the aggregate risk conditioned on the portfolio composition not having changed too much. In addition, second-order limits based on additional OCS control the stability of the portfolio composition.

The left side of Figure 1.4 depicts combinations of u_1 and u_2 with $u_3 = 1$ being fixed; the right side of the Figure depicts combinations of u_1 and u_3 with $u_2 = 1$ being fixed. The combinations below the green curve are admissible if risk limits are implemented based on the true risk measurement, i.e.

$$f(u) \leq 120$$

Using the OCS in Table 1.1, we allocate limits as

$$\left| (x_1^{OCS})^T u \right| \leq \sqrt{120^2 - 2 \cdot 15^2} = 118.11 \quad (1.27)$$

$$\left| (x_2^{OCS})^T u \right| \leq 15 \quad (1.28)$$

$$\left| (x_3^{OCS})^T u \right| \leq 15 \quad (1.29)$$

ensuring that

$$g_m(u) \leq 120$$

The left-hand sides of Ineq. (1.27) - (1.29) are linear in u_i and depicted in Figure 1.4 by the red line (gradient scenario), blue lines (second OCS) and dashed blue lines (third OCS). The gray colored area marks portfolios that meet all limits in Ineq. (1.27) - (1.29). In the $u_1 u_2$ -plane on the left-hand side Figure 1.4, the area of admissible portfolios is wider than in the $u_1 u_3$ -plane on the right-hand side: a substitution of the risks of segment 1 with those of segment 2 hardly impacts the risk profile given that they are both strongly connected with each other through the Gumbel copula. In contrast, if risks of segment 1 are substituted with those of segment 3, the risk profile changes more immediately, since risks of segment 3—which are currently well diversified—become more dominant for the risk profile. A practical implementation of the proposed limits in the given example could be that segments are allowed to increase their business by up to 20% (first-order limits) and a central department regularly supervises the adherence to second-order limits. If a second-order limit is breached, first-order limits have to be adjusted. Limits in the sense of Ineq. (1.27) - (1.29) should be conservative and account for a potential remainder of $f(u) - g_m(u)$, i.e. the right-hand sides of these inequalities should add up to a total limit of $120 - \max_{u \in U} |f(u) - g_m(u)|$.¹⁹ In the given example, $g_m(u)$ slightly overestimates $f(u)$, and the remainder hence does not appear in the limits.

¹⁹Starting points for assessing the remainder are provided by Paulusch and Schlütter (2022) Proposition 1 and Appendix I.

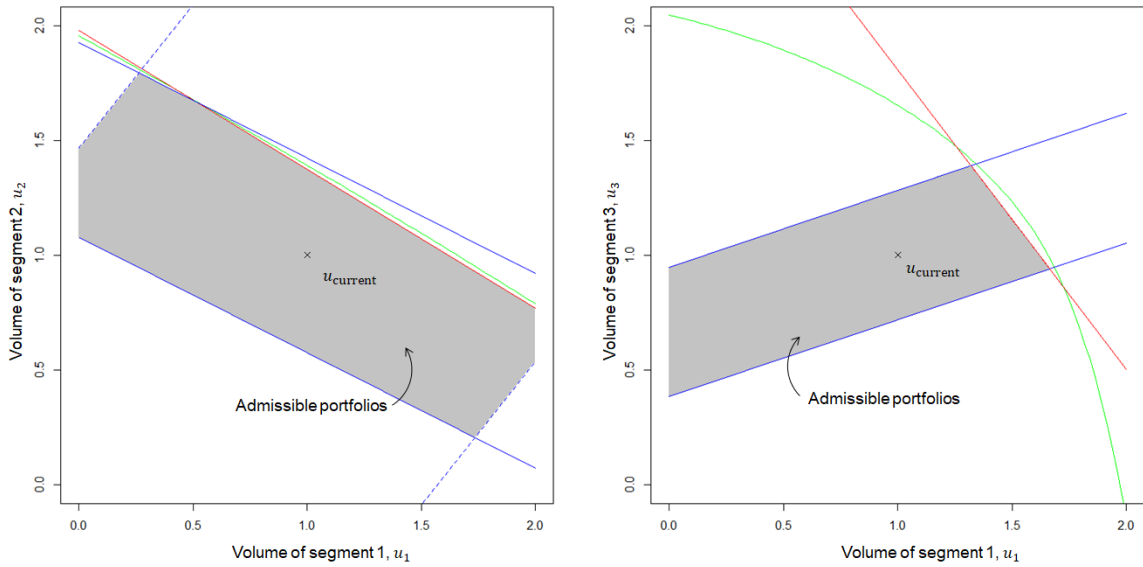


Figure 1.4 The green curves reflect u_1u_2 -combinations (left side, $u_3 = 1$ is fixed), and u_1u_3 -combinations (right side, $u_2 = 1$ is fixed), such that $f(u_1, u_2, u_3) = 120$. The red lines reflect combinations satisfying the gradient scenario limit in Ineq. (1.27) with equality. The blue lines (dashed blue lines) reflect combinations satisfying the further OCS limits in Ineq. (1.28) (Ineq. (1.29)) with equality. The gray colored area marks portfolios meeting all limits in Ineq. (1.27) - (1.29).

1.7 Conclusion

This paper proposes a new methodology for translating portfolio risk into multivariate scenarios of portfolio segments' profits and losses. Our proposed orthogonal convexity scenarios (OCS) extend the gradient capital allocation principle in the sense that they inform about second-order sensitivities of portfolio risk with respect to the volumes of portfolio components. Specifically, OCS demonstrate which combinations of expansions or reductions of portfolio segments can cause a substantial amplification of risk concentrations. OCS can also be viewed as a generalization of Principal Component Analysis, providing a second-order local approximation of portfolio risk without the need for assuming an elliptical distribution. We demonstrate applications of OCS in terms of risk communication, visualization and risk limiting.

Throughout this article, we assume that the risk model, i.e. the original risk measurement $f(u)$, is well established and allows for calculating first and second-order derivatives. The estimation of first- and/or second-order derivatives based on sample data or a Monte Carlo simulation is addressed in many articles, for example, in Gouriéroux et al. (2000),

Hong and Liu (2009), Gómez et al. (2022), Gribkova et al. (2022), Paulusch and Schlütter (2022). It seems promising that OCS can favor the estimation of second-order derivatives. For this purpose, one could set up an iterative process that uses OCS to identify particularly relevant directional derivatives to which the estimation could pay special attention. We leave this however beyond the scope of this paper and for future research.

1.8 Appendix

1.8.1 Proofs

1.8.1.1 Proof of Proposition 1.1

For all $v \in \mathbb{R}^n$, we have

$$\begin{aligned} \frac{\partial}{\partial h} g_1(u_{\text{initial}} + hv) \Big|_{h=0} &= (\nabla_u g_1(u_{\text{initial}}))^T \cdot v = \left(\nabla_u \left((x^{\text{grad}})^T \cdot u \right) \right)^T \cdot v \\ &= (x^{\text{grad}})^T \cdot v \stackrel{\text{Eq. (3.8)}}{=} (\nabla_u f(u_{\text{initial}}))^T \cdot v = \frac{\partial}{\partial h} f(u_{\text{initial}} + hv) \Big|_{h=0} \end{aligned}$$

Therefore, (QC2) holds with $V_1 = \mathbb{R}^n$ and (QC1) follows by line (1.4).

1.8.1.2 Proof of Proposition 1.2

Note that the standard deviation of $u^T \mathbf{X}$ is $\sqrt{u^T \Sigma u}$. Therefore, in both cases a. and b., the original risk measurement can be written as

$$f(u) = z \cdot \sqrt{u^T \Sigma u} \quad (1.30)$$

with a constant $z > 0$. For all $u \in \text{span}\{w_1, \dots, w_m\}$, there are constants $\lambda_1, \dots, \lambda_m \in \mathbb{R}$ such that

$$u = \sum_{i=1}^m \lambda_i w_i \quad (1.31)$$

and we have

$$\begin{aligned} g_m^2(u) &= \sum_{j=1}^m \left((x_j^{\text{PCA}})^T u \right)^2 \stackrel{\text{Eq. (1.7)}}{=} z^2 \cdot \sum_{j=1}^m \left(\frac{w_j^T \cdot \Sigma}{\sqrt{w_j^T \Sigma w_j}} \cdot u \right)^2 \\ &\stackrel{\text{Eq. (1.31)}}{=} z^2 \cdot \sum_{j=1}^m \left(\frac{w_j^T \cdot \Sigma}{\sqrt{w_j^T \Sigma w_j}} \cdot \sum_{i=1}^m \lambda_i w_i \right)^2 = z^2 \cdot \sum_{i,j=1}^m \lambda_i^2 \cdot \left(\frac{w_j^T \cdot \Sigma \cdot w_i}{\sqrt{w_j^T \Sigma w_j}} \right)^2 \\ &\stackrel{\text{Eq. (1.6)}}{=} z^2 \cdot \sum_{i=1}^m \lambda_i^2 \cdot \left(\frac{w_i^T \cdot \Sigma \cdot w_i}{\sqrt{w_i^T \Sigma w_i}} \right)^2 = z^2 \cdot \sum_{i=1}^m \lambda_i^2 \cdot w_i^T \cdot \Sigma \cdot w_i \\ &\stackrel{\text{Eq. (1.31)}}{=} z^2 \cdot u^T \cdot \Sigma \cdot u \stackrel{\text{Eq. (1.30)}}{=} f^2(u) \end{aligned}$$

By definition in lines (3.10) and (1.30), $g_m(u) \geq 0$ and $f(u) \geq 0$. Therefore, $g_m^2(u) = f^2(u)$ implies $g_m(u) = f(u)$. For $u_{\text{initial}} \in \text{span}\{w_1, \dots, w_m\}$, the statements about (QC1) and (QC3) thus follow immediately.

1.8.1.3 Proof of Lemma 1.1

With assumption (A), the second equation of (1.10) holds because the differential operator is linear. $\langle \cdot, \cdot \rangle_H$ defines a symmetric bilinear form, since we have for all $w_1, w_2, w_3 \in U$ and all $\lambda \in \mathbb{R}$: (i) $\langle w_1, w_2 \rangle_H = w_1^\top H w_2 = w_2^\top H w_1 = \langle w_2, w_1 \rangle_H$ due to the symmetry of H ; (ii) $\langle w_1 + w_2, w_3 \rangle_H = (w_1 + w_2)^\top H w_3 = w_1^\top H w_3 + w_2^\top H w_3 = \langle w_1, w_3 \rangle_H + \langle w_2, w_3 \rangle_H$; (iii) $\langle \lambda \cdot w_1, w_2 \rangle_H = (\lambda \cdot w_1)^\top H w_2 = \lambda \cdot w_1^\top H w_2 = \lambda \cdot \langle w_1, w_2 \rangle_H$.

1.8.1.4 Proof of Lemma 1.2

We have

$$\begin{aligned} \left((x_j^{\text{OCS}})^\top u \right)^2 &\stackrel{\text{Eq. (1.14)}}{=} \left(\left(\frac{H w_j}{\sqrt{2 w_j^\top H w_j}} \right)^\top u \right)^2 = \frac{1}{2 w_j^\top H w_j} \cdot (w_j^\top H u)^2 = \frac{(\langle w_j, u \rangle_H)^2}{2 \langle w_j, w_j \rangle_H} \\ &= \frac{(\langle w_j, u \rangle_H)^2}{2 (\langle w_j, w_j \rangle_H)^2} \cdot w_j^\top H w_j = 0.5 \cdot \left(\frac{\langle w_j, u \rangle_H}{\langle w_j, w_j \rangle_H} \cdot w_j \right)^\top H \left(\frac{\langle w_j, u \rangle_H}{\langle w_j, w_j \rangle_H} \cdot w_j \right) \\ &\stackrel{\text{Eq. (1.12)}}{=} 0.5 \tilde{u}_j^\top H \tilde{u}_j \end{aligned}$$

1.8.1.5 Proof of Theorem 1.1

By definition in lines (3.10) and (1.9), $g_m(u) \geq 0$ and $g_{\text{Taylor}}(u) \geq 0$ for all $u \in U$. Hence, Eq. (1.16) implies $g_m(u) = g_{\text{Taylor}}(u)$ for all $u \in \text{span}\{w_1, \dots, w_m\}$. This implies (QC1). According to Theorem 1 from Paulusch and Schlütter (2022), $g_{\text{Taylor}}(u)$ satisfies (QC2) and (QC3) with $V_1 = V_2 = \mathbb{R}^n$. Since $g_m(u) = g_{\text{Taylor}}(u)$ for $u \in \text{span}\{w_1, \dots, w_m\}$, we can conclude that (QC3) holds with $V_2 = \text{span}\{w_1, \dots, w_m\}$. Focusing on (QC2), we calculate with the definition of OCS in Eq. (1.14) in connection with Eq. (3.10)

$$g_m^2(u) = \sum_{i=1}^m \left((x_i^{\text{OCS}})^\top u \right)^2 = \sum_{i=1}^m \left(\frac{w_i^\top H u}{\sqrt{2 w_i^\top H w_i}} \right)^2$$

The gradient of $g_m^2(u)$ evaluated at u_{initial} is obtained as

$$\nabla_u g_m^2(u_{\text{initial}}) = 2 \cdot \sum_{i=1}^m \frac{w_i^\top H u_{\text{initial}}}{2 w_i^\top H w_i} \cdot w_i^\top H$$

Given that $u_{\text{initial}} \in \text{span}\{w_1, \dots, w_m\}$, we can write analogously to Eq. (1.11)

$$u_{\text{initial}} = \sum_{j=1}^m \frac{\langle w_j, u_{\text{initial}} \rangle_H}{\langle w_j, w_j \rangle_H} \cdot w_j \tag{1.32}$$

Noting that $w_i H w_j = 0$ for all $i \neq j$, we have

$$\begin{aligned} \nabla_u g_m^2(u_{\text{initial}}) &= \sum_{i,j=1}^m \frac{\langle w_j, u_{\text{initial}} \rangle_H}{\langle w_j, w_j \rangle_H} \frac{w_i^T H w_j}{w_i^T H w_i} \cdot w_i^T H = \sum_{i=1}^m \frac{\langle w_i, u_{\text{initial}} \rangle_H}{\langle w_i, w_i \rangle_H} \cdot w_i^T H \\ &= u_{\text{initial}}^T H \stackrel{\text{Eq. (1.8)}}{=} \nabla_u P_{f^2}(u_{\text{initial}}) \end{aligned} \quad (1.33)$$

According to Assumption (A), $f(u) > 0$ in an environment of u_{initial} . Therefore, line (1.33) implies

$$\nabla_u g_m(u_{\text{initial}}) = \nabla_u g_{\text{Taylor}}(u_{\text{initial}}) = \nabla_u f(u_{\text{initial}}), \quad (1.34)$$

where the last equality follows from Theorem 1 of Paulusch and Schlütter (2022).

1.8.1.6 Proof of Corollary 1.1

We have

$$\begin{aligned} x^{\text{grad}} &= \nabla_u f(u_{\text{initial}}) \stackrel{\text{Eq. (1.34)}}{=} \nabla_u g_m(u_{\text{initial}}) \stackrel{\text{Eq. (1.9)}}{=} \nabla_u \sqrt{0.5 u^T H u} \Big|_{u=u_{\text{initial}}} \\ &= \frac{H u_{\text{initial}}}{\sqrt{2 u_{\text{initial}}^T H u_{\text{initial}}}} \stackrel{\text{Eq. (1.14)}}{=} x_1^{\text{OCS}} \end{aligned}$$

where the last equation uses $w_1 = u_{\text{initial}}$.

1.8.1.7 Proof of Corollary 1.2

For all $j = 1, \dots, m$, we have

$$\begin{aligned} (x_j^{\text{OCS}})^T H^{-1} x_j^{\text{OCS}} &\stackrel{\text{Eq. (1.14)}}{=} \frac{1}{2 w_j^T H w_j} \cdot w_j^T H^T H^{-1} H w_j \\ &\stackrel{H \text{ is symmetric}}{=} \frac{1}{2 w_j^T H w_j} \cdot w_j^T H w_j = 0.5 \end{aligned}$$

1.8.1.8 Proof of Corollary 1.3

w_1 and w_2 , as defined, are orthogonal in the sense of $\langle \cdot, \cdot \rangle_H$, since

$$w_1^T H w_2 = (1, 0) \cdot \begin{pmatrix} 0 \\ -h_{12}^2/h_{11} + h_{22} \end{pmatrix} = 0$$

Inserting w_2 into Eq. (1.14) implies

$$x_2^{\text{OCS}} = \frac{1}{\sqrt{2(h_{22} - h_{12}^2/h_{11})}} \begin{pmatrix} 0 \\ h_{22} - h_{12}^2/h_{11} \end{pmatrix} = \frac{1}{\sqrt{2}} \begin{pmatrix} 0 \\ \sqrt{h_{22} - h_{12}^2/h_{11}} \end{pmatrix} \quad (1.35)$$

Corollary 1.1 implies $\nabla_u f(u_{\text{initial}}) = x_1^{\text{OCS}}$ and Eq. (1.4) implies

$$f(u_{\text{initial}}) = (\nabla_u f(u_{\text{initial}}))^{\text{T}} \cdot u_{\text{initial}} = (x_1^{\text{OCS}})^{\text{T}} \cdot u_{\text{initial}} = x_{11}^{\text{OCS}} \quad (1.36)$$

Let $H_g(u)$ and $H_{g^2}(u)$ denote the Hessian matrices of functions $g(u)$ and $g^2(u)$ evaluated at u . The chain rule and product rule for multivariate functions imply

$$\begin{aligned} H_{g^2}(u_{\text{initial}}) &= \nabla_u \left[2g(u) (\nabla_u g(u))^{\text{T}} \right] \Big|_{u=u_{\text{initial}}} \\ &= 2\nabla_u g(u) (\nabla_u g(u))^{\text{T}} + 2g(u) H_g(u) \Big|_{u=u_{\text{initial}}} \\ \Leftrightarrow H_g(u_{\text{initial}}) &= \frac{1}{g(u)} \left(0.5H_{g^2}(u) - \nabla_u g(u) (\nabla_u g(u))^{\text{T}} \right) \Big|_{u=u_{\text{initial}}} \\ \stackrel{\text{Theorem 1.1}}{\Leftrightarrow} H_f(u_{\text{initial}}) &= \frac{1}{f(u)} \left(0.5H - \nabla_u f(u) (\nabla_u f(u))^{\text{T}} \right) \Big|_{u=u_{\text{initial}}} \\ &\stackrel{\text{Eq. (1.36)}}{=} \frac{1}{x_{11}^{\text{OCS}}} \left(0.5H - x_1^{\text{OCS}} (x_1^{\text{OCS}})^{\text{T}} \right) \end{aligned} \quad (1.37)$$

Inserting $w_1 = (1, 0)^{\text{T}}$ into Eq. (1.36) provides

$$\begin{aligned} x_1^{\text{OCS}} (x_1^{\text{OCS}})^{\text{T}} &= \frac{1}{2w_1^{\text{T}} H w_1} H w_1 (H w_1)^{\text{T}} = \frac{1}{2h_{11}} \begin{pmatrix} h_{11} \\ h_{12} \end{pmatrix} (h_{11}, h_{12}) \\ &= \frac{1}{2} \begin{pmatrix} h_{11} & h_{12} \\ h_{12} & h_{12}^2/h_{11} \end{pmatrix} \end{aligned} \quad (1.38)$$

Inserting line (1.38) into (1.37) implies that entry (2,2) of $H_f(u_{\text{initial}})$ is

$$\frac{1}{2x_{11}^{\text{OCS}}} (h_{22} - h_{12}^2/h_{11}) \stackrel{\text{Eq. (1.35)}}{=} \frac{(x_{21}^{\text{OCS}})^2}{x_{11}^{\text{OCS}}}$$

and that all other entries of $H_f(u_{\text{initial}})$ are zero.

1.8.1.9 Proof of Proposition 1.3

a. Line (1.30) implies $f^2(u) = z^2 \cdot u^{\text{T}} \Sigma u$ and $H = \nabla_u (z^2 \cdot 2\Sigma u) \Big|_{u=u_{\text{initial}}} = 2z^2 \Sigma$.

b. Starting from the definition in line (1.14) and using assertion a., we have

$$x_j^{\text{OCS}} = \frac{H w_j}{\sqrt{2w_j^{\text{T}} H w_j}} = \frac{2z^2 \Sigma w_j}{\sqrt{2w_j^{\text{T}} 2z^2 \Sigma w_j}} = \frac{\Sigma w_j}{\sqrt{w_j^{\text{T}} \Sigma w_j}} \cdot z = x_j^{\text{PCA}}$$

c. To identify w_1 , we can neglect condition $\langle u, w_i \rangle_H = 0$ in U_{\perp} from Eq. (1.19), since there are no formerly selected w_i . Then, the eigenvector of Σ relating to its largest eigenvalue solves Eq. (1.21) noting that $g_{\text{Taylor}}^2(u) = z^2 u^{\text{T}} \Sigma u$. Due to $H = 2z^2 \Sigma$, the eigenvalues of Σ are a multiple of those of H , and the two matrices' eigenvectors coincide. With vectors

w_1, \dots, w_m being identified as eigenvectors corresponding to the m largest eigenvalues, the columns of matrix M in Appendix 1.8.2 can be set to the eigenvectors relating to the other positive eigenvalues of Σ . Therefore, $\Lambda = M^T H M$ includes the remaining eigenvalues of H . Since $M^T M$ is the identity matrix of dimension $\tilde{n} - m$, the smallest eigenvalue of $\Lambda^{-0.5} M^T M \Lambda^{-0.5}$ is the inverse of the largest eigenvalue of H , say λ_{\max}^{-1} . w_{m+1} from Eq. (1.41) is the corresponding eigenvector of Σ , since

$$w_{m+1}^T \Sigma w_{m+1} = \frac{w_{m+1}^T H w_{m+1}}{2z^2} = \frac{s^T \Lambda^{-0.5} M^T H M \Lambda^{-0.5} s}{2z^2 s^T \Lambda^{-0.5} M^T M \Lambda^{-0.5} s} = \frac{s^T s}{2z^2 \lambda_{\max}^{-1}} = \frac{\lambda_{\max}}{2z^2}$$

d. With $z = 1$, the conditions in lines (1.22) and (1.23) are equivalent, since $v^T H^{-1} v \leq 0.5 \Leftrightarrow v^T (2\Sigma)^{-1} v \leq 0.5 \Leftrightarrow v^T \Sigma^{-1} v \leq 1$.

e. With assertion b. and $w_1 = u_{\text{initial}}$, noting that Corollary 1.1 implies $x_1^{\text{OCS}} = x_1^{\text{grad}}$ and using Eq. (1.30), we have

$$\frac{x_{1j}^{\text{OCS}}}{f(u_{\text{initial}})} = \frac{\left(\frac{\Sigma w_1}{\sqrt{w_1^T \Sigma w_1}} \cdot z \right)_j}{z \cdot \sqrt{u_{\text{initial}}^T \Sigma u_{\text{initial}}}} = \frac{\Sigma_{j \cdot} \cdot u_{\text{initial}}}{u_{\text{initial}}^T \Sigma u_{\text{initial}}} = \frac{\text{cov}(X_j, \mathbf{X}^T \cdot u_{\text{initial}})}{\text{var}(\mathbf{X}^T \cdot u_{\text{initial}})} = \beta_j$$

1.8.2 Lagrange procedure for OCS selection

We start with the Lagrangian for identifying w_{m+1} , i.e.

$$L_1(w, \gamma_0, \gamma_1, \dots, \gamma_m) = g_{\text{Taylor}}(\tilde{u} + w) - g_m(\tilde{u} + w) + \gamma_0 \cdot (w^T w - 1) + \sum_{i=1}^m \gamma_i \cdot w_i^T H w$$

In this Lagrangian, we can omit the term $g_m(\tilde{u} + w)$, since it vanishes in the first-order condition: for any $w \in U_{\perp}$, we have $g_m(\tilde{u} + w) = g_m(\tilde{u})$, and hence $\nabla_w g_m(\tilde{u} + w) = 0$. Since the target function $g_{\text{Taylor}}(\tilde{u} + w)$ is non-negative, we can replace it with its square and rewrite

$$\begin{aligned} g_{\text{Taylor}}^2(\tilde{u} + w) &= 0.5 \cdot (\tilde{u} + w)^T H (\tilde{u} + w) = 0.5 \cdot (\tilde{u}^T H \tilde{u} + 2\tilde{u}^T H w + w^T H w) \\ &= 0.5 \tilde{u}^T H \tilde{u} + 0.5 w^T H w \end{aligned}$$

Omitting the constant term and the factor 0.5, the target function becomes $w^T H w$.

Let $\tilde{n} \leq n$ denote the rank of H . We assume that $m < \tilde{n}$, since Theorem 1 otherwise implies that there is no remaining error part 2. Define a matrix $M \in \mathbb{R}^{n \times (\tilde{n} - m)}$ with $\text{rank}(HM) = \tilde{n} - m$, $Mv \in U_{\perp}$ for all $v \in \mathbb{R}^{\tilde{n} - m}$ and the columns of M being orthogonal in the sense of $\langle \cdot, \cdot \rangle_H$. To ensure that $w \in U_{\perp}$, we set $w = Mv$ and identify v maximizing

$g_{\text{Taylor}}^2(Mv)$ using the simpler Lagrangian

$$L_2(v, \gamma) = v^T M^T H M v + \gamma (v^T M^T M v - 1) \quad (1.39)$$

We define $\Lambda = M^T H M$, which by construction is a diagonal matrix with all diagonal elements being positive, since $\text{rank}(HM) = \tilde{n} - m$ and H is positive semidefinite. Let $\lambda_1, \dots, \lambda_{\tilde{n}-m}$ denote the diagonal elements of Λ and let the matrix $\Lambda^{-0.5}$ be a diagonal matrix with diagonal entries $\lambda_1^{-0.5}, \dots, \lambda_{\tilde{n}-m}^{-0.5}$. We substitute $v = \Lambda^{-0.5} s$ and rewrite the Lagrangian in line (1.39) as

$$\begin{aligned} L_2(s, \gamma) &= s^T \Lambda^{-0.5} \Lambda \Lambda^{-0.5} s + \gamma s^T \Lambda^{-0.5} M^T M \Lambda^{-0.5} s \\ &= s^T s + \gamma s^T \Lambda^{-0.5} M^T M \Lambda^{-0.5} s \end{aligned}$$

The first-order condition of maximizing $L_2(s, \gamma)$ includes

$$\nabla_s L_2(s, \gamma) = 2s + 2\gamma \Lambda^{-0.5} M^T M \Lambda^{-0.5} s = 0 \quad (1.40)$$

which is satisfied if s is an eigenvector of $\Lambda^{-0.5} M^T M \Lambda^{-0.5}$. We select s relating to the smallest eigenvalue of $\Lambda^{-0.5} M^T M \Lambda^{-0.5}$. Finally, we determine portfolio w_{m+1} with the largest approximation error and satisfying $\|w_{m+1}\|_2 = 1$ as

$$w_{m+1} = \frac{1}{\sqrt{s^T \Lambda^{-0.5} M^T M \Lambda^{-0.5} s}} \cdot M \Lambda^{-0.5} s \quad (1.41)$$

Scenario w_{m+2} can immediately be identified by inserting the eigenvector relating to the second smallest eigenvalue into line (1.41) and so on.

1.8.3 Asset selection

Consider an investor with initial wealth w_0 who selects the portfolio weight α of a capital asset I with stochastic return r_I and invests $1 - \alpha$ into the market portfolio with stochastic return r_M . Portfolio risk is measured analogous to line (1.2). Based on α , the function is

$$\tilde{f}(\alpha) = \varrho(w_0 \cdot (\alpha \cdot r_I + (1 - \alpha) \cdot r_M)) - \mathbb{E}(w_0 \cdot (\alpha \cdot r_I + (1 - \alpha) \cdot r_M)) \quad (1.42)$$

With $X_1 = w_0 \cdot r_M$, $X_2 = w_0 \cdot r_I$ and $u_{\text{initial}} = (1, 0)^T$, define x_i^{OCS} as in Corollary 1.3. For general distributions of returns, OCS explain how adding asset I to the portfolio affects

portfolio risk:

$$\tilde{f}(0) = x_{11}^{\text{OCS}} \quad (1.43)$$

$$\frac{\partial}{\partial \alpha} \tilde{f}(0) = x_{12}^{\text{OCS}} - x_{11}^{\text{OCS}} \quad (1.44)$$

$$\frac{\partial^2}{\partial \alpha^2} \tilde{f}(0) = \frac{(x_{22}^{\text{OCS}})^2}{x_{11}^{\text{OCS}}} \quad (1.45)$$

Assume now that the returns r_M and r_I jointly follow a normal distribution with standard deviations σ_M and σ_I and correlation ρ . Let ϱ be the Value-at-Risk with confidence level ζ and z_ζ denote the ζ -percentile of the standard normal distribution. We can then specify Equations (1.43), (1.44) and (1.45) as

$$\tilde{f}(0) = x_{11}^{\text{OCS}} = z_\zeta \cdot w_0 \cdot \sigma_M \quad (1.46)$$

$$\frac{\partial}{\partial \alpha} \tilde{f}(0) = x_{11}^{\text{OCS}} \cdot \frac{x_{12}^{\text{OCS}} - x_{11}^{\text{OCS}}}{x_{11}^{\text{OCS}}} = x_{11}^{\text{OCS}} \cdot (\beta_I - 1) \quad (1.47)$$

$$\frac{\partial^2}{\partial \alpha^2} \tilde{f}(0) = x_{11}^{\text{OCS}} \cdot \sigma_I^2 / \sigma_M^2 \cdot (1 - \rho^2) \quad (1.48)$$

According to line (1.47), the classical CAPM-beta, $\beta_I = \text{cov}(r_I, r_M) / \text{var}(r_M)$, reflects the first-order derivative of the portfolio Value-at-Risk with respect to adding asset I . Line (1.48) states that convexity is large if the return on asset I has a large standard deviation σ_I and is uncorrelated with the return of the market portfolio. The right part of Figure

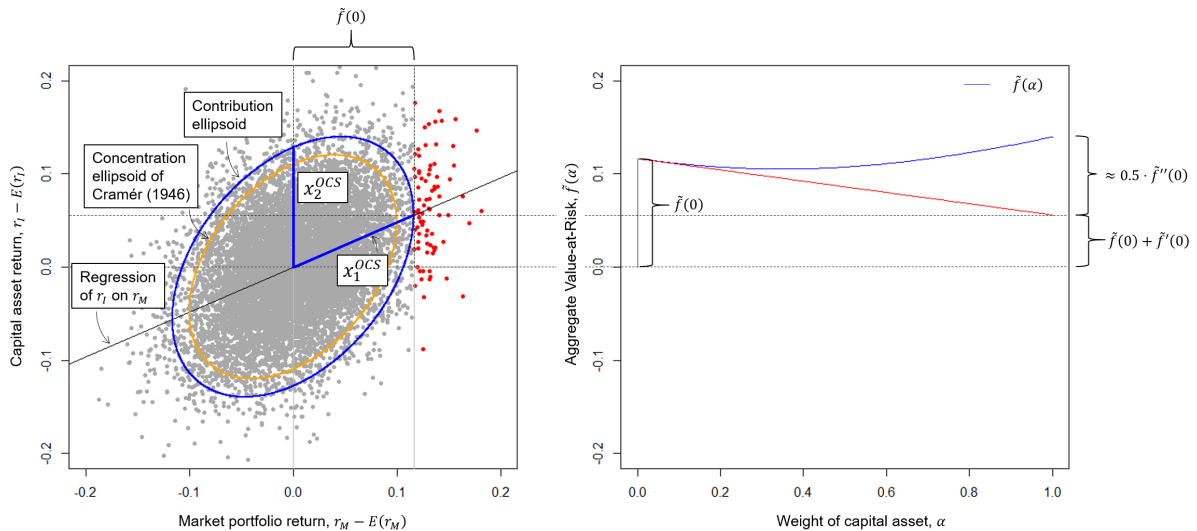


Figure 1.5 Asset selection with normally distributed returns. Left-hand side: scatter plot of asset I 's returns vs. market portfolio returns together with ellipsoids, linear regression and OCS. Right part: Portfolio Value-at-Risk according to true risk measurement, $\tilde{f}(\alpha)$, (blue curve) and first-order approximation of $\tilde{f}(\alpha)$ at $\alpha = 0$ (red line).

1.5 depicts function $\tilde{f}(\alpha)$ for normally distributed returns with $w_0 = 1$,²⁰ $\sigma_M = 0.05$, $\sigma_I = 0.06$, $\rho = 0.4$ and $\zeta = 99\%$. In $\alpha = 0$, $\tilde{f}(\alpha)$ decreases, since marginally adding asset I improves portfolio diversification. For larger α -values, the portfolio becomes more concentrated in risks of asset I , and hence $\tilde{f}(\alpha)$ increases. The left part of Figure 1.5 shows both OCS in a scatter plot of 10,000 realizations of unexpected returns, i.e. $r_I - E(r_I)$ vs. $r_M - E(r_M)$. Realizations are colored in red if the market portfolio experiences a loss beyond the 99% Value-at-Risk and gray otherwise.

There are clear connections between the two parts of the Figure: The x-coordinate of \tilde{x}_1^{OCS} is the portfolio Value-at-Risk for w_0 being invested completely in the market portfolio. The y-coordinate of \tilde{x}_1^{OCS} provides an assessment of $\tilde{f}(1)$ in the sense of a linear approximation starting at $\alpha = 0$ (cf. the red line on the right side of Figure 1.5). The y-coordinate of \tilde{x}_2^{OCS} translates via Eq. (1.45) into the convexity $\tilde{f}''(0) = (x_{22}^{OCS})^2 / x_{11}^{OCS} = 0.128^2 / 0.116 = 0.1407$.

²⁰Thanks to $w_0 = 1$, the left part of Figure 1.5 plots the unexpected returns; for general values of w_0 , we had to plot realizations of $X_i - E(X_i) = w_i \cdot r_i$ for $i \in \{I, M\}$.

References

- Aven, T., 2016. Risk assessment and risk management: Review of recent advances on their foundation. *European Journal of Operational Research* 253, 1–13.
- Breuer, T., Csiszár, I., 2013. Systematic stress tests with entropic plausibility constraints. *Journal of Banking & Finance* 37, 1552–1559.
- Buch, A., Dorfleitner, G., Wimmer, M., 2011. Risk capital allocation for RORAC optimization. *Journal of Banking & Finance* 35, 3001–3009.
- Christensen, J.H., Rudebusch, G.D., 2015. Estimating shadow-rate term structure models with near-zero yields. *Journal of Financial Econometrics* 13, 226–259.
- Clay, D., Lay, S.R., McDonald, J.J., 2015. *Linear Algebra and Its Applications*, 5th Edition. Pearson.
- Cramér, H., 1946. A contribution to the theory of statistical estimation. *Scandinavian Actuarial Journal* 1946, 85–94.
- Darmois, G., 1945. Sur les limites de la dispersion de certaines estimations. *Revue de l'Institut International de Statistique*, 9–15.
- Eling, M., Schmeiser, H., 2010. Insurance and the credit crisis: Impact and ten consequences for risk management and supervision. *The Geneva Papers on Risk and Insurance—Issues and Practice* 35, 9–34.
- Erel, I., Myers, S.C., Read Jr, J.A., 2015. A theory of risk capital. *Journal of Financial Economics* 118, 620–635.
- Financial Stability Board, 2013. *Principles for an effective risk appetite framework. Consultative Document*.
- Frye, J., 1997. Principals of risk: Finding var through factor-based interest rate scenarios, in: *VAR: Understanding and Applying Value at Risk*. Risk Publications, London, pp. 275–288.

- Golub, B.W., Tilman, L.M., 1997. Measuring yield curve risk using principal components analysis, value at risk, and key rate durations. *Journal of Portfolio Management* 23, 72.
- Gómez, F., Tang, Q., Tong, Z., 2022. The gradient allocation principle based on the higher moment risk measure. *Journal of Banking & Finance* 143, 106544.
- Gourieroux, C., Laurent, J.P., Scaillet, O., 2000. Sensitivity analysis of values at risk. *Journal of Empirical Finance* 7, 225–245.
- Gribkova, N., Su, J., Zitikis, R., 2022. Inference for the tail conditional allocation: large sample properties, insurance risk assessment, and compound sums of concomitants. *Insurance: Mathematics and Economics* 107, 199–222.
- Gründl, H., Schmeiser, H., 2007. Capital allocation for insurance companies—what good is it? *Journal of Risk and Insurance* 74, 301–317.
- Hong, L.J., Liu, G., 2009. Simulating sensitivities of conditional value at risk. *Management Science* 55, 281–293.
- Hull, J.C., 2018. *Risk Management and Financial Institutions*. Wiley Finance Series. 5th Edition.
- Jorion, P., 2006. *Value at risk: The new benchmark for managing financial risk*. New York: McGraw–Hill .
- Lintner, J., 1965. Security prices, risk, and maximal gains from diversification. *The Journal of Finance* 20, 587–615.
- McNeil, A.J., Frey, R., Embrechts, P., 2015. *Quantitative Risk Management: Concepts, Techniques and Tools - Revised Edition*. Princeton Series in Finance.
- McNeil, A.J., Smith, A.D., 2012. Multivariate stress scenarios and solvency. *Insurance: Mathematics and Economics* 50, 299–308.
- Mildenhall, S.J., 2004. A note on the myers and read capital allocation formula. *North American Actuarial Journal* 8, 32–44.

- Mossin, J., 1966. Equilibrium in a capital asset market. *Econometrica: Journal of the Econometric Society* , 768–783.
- Myers, S.C., Read, J.A., 2001. Capital allocation for insurance companies. *Journal of Risk and Insurance* 68, 545–580.
- Nordström, K., 1991. The concentration ellipsoid of a random vector revisited. *Econometric Theory* 7, 397–403.
- Panjer, H.H., 2002. Measurement of risk, solvency requirements and allocation of capital within financial conglomerates. Institute of Insurance and Pension Research, University of Waterloo, Research Report , 01–15.
- Paulusch, J., 2017. The Solvency II standard formula, linear geometry, and diversification. *Journal of Risk and Financial Management* 10, 11.
- Paulusch, J., Schlütter, S., 2022. Sensitivity-implied tail-correlation matrices. *Journal of Banking & Finance* 134, 106333.
- Rockafellar, R.T., Uryasev, S., et al., 2000. Optimization of conditional value-at-risk. *Journal of Risk* 2, 21–42.
- Rosenberg, J.V., Schuermann, T., 2006. A general approach to integrated risk management with skewed, fat-tailed risks. *Journal of Financial Economics* 79, 569–614.
- Schilling, K., Bauer, D., Christiansen, M.C., Kling, A., 2020. Decomposing dynamic risks into risk components. *Management Science* 66, 5738–5756.
- Schlütter, S., 2021. Scenario-based measurement of interest rate risks. *The Journal of Risk Finance* 22 No. 1, 56–77.
- Sharpe, W.F., 1964. Capital asset prices: A theory of market equilibrium under conditions of risk. *The Journal of Finance* 19, 425–442.
- Stulz, R.M., 2008. Risk management failures: What are they and when do they happen? *Journal of Applied Corporate Finance* 20, 39–48.
- Tasche, D., 2008. Capital allocation to business units and sub-portfolios: The Euler principle, in: Resti, A. (Ed.), *Pillar II in the New Basel Accord: The Challenge of Economic Capital*. Risk Books, London, pp. 423–453.

Wilson, T.C., 2015. Value and Capital Management: A Handbook for the Finance and Risk Functions of Financial Institutions, 1st Edition. Wiley.

Zanjani, G., 2002. Pricing and capital allocation in catastrophe insurance. *Journal of Financial Economics* 65, 283–305.

Chapter 2

Identifying Scenarios for the Own Risk and Solvency Assessment of Insurance Companies^{*}

Abstract

Most insurers in the European Union determine their regulatory capital requirements based on the standard formula of Solvency II. However, there is evidence that the standard formula inaccurately reflects insurers' risk situation and may provide misleading steering incentives. In the second pillar, Solvency II requires insurers to perform a so-called "Own Risk and Solvency Assessment" (ORSA). In their ORSA, insurers must establish their own risk measurement approaches, including those based on scenarios, in order to derive suitable risk assessments and address shortcomings of the standard formula. The idea of this paper is to identify scenarios in such a way that the standard formula in connection with the ORSA provides a reliable basis for risk management decisions. Using an innovative method for scenario identification, our approach allows for a simple but relatively precise assessment of marginal and even non-marginal portfolio changes. We numerically evaluate the proposed approach in the context of market risk employing an internal model from the academic literature and the Solvency Capital Requirement (SCR) calculation under Solvency II.

JEL classification: G22, G28, G32.

Keywords: Risk measurement, Enterprise Risk Management, Own Risk and Solvency Assessment, Solvency II

^{*}Earlier versions of this paper were presented at the annual meeting of the DVfVW 2022, the International Congress of Insurance: Mathematics and Economics 2022 and the ARIA annual meeting 2022.

2.1 Introduction

Even in modern regulation systems such as Solvency II, the majority of insurance companies determine their capital requirements using a pre-specified standard formula rather than a self-developed internal risk capital model.¹ However, various academic papers show that the risk landscape may not be realistically depicted on the basis of such a standardized approach, which can lead to incorrect steering incentives when portfolio decisions are made. A relatively well known deficiency of the Solvency II standard formula is that it disregards credit risks of any government counterparties in the European Economic Area (EEA) or the Organisation for Economic Co-operation and Development (OECD).² Gatzert and Martin (2012), for instance, identify this problem and show that there is a gap between the results of an internal risk model and those of the standard formula in the context of market risks. Becker and Ivashina (2015) find empirical evidence that regulatory constraints on insurance companies investing in the corporate bond market can lead to portfolio distortions. Chen et al. (2019) find that relying on the square root rule for the calculation of risk-based capital (RBC) may provide a misleading view of changing diversification effects. In the case of equity risk, Fischer and Schlütter (2015) show that insurers' asset selection is highly sensitive to parameters of the standard formula and can end up too risky or conservative. Braun et al. (2017) find that the standard formula is likely to have an adverse impact on life insurers' asset allocation, as it hinders insurers in selecting an efficient investment portfolio. Furthermore, Pfeifer and Strassburger (2008) provide evidence that for several classes of distributions, the standard formula underestimates the true Solvency Capital Requirements (SCR). A more general criticism regarding the regulatory framework is formulated by Scherer and Stahl (2021), stating that the Solvency II standard formula "lacks sound economic and mathematical reasoning". A mitigation of the standard formula's deficiencies could potentially be offered by second pillar requirements. These requirements aim to improve insurers' Enterprise Risk Management and to this end require — in addition to the standard formula — stress tests and scenario analyses. These approaches aim to extend the regulatory risk measurement "in order to provide an adequate basis for the assessment of the overall solvency

¹For instance, the European Insurance and Occupational Pensions Authority (EIOPA) states in their annual Insurance Statistics report regarding the own funds, cf. EIOPA (2019), that 2,470 of the 2,658 insurers evaluated base their risk calculations on the standard formula provided by Solvency II.

²Cf. BaFin (2016).

needs”, cf. EIOPA (2015), Guideline 7. Similarly, the requirements for the Own Risk and Solvency Assessment (ORSA) of an insurer expect to “also take into account risks that are not or not adequately included in the standard formula, and must develop a suitable assessment procedure for them”, cf. BaFin (2016).

In general, stress scenarios are a tool to “help decision makers understand better the level of resilience of the organization”, cf. Albrecher et al. (2018, Chapter 5.5). In the literature, there are several different suggestions on how to identify (reverse) stress scenarios by stressing the underlying distribution of risk drivers: for example, Korn and Müller (2021) apply the worst-case scenario in the setting of a portfolio optimization. Pesenti et al. (2019) employ the Kullback-Leibler divergence measure, Makam et al. (2021) use the χ^2 divergence considering a discrete sample to derive stress scenarios. Breuer and Csiszár (2013) suggest identifying stress scenarios by using a relative entropy measure to ensure plausibility. However, they do not address the ORSA requirements explicitly to quantify scenarios that are not captured by the standard formula. A different idea more in line with the ORSA requirements is provided by McNeil and Smith (2012), proposing the so-called “least solvent likely event” (LSLE), a deterministic scenario that allows for a reliable evaluation of risk resulting from a given portfolio.³

This paper proposes a new approach to identify ORSA scenarios. We assume that the insurer’s strategy can be expressed by an exposure vector $u \in R^n$. The entries of u can represent, for example, investments in asset categories or sizes of the insurer’s lines of business. Corresponding to strategy u , the function $f^{\text{true}}(u)$ provides the capital requirement which satisfies the safety level defined in pillar 1 (i.e. the 99.5% Value-at-Risk). $f^{\text{true}}(u)$ can be considered as the outcome of a perfect internal model. Function $f^{\text{SF}}(u)$ presents the capital requirement according to the standard formula. Our target is to identify scenarios which approximate the residual

$$f^{\text{true}}(u) - f^{\text{SF}}(u) \tag{2.1}$$

To this end, we consider $g_m(u)$ as the risk measurement of strategy u based on m scenarios. If $g_m(u)$ approximates the residual in (2.1), then the standard formula in connection with

³Notably, McNeil and Smith (2012, Corollary 4.4) show that their suggestion coincides with the so-called “gradient scenario”, which is often also referred to as Euler allocation, cf. for instance Tasche (2008).

ORSA scenarios provides an approximation of the true risk:

$$f^{\text{true}}(u) \approx f^{\text{SF}}(u) + g_m(u) \quad (2.2)$$

Our technical basis to derive scenarios for function $g_m(u)$ are so-called “orthogonal convexity scenarios” (OCS) as proposed by Aigner and Schlütter (2022). The aim of OCS is to translate the risk measurement of a portfolio into a small number of multivariate realization vectors. In contrast to the aforementioned stress scenario literature, OCS therefore do not change the risk distribution. By construction, OCS are orthogonal in the sense of sensitivity-implied tail correlations, as proposed by Paulusch and Schlütter (2022), and hence their use is not limited to elliptical distributions. Additionally, by employing deterministic scenarios, a combination with the standard formula leads to a deterministic risk measurement in the right-hand side of Eq. (2.2). We show that such a combination with only a single OCS can then be set to reflect the outcome of the internal model for the initial portfolio as well as all first-order derivatives. The approach thus coincides with the well known Euler capital allocation.⁴ When additional scenarios are taken into account, second-order derivatives are also reflected correctly. By approximating the internal model not only in a linear way, the scenarios reflect how portfolio-wide diversification effects alter when the portfolio volumes are changed. Deriving scenarios for a representative insurer could thereby provide a regulatory authority with a tool that can be handed out to insurance companies as an addition to the standard formula.

Numerically, the suggestion is evaluated based on Gatzert and Martin (2012) and Eckert et al. (2016) dealing with market risks. In the latter, the authors employ an internal model which comprises the risks of three sub-modules, the outcome of which is considered as the true portfolio risk. A difference in risk capital between the internal model and the standard formula is found, providing a good starting point for the scenario-based extension of the regulatory approach.

This article contributes to the literature in three ways: Firstly, it highlights the shortcomings of a standardized approach to risk measurement. Secondly, a practical idea is presented on how to formalize and implement the suggestions of the ORSA. Thirdly, empirical indications are given as to what meaningful scenarios in the sense of the ORSA might look like for an example company.

⁴Cf. for instance Tasche (2008), Buch et al. (2011), or Guo et al. (2021).

The remainder of this article is structured as follows. section 2.2 presents the ideas of Aigner and Schlütter (2022) for the determination of scenarios. Section 2.3 summarizes the suggestion of Solvency II for the measurement of market risk as well as an internal model counterpart given by Eckert et al. (2016) and Gatzert and Martin (2012). Section 2.4 numerically evaluates the goodness of the suggested extension of the standard formula. Section 2.5 provides concluding remarks about the concrete practical usefulness of the proposed approach.

2.2 Orthogonal convexity scenarios for the ORSA

We suppose that a company’s risk can be specified by inspecting a random vector

$$\mathbf{X} = (X_1, \dots, X_n)^T$$

with X_i modeling the losses (or gains in case of negative values) of the i th risk driver. The X_i could be losses resulting from risks of the various submodules in the standard formula, but they could also be defined at a more granular level. For example, in section 2.3, we will consider the X_i to reflect losses from single equity and bond investments. It is further assumed that the insurer can change its portfolio by linearly scaling the X_i . To this end, we introduce an exposure vector $u \in \mathbb{R}^n$ representing the portfolio volumes. The true risk function can then be defined, in line with Solvency II, as

$$\begin{aligned} f^{\text{true}} : \mathbb{R}^n &\rightarrow \mathbb{R} \\ u &\mapsto \varrho(\mathbf{X}^T u) - \mathbb{E}(\mathbf{X}^T u) \end{aligned} \tag{2.3}$$

with ϱ being a risk measure. For the identification of scenarios later on, it is sufficient to assume that ϱ is homogeneous of degree one and law-invariant. Paulusch (2017) ensures that the common risk measure under Solvency II, the 99.5% Value-at-Risk, fulfills this property. Notably, our method could also be applied in connection with the Expected Shortfall, for example, cf. also Paulusch (2017). The function f^{true} could then be derived from a stochastic model or a “perfect” internal model.

Secondly, we will inspect the regulatory standard formula that measures the risk of portfolio u in terms of

$$f^{\text{SF}} : \mathbb{R}^n \rightarrow \mathbb{R}, u \mapsto f^{\text{SF}}(u) \tag{2.4}$$

which is explicitly specified in the ORSA, cf. EIOPA (2015).⁵ We assume that both functions, $f^{\text{true}}(u)$ and $f^{\text{SF}}(u)$, are twice continuously differentiable in a neighborhood of an initial portfolio u_{initial} . The central concern that we would like to tackle is that $f^{\text{true}}(u)$ and $f^{\text{SF}}(u)$ may deviate, and we will thus inspect and approximate the residual

$$f^{\text{diff}}(u) = f^{\text{true}}(u) - f^{\text{SF}}(u) \quad (2.5)$$

Here, situations that are not captured by the standard formula can be considered. In order to approximate $f^{\text{diff}}(u)$ relying on deterministic scenarios also taking into account tail dependencies, the approach presented by Aigner and Schlütter (2022) will be used.⁶ The authors suggest employing so-called “orthogonal convexity scenarios” (OCS) resulting in a scenario-based risk-measurement function

$$g_m : \mathbb{R}^n \rightarrow \mathbb{R} \quad (2.6)$$

$$u \mapsto \sqrt{\sum_{i=1}^m \left((x_i^{\text{OCS}})^{\text{T}} u \right)^2}$$

with $1 \leq m \leq n$ a pre-specified number of scenarios that should be considered and x_i^{OCS} , $i = 1, \dots, m$, denoting the OCS.⁷ The latter are defined as

$$x_i^{\text{OCS}} = \frac{w_i^{\text{T}} H}{\sqrt{2 \cdot w_i^{\text{T}} H w_i}} \quad (2.7)$$

with weightvectors $w_1, \dots, w_m \in \mathbb{R}^n$ and H the Hessian matrix of $(f^{\text{diff}})^2$.⁸ The weightvectors have to be specified by the user of the method and are supposed to be selected orthogonally in the sense of the bilinearform

$$\langle w_i, w_j \rangle_H = w_i^{\text{T}} H w_j \quad (2.8)$$

⁵Although this paper focuses on the standard formula for insurance companies, the methodology could also be adapted to other models which are to be compared to a benchmark model.

⁶There is some literature dealing with tail dependencies such as Mittnik (2014) and Paulusch and Schlütter (2022).

⁷These scenarios can be understood as realizations of the risk vector \mathbf{X} in Eq. (2.9).

⁸Appendix 2.6.2 highlights how to calibrate the Hessian matrix.

with H as before. Appendix 2.6.3 provides some guidance on how to identify the necessary weightvectors. Explicitly, it can be ensured that

$$x_1^{\text{OCS}} = \nabla_u f^{\text{diff}}(u_{\text{initial}})$$

such that the first scenario coincides with the Euler allocation of f^{diff} . The OCS approach can also be interpreted as an extension of the "Least solvent likely event" (LSLE) introduced by McNeil and Smith (2012) by including additional scenarios that can capture the convexity of the approximated risk measurement.

By basing the identification of the scenarios on the Hessian matrix, the function g_m is capable of capturing non-linear dependencies and heavy tails in the portfolio as outlined by Paulusch and Schlütter (2022).⁹ When now approximating $f^{\text{true}}(u)$ by the sum $f^{\text{SF}}(u) + g_m(u)$, it fulfills the properties summarized in Proposition 2.1.

Proposition 2.1. Let $1 \leq m \leq n$, $f^{\text{true}}(u)$ and $f^{\text{SF}}(u)$ as before and $f^{\text{true}}(u_{\text{initial}}) > f^{\text{SF}}(u_{\text{initial}})$. Then, it holds:

- 1) $f^{\text{true}}(u_{\text{initial}}) = f^{\text{SF}}(u_{\text{initial}}) + g_m(u_{\text{initial}})$

- 2) For all $v \in \mathbb{R}^n$, it is

$$\frac{\partial}{\partial h} f^{\text{true}}(u_{\text{initial}} + hv) \Big|_{h=0} = \frac{\partial}{\partial h} (f^{\text{SF}}(u_{\text{initial}} + hv) + g_m(u_{\text{initial}} + hv)) \Big|_{h=0}$$

- 3) For $v_1, v_2 \in \text{span}\{w_1, \dots, w_m\}$, it is

$$\begin{aligned} & \frac{\partial^2}{\partial h_1 \partial h_2} f^{\text{true}}(u_{\text{initial}} + h_1 v_1 + h_2 v_2) \Big|_{h_1=h_2=0} = \\ & = \frac{\partial^2}{\partial h_1 \partial h_2} (f^{\text{SF}}(u_{\text{initial}} + h_1 v_1 + h_2 v_2) + g_m(u_{\text{initial}} + h_1 v_1 + h_2 v_2)) \Big|_{h_1=h_2=0} \end{aligned}$$

Therein, g_m is as in Eq. (2.6) in connection with x_i^{OCS} 's as in (2.7).

The proof is presented in Appendix 2.6.1. From Proposition 2.1, we see that an extension of the standard formula adding risk resulting from OCS indeed allows an approximation of the true risk measurement function in the sense of first and second order sensitivities.

⁹In the literature, it is often suggested to identify scenarios on the basis of the covariance matrix such that the scenarios can be found through the application of Principal Component Analysis (PCA), cf. for instance Hull (2018). Aigner and Schlütter (2022) highlight that relying on such a linear measure may lead to a misinterpretation of the company's risk situation.

2.3 Calibration of ORSA scenarios for market risk

To derive ORSA scenarios in the sense of section 2.2, we have to calibrate the two risk measurements based on the true risk which will be represented by an internal model and the one based on the regulatory requirements. This is done in the following two subsections. Specifically, we restrict the analysis to a market risk setting including equity, interest rate and spread risk, and set up a specific portfolio.

2.3.1 Specification of f^{true}

To meet the requirements of the regulatory authority in Europe, we employ as risk measure ϱ in (2.3) the VaR to a confidence level of 99.5% such that the true risk is given by

$$\begin{aligned} f^{\text{true}} : \mathbb{R}^n &\rightarrow \mathbb{R} \\ u &\mapsto \text{VaR}_{0.995}(\mathbf{X}^T u) - \mathbb{E}(\mathbf{X}^T u) \end{aligned}$$

with a random risk vector

$$\mathbf{X} = (X_1, \dots, X_n)^T \tag{2.9}$$

consisting of $n = n_B + n_S$ risk drivers comprising $n_B \in \mathbb{N}$ bond and $n_S \in \mathbb{N}$ stock investments. Without loss of generality, we assume that X_1, \dots, X_{n_B} reflect the losses/gains resulting from bonds and $X_{n_B+1}, \dots, X_{n_B+n_S}$ those from stock investments. For f^{true} to be well-defined, we then have to specify \mathbf{X} . For notational reasons, we rewrite the risk vector $\mathbf{X} = (X^B, X^S)^T$ to represent losses/gains resulting from bonds and stocks separately after one year. In order to determine these stochastic vectors

$$\begin{aligned} X^B &= (X_1^B, \dots, X_{n_B}^B)^T \\ X^S &= (X_1^S, \dots, X_{n_S}^S)^T \end{aligned}$$

we follow Eckert et al. (2016), who suggest modeling stock investments in combination with a reduced form credit risk model for defaultable bond exposure. Therefore, they let the stochastic default intensity (hazard rate) $h(t)$ follow a Vasicek (1977) process. The resulting model in Eckert et al. (2016) can be written as

$$\begin{aligned}
dr(t) &= \kappa \cdot (\theta - r(t)) dt + \zeta dW_r(t) \\
dh_1(t) &= \chi_1 \cdot (o_1 - h_1(t)) dt + \Gamma_1 dW_{h_1}(t) \\
&\dots \\
dh_{n_B}(t) &= \chi_{n_B} \cdot (o_{n_B} - h_{n_B}(t)) dt + \Gamma_{n_B} dW_{h_{n_B}}(t) \\
dS_1(t) &= \mu_1 S_1(t) dt + \sigma_1 \cdot S_1(t) dW_{S_1}(t) \\
&\dots \\
dS_{n_S}(t) &= \mu_{n_S} S_{n_S}(t) dt + \sigma_{n_S} \cdot S_{n_S}(t) dW_{S_{n_S}}(t)
\end{aligned}$$

where $W(t) = (W_r(t), W_{h_1}(t), \dots, W_{h_{n_B}}(t), W_{S_1}(t), \dots, W_{S_{n_S}}(t))^T$ is a standard Brownian motion with a symmetric correlation matrix R_{IM} implying that the valuation of market risk takes into account interest rate risk, credit risk, equity risk as well as dependencies between them.¹⁰ Herein, κ and χ_i define the speeds of mean reversion, θ and o_i the long-term means, and ζ and Γ_i the volatilities of the processes for $i = 1, \dots, n_B$. Additionally, stock investments are assumed to follow geometric Brownian motions.¹¹ Here, there are closed form solutions for the pricing of stock investments given by

$$S_i(t) = S_i(0) \cdot \exp\left(\mu_{S_i} - \frac{\sigma_{S_i}^2}{2} \cdot t + \sigma_{S_i} \cdot \sqrt{t} W_{S_i}\right)$$

for $i = n_B + 1, \dots, n_B + n_S$, cf. for instance Gatzert and Martin (2012, Eq. (7)), modeling the stock value at time t . Since we are interested in the stochastic losses of each stock investment, we set

$$(X^S)_i := -(S_i(1) - S_i(0)) \quad (2.10)$$

for $i = 1, \dots, n_S$.¹² Notably, we will set $S_i(0) = 1$ later on.

For the evaluation of bond investments, we have to take into account spread and interest rate risk. As our model states, we assume the interest rate process to follow a Vasicek (1977) process

$$dr(t) = \kappa \cdot (\theta - r(t)) dt + \zeta dW_r(t)$$

¹⁰For more details on the model, cf. Eckert et al. (2016).

¹¹The selection of geometric Brownian motions for modeling stocks is quite common in the literature, cf. for instance Islam and Nguyen (2020) or Graf and Korn (2020).

¹²In Eq. (2.10), negative values are reported such that positive values represent losses later on.

allowing us to determine the price of a non-defaultable zero coupon bond with maturity T as¹³

$$\begin{aligned} P(t, T) &= \exp(-M_r(t, T) + 0.5 \cdot V_r^2(t, T)), \text{ with} \\ M_r(t, T) &= r(t) \cdot \frac{1 - \exp(-\kappa \cdot (T - t))}{\kappa} + \theta \cdot \left((T - t) - \frac{1 - \exp(-\kappa \cdot (T - t))}{\kappa} \right) \\ V_r^2(t, T) &= \frac{\zeta^2}{\kappa^2} \left((T - t) - 2 \cdot \frac{1 - \exp(-\kappa(T - t))}{\kappa} + \frac{1 - \exp(-2\kappa(T - t))}{2\kappa} \right) \end{aligned}$$

Furthermore, in line with Eckert et al. (2016) we follow Duffie and Singleton (1999) to account for credit risk in the valuation of defaultable bonds. Therefore, default events for a given bond i are modeled by a Cox process with a stochastic hazard rate $h_i(t)$. Moreover, the model of Duffie and Singleton (1999) allows us to take into account dependencies between credit spread and interest rate by using correlated Brownian motions $W_r(t), W_{h_i}(t)$, $i = 1, \dots, n_B$. Additionally, a recovery of the market value is assumed such that in the case of a default at time τ , each bond pays a fraction of its value before the default

$$\delta_R(\tau) \cdot P^{RMV}(\tau-, T)$$

with $\delta_R(t)$ denoting the recovery rate,¹⁴ $P^{RMV}(t-, T) = \lim_{s \nearrow \tau} P^{RMV}(s, T)$ and $P^{RMV}(t, T)$ the pre-default price at time $t < \tau$ of a recovery of market value (RMV) defaultable bond with maturity T . Then, the price of a defaultable bond is

$$P^{RMV}(t, T) = E^{\mathbb{Q}} \left(\exp \left(- \int_t^T (r(u) + s_i(u)) du \right) \right)$$

with the credit spread $s_i(t) = (1 + \delta_R(t)) \cdot h_i(t)$. Since the hazard rates are assumed to follow a Vasicek (1977) process, the spread risks $s_i(t)$ follow —according to Itô's Lemma— again a Vasicek (1977) process given by

$$ds_i(t) = \chi_i \cdot (\hat{o}_i - s_i(t))dt + \hat{\Gamma}_i dW_{h_j}$$

with $\hat{o}_i = (1 - \delta_R) \cdot o_i$, $\hat{\Gamma}_i = (1 - \delta_R)\Gamma_i$ and a constant recovery rate $\delta_R(t) = \delta_R$. Then, Eckert et al. (2016) provide the following closed form solutions for the price of a RMV

¹³These formulas are presented for example in Eckert et al. (2016) and Schönbucher (2003).

¹⁴In general, the recovery rate could be stochastic, but for simplicity, we assume a constant recovery rate later on.

defaultable bond as

$$\begin{aligned}
P_i^{RMV}(t, T) &= P(t, T) \exp(-M_{s_i}(t, T) + 0.5 \cdot V_{s_i}^2 + C_i(t, T)), \text{ with} \\
M_{s_i}(t, T) &= s_i(t) \cdot \frac{1 - \exp(-\chi_i(T-t))}{\chi_i} + \hat{\sigma}_i \cdot \left((T-t) - \frac{1 - \exp(-\chi_i(T-t))}{\chi_i} \right) \\
V_{s_i}^2(t, T) &= \frac{\hat{\Gamma}_i^2}{\chi_i^2} \left((T-t) - 2 \cdot \frac{1 - \exp(-\chi_i(T-t))}{\chi_i} + \frac{1 - \exp(-2\chi_i(T-t))}{2\chi_i} \right), \text{ and} \\
C_i(t, T) &= \rho_{r, h_i} \frac{\zeta \hat{\Gamma}_i}{\kappa \chi_i} \left((T-t) - \frac{1 - \exp(-\kappa(T-t))}{\kappa} - \frac{1 - \exp(-\chi(T-t))}{\chi_i} \right. \\
&\quad \left. + \frac{1 - \exp(-(\kappa + \chi_i)(T-t))}{\kappa + \chi_i} \right)
\end{aligned}$$

where ρ_{r, h_i} reflects the correlation of the standard Brownian motions $W_r(t)$ and $W_{h_i}(t)$. The price of a defaultable bond i with hazard rate h_i and maturity T_i at time t is then derived as

$$B_i(t) = \sum_{h=t+1}^{T_i} CF_i(h) \cdot P_i^{RMV}(t, h)$$

with cash flows

$$CF_i(t) = \begin{cases} c_i(t) \cdot FV_i, & \text{if } (t < T_i) \wedge (\tau_i^B > t) \\ (1 + c_i(t)) \cdot FV_i, & \text{if } (t = T_i) \wedge (\tau_i^B > t) \\ \delta_R \cdot B_i(t-1), & \text{if } t = \tau_i^B \\ 0, & \text{else} \end{cases} \quad (2.11)$$

depending on the time of default τ_i^B , coupon $c_i(t)$ and time t . Herein, the face values FV_i are scaled such that $B_i(0) = 1$ for all $i = 1, \dots, n_B$. Since we are again interested in potential losses/gains after one year, we set

$$(X^B)_i = -(B_i(1) - B_i(0)) \quad (2.12)$$

with $i = 1, \dots, n_B$. In case of a mixed portfolio consisting of stocks and bonds, the market value risk vector is then

$$\mathbf{X} = ((X^B)^T, (X^S)^T)^T$$

with X_B and X_S as in (2.12) and (2.10) respectively. Here, the risk measure function in (2.3) is well-defined. By selecting the face value as in (2.11), the cash flows are adjusted

in a way that ensures that $(\mathbf{X}^T u)_i$ represents a loss with a value of u_i at $t = 0$. The portfolio volumes can be steered by adjusting the u_i .

2.3.2 Specification of f^{SF}

The Solvency II framework suggests a module structure making it necessary to calculate *equity*, *interest rate* and *spread* risks separately on a sub-module basis, cf. Figure 2.1. The risks are then aggregated towards the market module by the so-called square-root formula denoted by f^{SF} . In particular, we calculate three different values: Mkt_{eq} , Mkt_{int} and

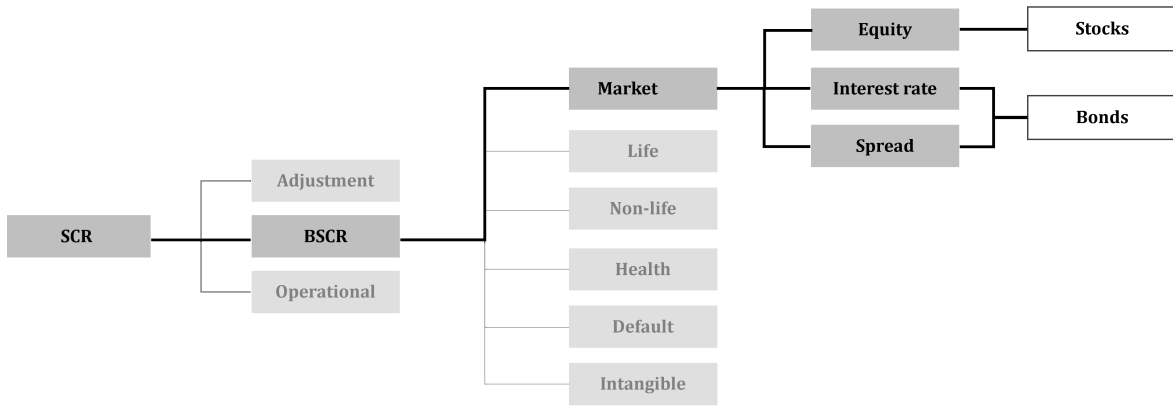


Figure 2.1 Structure for the SCR calculation in the style of Gatzert and Martin (2012); only sub-modules that are taken into account later on are presented.

Mkt_{sp} representing the capital requirement of the sub-modules respectively. Liquidity, concentration, property and currency risk will be excluded in the following analysis for the sake of simplicity. In this section, we mainly adopt the notation of Gatzert and Martin (2012). For notational reasons, we set the exposure vector as $u = \left((u^B)^T, (u^S)^T \right)^T \in \mathbb{R}^n$ with

$$u^B = (u_1^B, \dots, u_{n_b}^B)^T \in \mathbb{R}^{n_B}$$

$$u^S = (u_1^S, \dots, u_{n_s}^S)^T \in \mathbb{R}^{n_S}$$

distinguishing between exposures referring to bond investments, $u^B \in \mathbb{R}^{n_B}$, and those referring to stocks, $u^S \in \mathbb{R}^{n_S}$.

2.3.2.1 Interest rate risk

First, the risk resulting from a change of the term structure is determined within the *interest rate risk* sub-module. For this purpose, we calculate the present value (PV) of

all interest-rate-sensitive exposures—namely u^B —by discounting their cash flows (CF) using the risk-free interest rate structure $r_f(t)$ which is published monthly by EIOPA, cf. Table 2.7. Specifically, we have to calculate for $i = 1, \dots, n_B$

$$PV_i^{int} = \sum_{t=1}^{T_i} \frac{\overline{CF}_i(t)}{(1 + r_f(t))^t} \quad (2.13)$$

with T_i the maturity and $\overline{CF}_i(t)$ the cash flow of investment i at time t . For face values FV_i as discussed in the section before and a coupon payment $c_i(t)$ at time t , the cash flow for bond i is given by

$$\overline{CF}_i(t) = \begin{cases} c_i(t) \cdot FV_i, & \text{if } t < T_i \\ (1 + c_i(t)) \cdot FV_i, & \text{if } t = T_i \end{cases} \quad (2.14)$$

for $i = 1, \dots, n_B$. The upward shocked present values are then calculated as

$$(PV_{up}^{int})_i = \sum_{t=1}^{T_i} \frac{\overline{CF}_i(t)}{(1 + \max(r_f(t) \cdot (1 + s^{up}(t)), 0.01))^t} \quad (2.15)$$

where the maximum in the denominator is in line with European Commission (2015, Article 166) and ensures that there is at least a shock of one percent. Furthermore, for the downward shock we calculate

$$(PV_{down}^{int})_i = \sum_{t=1}^{T_i} \frac{\overline{CF}_i(t)}{(1 + \max(r_f(t) \cdot (1 + s^{down}(t)), 0))^t} \quad (2.16)$$

with the maximum in the denominator accounting for the current low-level interest rate environment. In both cases, it is again $i = 1, \dots, n_B$. The shocks $s^{up}(t)$, $s^{down}(t)$ are provided by European Commission (2015, Article 166 and 167) and shown in Table 2.7. Interpreting the results in Eq. (2.13), (2.15) and (2.16) as vectors in \mathbb{R}^{n_B} , allows us to determine the overall risk of the sub-module *interest rate* as

$$Mkt_{int}(u^B) = \max \left((PV^{int} - PV_{int}^{up})^T u^B, (PV_{int} - PV_{int}^{down})^T u^B \right)$$

depending on the part of the exposure vector reflecting bond investments.

2.3.2.2 Spread risk

Changes in the credit spread on exposures are considered in the rating-based risk sub-module of the Solvency II standard approach. The risk consists of three uncorrelated

groups: the SCR of bonds Mkt_{sp}^{bonds} , of securization positions $Mkt_{sp}^{securization}$ and of credit derivatives Mkt_{sp}^{cd} which are then easily added up to the total risk of the sub-module *spread*

$$Mkt_{sp} = Mkt_{sp}^{bonds} + Mkt_{sp}^{securization} + Mkt_{sp}^{cd}$$

For simplicity, we will restrict our analysis only to bond assets, ignoring securization positions and credit derivatives. The SCR calculation for spread risk then takes into account the current value $MV_{sp,i}(0) = u_i^B$ of bond $i = 1, \dots, n_B$. The stress referring to each bond depends on shocks that can be specified by including their ratings, which are publicly available, and their durations. In order to determine the latter, we rely on the Macaulay (1938) duration with a floor of one, as suggested by European Commission (2015, Article 176). Given that there is only one coupon period per year, it can be determined as

$$duration_i = \min \left(\frac{\sum_{t=1}^T t \cdot \overline{CF}_i(t) \cdot (1 + r_f(t))^{-t}}{\sum_{t=1}^T \overline{CF}_i(t) \cdot (1 + r_f(t))^{-t}} \cdot \frac{1}{1 + r_{YtM}}, 1 \right)$$

for $i = 1, \dots, n_B$ with r_f and $\overline{CF}_i(t)$ the cash flow as before. Furthermore, we need to specify the yield to maturity r_{YtM} which is obtained by solving

$$PV_i^{int} = \sum_{t=1}^{T_i} \overline{CF}_i(t) \cdot (1 + r_{YtM})^{-t}$$

where PV_i^{int} is calculated as in (2.13) and T_i as before.¹⁵ Given the rating and the duration of each bond, European Commission (2015, Article 176) further outlines how to specify the stresses $stress_i$ for $i = 1, \dots, n_B$ explicitly, cf. Tables 2.8 and 2.9. Here, the SCR of the spread risk sub-module (in the simplified version only including bonds) is calculated as

$$Mkt_{sp}(u^B) = \max \left(\sum_{i=1}^{n_B} u_i^B \cdot stress_i, 0 \right) = \max (stress^T u^B, 0)$$

It should be noted that for bonds issued by governments belonging to the EEA or the OECD, the stress, according to BaFin (2016), is always zero percent, and hence the Mkt_{sp} is also zero when the exposure is a respective bond.

¹⁵For the numerical calculation, there are several common approaches, such as the Newton-Raphson method which we will employ later on.

2.3.2.3 Equity risk

In order to calculate the capital requirements resulting from equity risk, we first have to cluster the n_S stock assets within our portfolio in (2.9) into “global” and “other”. The class “global” comprises all exposures transacted in countries that are members of the European Economic Area (EEA) or the Organisation for Economic Co-operation and Development (OECD), cf. CEIOPS (2010) and European Commission (2015). Without loss of generality, we assume that the first $k_{global} \in \mathbb{N}$ entries of u represent the exposure to “global” investments and the rest $k_{other} = n_S - k_{global}$ the exposure to “other” investments. “Global” stocks are easily multiplied with $shock_{global} = 0.3$ and “other” investments are assumed to have a higher risk and therefore are assigned a shock of $shock_{other} = 0.4$.¹⁶ With these specifications, one can directly calculate the market values of both classes by summing up the market values at time $t = 0$, denoted by $MV_{eq,i}(0) = u_i^S$, $i = 1, \dots, n_S$ for all assets in the respective class and multiplying it with the respective shock parameter

$$Mkt_{eq, global}(u^S) = \max \left(0.3 \cdot \sum_{i=1}^{k_{global}} u_i^S, 0 \right)$$

$$Mkt_{eq, other}(u^S) = \max \left(0.4 \cdot \sum_{i=k_{global}+1}^{n_S} u_i^S, 0 \right)$$

with $k_{global} + k_{other} = n_S$.¹⁷ In order to aggregate the classes with respect to diversification effects, EIOPA (2011) recommends the aggregation via the square-root formula

$$Mkt_{eq}(u^S) = \sqrt{x^T R_{eq} x}$$

with $x = (Mkt_{eq,global}(u^S), Mkt_{eq,other}(u^S))^T$ and the correlation matrix

¹⁶The stresses are adjusted here to avoid pro-cyclical effects of adverse capital market developments, cf. Gatzert and Martin (2012) for more details.

¹⁷For further details on the specification of the shocks including strategic participation, adjustments etc. cf. Gatzert and Martin (2012). These are excluded in this paper for the sake of tractability, but the process in the simulation study later on would work equivalently.

$$R_{\text{eq}} = \begin{array}{cc} & \begin{array}{cc} \textit{Global} & \textit{Other} \end{array} \\ \begin{pmatrix} 1 & 0.75 \\ 0.75 & 1 \end{pmatrix} & \begin{array}{l} \textit{Global} \\ \textit{Other} \end{array} \end{array}$$

Notably, a portfolio only consisting of stocks is just exhibited to the equity sub-module, and the solvency capital requirement (SCR) calculation of the market risk module ends with this sub-module, cf. Figure 2.1.

2.3.2.4 Aggregation of the sub-modules

Following European Commission (2015), the three sub-modules, *equity*, *interest rate* and *spread* are assumed to be correlated by

$$R_{\text{SF}} = \begin{array}{ccc} & \begin{array}{ccc} \textit{Interest rate} & \textit{Equity} & \textit{Spread} \end{array} \\ \begin{pmatrix} 1 & A & A \\ A & 1 & 0.75 \\ A & 0.75 & 1 \end{pmatrix} & \begin{array}{l} \textit{Interest rate} \\ \textit{Equity} \\ \textit{Spread} \end{array} \end{array}$$

where the correlation parameter A is conditional on the result of Mkt_{int} as

$$A = \begin{cases} 0.5, & \text{if } Mkt_{\text{int}}(u^B) = (PV_{\text{int}} - PV_{\text{int}}^{\text{down}})^T u^B \\ 0, & \text{if } Mkt_{\text{int}}(u^B) = (PV_{\text{int}} - PV_{\text{int}}^{\text{up}})^T u^B \end{cases}$$

Then, the overall market risk of a portfolio $u \in \mathbb{N}^{n_S+n_B}$ can be calculated with a square-root formula resulting in a specification of the function in (2.4) as

$$\begin{aligned} f^{\text{SF}} : \mathbb{R}^n &\rightarrow \mathbb{R} \\ u &\mapsto \sqrt{x^T R_{\text{SF}} x} \end{aligned} \tag{2.17}$$

with $x = (Mkt_{\text{int}}(u^B), Mkt_{\text{eq}}(u^S), Mkt_{\text{sp}}(u^B))^T \in \mathbb{R}^n$ and $n = n_B + n_S$. It is shown in Appendix 2.6.5 that f^{SF} is indeed homogeneous of degree one, a necessary property for the application of OCS in the latter.

2.3.3 Portfolio set-up

Let us now construct a (theoretical) portfolio, the market risk of which will be determined on the basis of the approaches presented in the last two sections. We assume an investment portfolio consisting of $n_B = 5$ bond investments, cf. Table 2.1, and $n_S = 2$ stocks, cf. Table 2.2. Furthermore, we assume that we are equally invested in each of those positions such that we set the initial portfolio as $u_{\text{initial}} = \mathbb{1}_7$ – with u_1, \dots, u_5 presenting the bond and u_6, u_7 the stock investments.¹⁸ Since there is a strict distinction between *spread* and *default* risk in the regulatory requirements, we assume that none of the bonds default until their maturity. We exclude *default* risk in the internal model here, such that the numerical analysis is indeed in line with the solvency calculation of the market risk module.

The SCR based on the standard formula can now directly be derived on the basis of the given specifications. Notably, the spread risk for the governmental bonds is set to zero, since Germany and Spain are both part of the EEA.

For the internal model, we take into account correlated standard Wiener processes with

B_i	Type _{i}	rating _{i}	maturity _{i}	Coupon (in %) c_i	χ_i	o_i	Γ_i
1	Corporate	AA	16	8.00	0.0392	0.0269	0.0004
2	Corporate	A	12	2.95	0.0180	0.0240	0.0009
3	Corporate	BBB	11	5.75	0.0373	0.0453	0.0027
4	Government	BB	10	1.75	0.2201	0.5670	0.2299
5	Government	A	10	0.50	0.0139	-0.0070	0.0022

Table 2.1 Specifications of the bonds that are taken into account. B_1 : Deutsche Bank AG, B_2 : Commerzbank AG, B_3 : E.ON SE, B_4 : Greece and B_5 : Spain. The parameters χ_i , o_i and Γ_i refer to the Vasicek processes and are estimated on the basis of spread data between 09/2011 and 09/2021.

the correlation matrix R_{IM} as discussed in section 2.3.1. The entries of R_{IM} have been estimated relying on monthly data between 09/2011 and 09/2021 and are presented in Table 2.3. The stocks are then modeled by Monte Carlo simulations with 5,000,000 paths following geometric Brownian motions with the parameters as in Table 2.2. Here, S_1 , namely Euro Stoxx, represents the investment in a “global” asset and S_2 , Shanghai Stock Exchange (SSE) composite index, in an “other” asset. Both potential classes in

¹⁸The choice of the initial portfolio is arbitrary thanks to homogeneity of f^{true} and f^{SF} as long as $f^{\text{true}}(u_{\text{initial}}) > f^{\text{SF}}(u_{\text{initial}})$.

the equity risk sub-module are thus covered.

The interest rate is modeled on the basis of a Vasicek (1977) process with a long-term

S_i	Index $_i$	category $_i$	μ_i	σ_i
1	Euro Stoxx	Global	0.0750	0.1611
2	Shanghai SE composite index	Other	0.0632	0.2091

Table 2.2 Annualized parameters for the specification of the geometric Brownian motions representing stock investments. The values are estimated on monthly data between 09/2011 and 09/2021.

mean $\theta = -0.0225$, the speed of mean reversion of $\kappa = 0.0046$ and a drift of $\sigma = 0.0015$. The parameters have been estimated on the basis of monthly EURIBOR data between 09/2011 and 09/2021 and relying on Maximum Likelihood estimation, cf. for instance Fergusson and Platen (2015). Furthermore, the initial value is set to $r(0) = \theta$.

As possible bond investments, a mixture of corporate and government bonds is considered. Their specifications are presented in Table 2.1. Employing again Maximum Likelihood estimation, the hazard processes can be fitted with the parameters presented in Table 2.1. Additionally, the recovery rate is set constant to $\delta_R = 0.61$.¹⁹

With these specifications, we can now define

	r	h_1	h_2	h_3	h_4	h_5	S_1	S_2
r	1							
h_1	0.1864	1						
h_2	0.1025	0.4518	1					
h_3	0.0848	0.2443	0.3165	1				
h_4	-0.0186	0.0310	-0.0846	-0.0147	1			
h_5	0.1617	0.4263	0.6409	0.5236	-0.0832	1		
S_1	-0.0865	-0.0213	0.0916	-0.2930	-0.0095	-0.1998	1	
S_2	-0.2118	0.0629	-0.1576	-0.1366	0.0789	-0.1818	0.3365	1

Table 2.3 The entries of correlation matrix R_{IM} . The values represent the correlation between stocks, bonds and interest rate r based on monthly data from 09/2011 to 09/2021.

$$f^{\text{diff}}(u) = f^{\text{true}}(u) - f^{\text{SF}}(u)$$

We can now identify OCS as in Eq. (2.7) such that $g_m(u)$ as in Eq. (2.6) approximates f^{diff} . To this end, Appendix 2.6.2 and Appendix 2.6.3 provide the necessary technical

¹⁹Eckert et al. (2016) note a high sensitivity of the model to changes of δ_R , but for our purpose a change in the recovery rate would lead to similar results.

details specifying the Hessian matrix H of $(f^{\text{diff}})^2$ and the weightvectors w_i , $i = 1, \dots, m$, which are crucial for the definition.

2.4 Results

Let us put ourselves in the situation of an investor who has seven units to invest in the portfolio specified in section 2.3.3. Table 2.4 shows what the risk capital looks like when investing all units separately in each asset and when investing in an equally weighted portfolio $u_{\text{initial}} = \mathbb{1}_7$. We observe that there is a severe gap between the two approaches

u	$f^{\text{SF}}(u)$	$f^{\text{true}}(u)$	Relative difference
$(7, 0, 0, 0, 0, 0, 0)^{\text{T}}$	0.933	0.931	0.21%
$(0, 7, 0, 0, 0, 0, 0)^{\text{T}}$	1.008	0.848	18.87%
$(0, 0, 7, 0, 0, 0, 0)^{\text{T}}$	1.469	0.806	82.26%
$(0, 0, 0, 7, 0, 0, 0)^{\text{T}}$	3.367	6.697	-49.72%
$(0, 0, 0, 0, 7, 0, 0)^{\text{T}}$	0.602	0.887	-32.13%
$(0, 0, 0, 0, 0, 7, 0)^{\text{T}}$	2.1	2.626	-20.03%
$(0, 0, 0, 0, 0, 0, 7)^{\text{T}}$	2.8	3.198	-12.45%
u_{initial}	1.300	1.478	-12.04%

Table 2.4 The SCRs based on f^{true} investing seven units separately in each of the seven assets and in an equally weighted portfolio are presented.

when investing in assets separately. And even including diversification effects, we observe a severe underestimation of the true risk by

$$\frac{f^{\text{SF}}(u_{\text{initial}})}{f^{\text{true}}(u_{\text{initial}})} - 1 = \frac{1.300}{1.478} - 1 = -12.04\%$$

Such an underestimation may lead to a capital buffer too low to cover investment risks, as outlined for instance by Asadi and Al Janabi (2020).

Inspecting a common tool of capital allocation, the Euler allocation, of both measurements at u_{initial} , cf. Table 2.5, also provides evidence that there is a severe gap between the two approaches. Notably, the entries of the gradient add up to the capital requirement for u_{initial} in both cases, cf. Tasche (2008). We can thus conclude that changing diversification effects are not captured when basing risk measurement on the square-root formula, since the slope of the two functions in u_{initial} strongly differ. This observation is in line with Chen et al. (2019), who find empirical evidence that the standard formula does not reflect changing diversification effects correctly.

To approximate then the difference $f^{\text{diff}}(u) = f^{\text{true}}(u) - f^{\text{SF}}(u)$ the OCS provided in Ta-

i	$\nabla_u f_i^{\text{SF}}$	$\nabla_u f_i^{\text{true}}$	Relative difference
1	0.126	0.068	85.29%
2	0.136	0.062	122.95%
3	0.190	0.058	229.34%
4	0.316	0.756	-58.20%
5	0.056	0.064	-11.11%
6	0.201	0.203	-1.96%
7	0.277	0.267	3.74%
\sum	1.300	1.478	-12.04%

Table 2.5 Euler allocations of f^{true} and f^{SF} and their relative difference. ∇_u represents the gradient.

ble 2.6 are determined as suggested in section 2.2 such that we obtain an approximation $f^{\text{SF}}(u) + g_m(u)$ of $f^{\text{true}}(u)$ in the sense of Proposition 2.1.²⁰ In a first step, we use only a

i	Asset _i	$x_{1_i}^{\text{OCS}}$	$x_{2_i}^{\text{OCS}}$	$x_{3_i}^{\text{OCS}}$	$x_{4_i}^{\text{OCS}}$	$x_{5_i}^{\text{OCS}}$	$x_{6_i}^{\text{OCS}}$	$x_{7_i}^{\text{OCS}}$
1	B_1	-0.057	-0.001	0.027	-0.034	0.013	0.012	0.004
2	B_2	-0.075	-0.001	0.026	-0.031	0.011	0.008	0.002
3	B_3	-0.130	0.002	0.044	-0.016	-0.011	-0.008	-0.002
4	B_4	0.440	-0.002	-0.020	0.113	-0.088	-0.003	-0.016
5	B_5	0.006	-0.002	-0.004	-0.048	0.040	-0.006	0.004
6	S_1	0.005	0.071	-0.038	0.007	0.006	-0.005	0.071
7	S_2	-0.011	-0.069	-0.034	0.008	0.029	0.002	-0.063

Table 2.6 Orthogonal convexity scenarios for the definition of the approximation function $g_m(u)$ as in section 2.2.

single scenario. That scenario x_1^{OCS} mainly reflects losses in bond investment B_4 and is equal to the Euler allocation of f^{diff} such that

$$\sum_{i=1}^7 x_{1_i}^{\text{OCS}} = 0.178 = f^{\text{diff}}(u_{\text{initial}}) = f^{\text{true}}(u_{\text{initial}}) - f^{\text{SF}}(u_{\text{initial}})$$

Including this additional scenario comes with two advantages: Firstly, we ensure that the risk resulting from the initial portfolio u_{initial} is estimated precisely. Secondly, first order sensitivities of the true risk are met by our approximation. Employing further scenarios then allows us to fit a quadratic approximation of f^{true} in u_{initial} even allowing us to meet second order sensitivities of the true risk landscape.

²⁰Notably, for the determination it has been set $w_1 = u_{\text{initial}}$, $w_2 = (0, 0, 0, 0, 0, 1, -1)^{\text{T}}$ and $w_3 = (0.2, 0.2, 0.2, 0.2, 0.2, 0.5, -0.5)^{\text{T}}$ since those are the business decisions we want to evaluate later on. Appendix 2.6.3 sketches how Aigner and Schlütter (2022) select the OCS without pre-given decisions considered as well, and the following calculations could be conducted in the same way.

For illustration, let us numerically evaluate the goodness of the approximation. Therefore, we shift the portfolio in the direction

$$u_{\text{new}}(h) = u_{\text{initial}} + h \cdot (0, 0, 0, 0, 0, 1, -1)^{\text{T}} \quad (2.18)$$

for $h \in \mathbb{R}$. This new portfolio represents a shift between stock investments keeping the exposure to the five bond investments constant. For positive values of h , we shift our portfolio from the “other” investment, S_2 , in the direction of the “global” one, S_1 . For negative h the shift is opposite, from “global” to “other”.

The resulting SCRs based on the different approaches are presented in Figure 2.2 for $h \in [-1, 1]$. There, we see that the overall capital requirement according to the standard formula (red curve) always underestimates the true risk (black curve). Furthermore, we see that it strictly decreases when shifting the portfolio away from S_2 in the direction of S_1 , which is reflected by the consistently negative slope. However, the true risk actually increases if the portfolio is shifted “too far” away from S_2 (positive h) due to changing diversification effects that are not captured by the standard formula. Generally, we can say that first and second order sensitivities in $u_{\text{initial}} = \mathbb{1}_7$ (for $h = 0$) are not reflected correctly.

By extending the standard formula with only $m = 1$ OCS (orange curve), we can adjust the risk measurement function in a sense that the true risk in u_{initial} is reflected correctly and that even first order sensitivities of f^{true} in all directions are met. The latter is due to the selection of the Euler allocation of f^{diff} as first scenario. Such an extension is a good starting point, but also does not take into account changing diversification effects, since it still has a consistently negative slope in line with the standard formula.

Including $m = 2$ scenarios (blue curve) allows a fit with a quadratic approximation function that also overcomes this second problem. We observe that now—additional to the properties of the extension with one scenario—even second order sensitivities are met in a neighbourhood of u_{initial} . We thus obtain a risk measurement function that is also capable of evaluating non-marginal portfolio shifts.

In order to inspect the goodness of the extension more granularly, let us inspect a more complex shift impacting all portfolio positions simultaneously

$$u_{\text{new}}(h_1, h_2) = u_{\text{initial}} + h_1 \cdot \left(\frac{1}{5}, \frac{1}{5}, \frac{1}{5}, \frac{1}{5}, \frac{1}{5}, -\frac{1}{2}, -\frac{1}{2} \right)^{\text{T}} + h_2 \cdot (0, 0, 0, 0, 0, 1, -1)^{\text{T}} \quad (2.19)$$

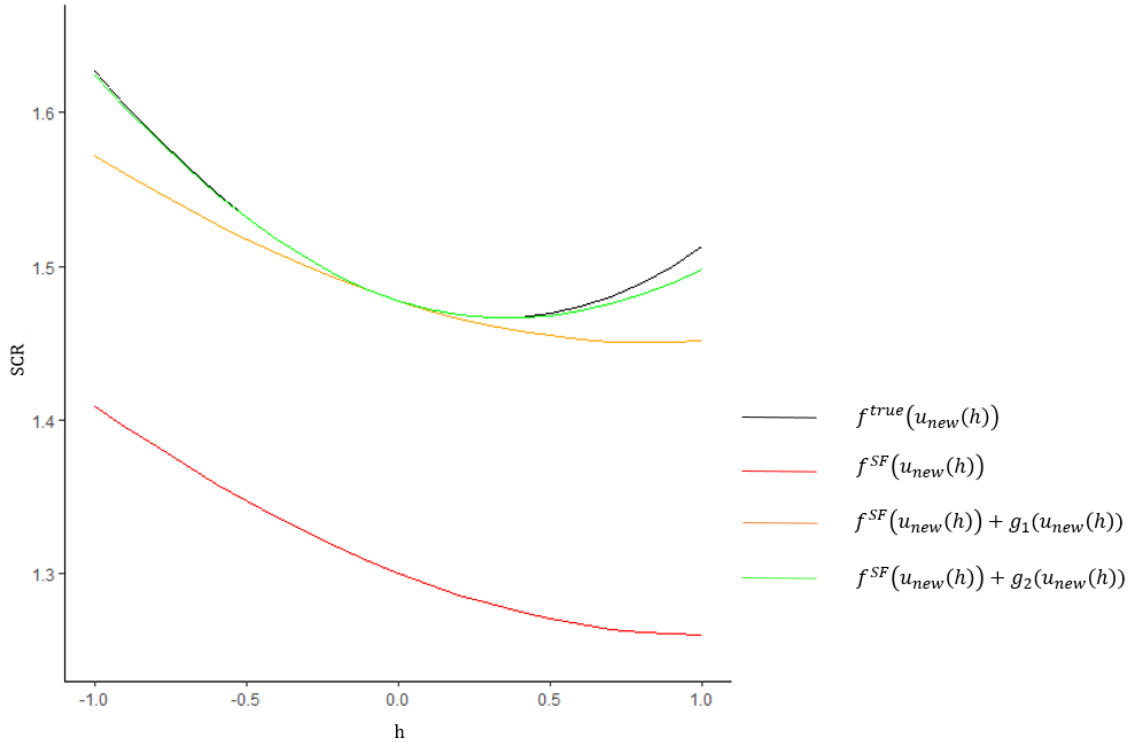


Figure 2.2 SCRs on the basis of the different risk measurement functions evaluating $u_{new}(h)$ as in Eq. (2.18).

for $h_1, h_2 \in \mathbb{R}$. If we set there $h_1 = 0$, we would again inspect a portfolio shift in the sense of Eq. (2.18). Setting $h_2 = 0$ would then reflect a shift away from stock into bond investments for positive h and vice versa for negative ones. Notably, the directions have been chosen such that the overall investment sum does not change. Comparing the resulting SCRs on the basis of OCS leads to the results presented in Figure 2.3 for $h_1, h_2 \in [-1, 1]$.

There, the left part shows the relative error of the standard formula extended by $m = 1$ scenario. It should be noted that we thereby obtain a reasonable approximation of f^{true} if we only evaluate marginal portfolio changes. When h_2 is de-/increased too far, the underlying curvature of the true risk measurement function cannot be reflected any more. That misestimation is represented by the relative errors of $f^{SF}(u_{new}(h_1, h_2)) + g_1(u_{new}(h_1, h_2))$ (red parts in the figure).

By including a second scenario, we are still able to approximate the true risk in a neighborhood of $u_{initial}$, but changing diversification effects are also considered. In the middle part of Figure 2.3, we observe that the gray parts—reflecting a relative error of about 0%—are not linear any more, but are instead spread in all directions. At the same

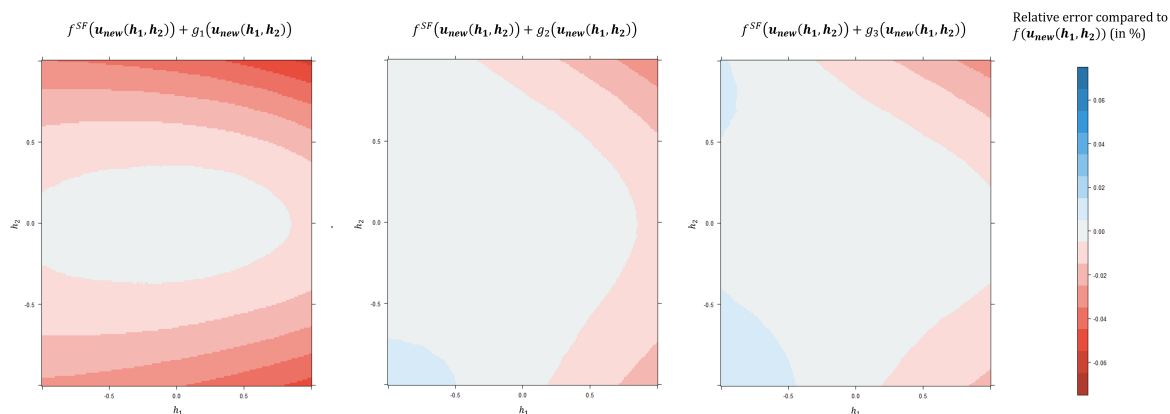


Figure 2.3 Relative errors measuring risks of portfolios $u_{\text{new}}(h_1, h_2)$ as in (2.19) on the basis of the standard formula and its extension via orthogonal scenarios for $m = 1, 2$ and 3 scenarios. All results are compared to $f^{\text{true}}(u_{\text{new}}(h_1, h_2))$.

time, we have to accept that a slight overestimation of the true risk may occur (blue parts), which is due to the fact that we extend the standard formula by a strictly positive function g . Numerically, including a second and third scenario reduces the absolute amount of the relative error from 5.86% (left) to 3.39% (middle). Notably, the inclusion of the third scenario (right part) does not have a great impact on the maximal relative error (3.00%), but indeed the neighbourhood region in which the approximation meets the true risk (gray parts in the right) can be widened. The inclusion of even more scenarios here also seems reasonable.

2.5 Conclusion

This paper suggests “orthogonal convexity scenarios” (OCS) to address the requirement for the Own Risk and Solvency Assessment (ORSA) of an insurer employing scenario analyses. Explicitly, it is expected to “also take into account risks that are not or not adequately included in the standard formula, and [...] develop a suitable assessment procedure for them” (BaFin (2016)). We show that the OCS allow the derivation of a deterministic extension of the standard formula such that the overall risk is in line with the true portfolio risk. The approach is applied in the context of market risks comprising interest rate, spread and equity risks. For the set-up of the standard formula, we follow the regulatory requirements and the approaches from the literature. Additionally, we use an internal model which is supposed to represent the true risk resulting from an asset portfolio. Notably, the true risk is generally unknown in practice, at which point an approximation becomes necessary. We find that extending the standard formula by OCS provides a reasonable approximation of the true risk in the sense of first and second order sensitivities. The latter property allows the evaluation of even non-marginal portfolio shifts, since changing diversification effects are considered by the resulting risk measurement. Although the approximation is only local, the examples in Paulusch and Schlütter (2022) indicate that the methodology is useful for other portfolios in addition to the calibration portfolio. The suggested approach can thus be seen as an answer to the question of how to select scenarios in the ORSA to measure risks that are not captured by the standard formula. Notably, since only deterministic scenarios are taken into account, we provide an easy tool for communicating the difference between an internal model and the standard formula to decision-makers, which has been identified as one of the fundamental aims of stress scenarios, cf. Albrecher et al. (2018, Chapter 5.5).

2.6 Appendix

2.6.1 Proof of Proposition 2.1

Let u_{initial} be arbitrary and assume $f^{\text{true}}(u_{\text{initial}}) > f^{\text{SF}}(u_{\text{initial}})$. Furthermore, assume that f^{true} and f^{SF} are homogeneous of degree one and twice continuously differentiable in u_{initial} . Then

$$f^{\text{diff}}(u) := f^{\text{true}}(u) - f^{\text{SF}}(u)$$

directly fulfills these properties as well. According to Aigner and Schlütter (2022, Theorem 1) it then holds for the approximation function g as specified in section 2.2

$$\begin{aligned} f^{\text{diff}}(u_{\text{initial}}) &= g_m(u_{\text{initial}}) \\ \frac{\partial}{\partial h} f^{\text{diff}}(u_{\text{initial}} + hv) \Big|_{h=0} &= \frac{\partial}{\partial h} (g_m(u_{\text{initial}} + hv)) \Big|_{h=0} \\ \frac{\partial^2}{\partial h_1 \partial h_2} f^{\text{diff}}(u_{\text{initial}} + h_1 v_1 + h_2 v_2) \Big|_{h_1=h_2=0} &= \frac{\partial^2}{\partial h_1 \partial h_2} g_m(u_{\text{initial}} + h_1 v_1 + h_2 v_2) \Big|_{h_1=h_2=0} \end{aligned}$$

for all $v \in \mathbb{R}^n$ and $v_1, v_2 \in \text{span}\{w_1, \dots, w_m\}$. Thereby, Proposition 2.1 follows.

2.6.2 Estimation of the Hessian matrix

For the identification of OCS in Eq. (2.7), we have to estimate the Hessian matrix of $(f^{\text{diff}})^2$. Employing the chain rule leads to

$$H = 2 \cdot (H_{f^{\text{true}}} - H_{f^{\text{SF}}}) \cdot (f^{\text{diff}}(u_{\text{initial}})) + 2 \cdot (\nabla_u f^{\text{diff}}(u_{\text{initial}}))^{\text{T}} \cdot \nabla_u f^{\text{diff}}(u_{\text{initial}}) \quad (2.20)$$

with $H_{f^{\text{true}}}$ and $H_{f^{\text{SF}}}$ the Hessian matrices of f^{SF} and f^{true} respectively, and $\nabla_u f^{\text{diff}}$ the gradient of f^{diff} all evaluated at u_{initial} . Furthermore, the gradient simplifies to

$$\nabla_u f^{\text{diff}}(u_{\text{initial}}) = \nabla_u f^{\text{true}}(u_{\text{initial}}) - \nabla_u f^{\text{SF}}(u_{\text{initial}})$$

It is then necessary to estimate the single parts of Eq. (2.20). On the one hand, $H_{f^{\text{SF}}}$ and $\nabla_u f^{\text{SF}}(u_{\text{initial}})$ can be determined easily by numerical derivation providing a reasonable result, since f^{SF} is deterministic. The identification of $H_{f^{\text{true}}}$ and $\nabla_u f^{\text{true}}(u_{\text{initial}})$, on the other hand, is more challenging. Monte Carlo simulations can be applied in line with Gourieroux et al. (2000) and Tasche (2009) who suggest Kernel estimators leading to a consistent estimation of $H_{f^{\text{true}}}$ and $\nabla_u f^{\text{true}}(u_{\text{initial}})$. Thanks to Slutsky's Theorem, (cf.

Casella and Berger, 2002, p. 239 f.), we can then consistently estimate H in (2.20), since it is a composition of consistent estimations.

2.6.3 Selection of weightvectors

For the identification of the necessary weightvectors w_1, \dots, w_m in Eq. (2.7), the user of the methodology could follow Appendix B in Aigner and Schlütter (2022) and set $w_1 = u_{\text{initial}}$. For the identification of w_2, \dots, w_m , the authors define a matrix $M \in \mathbb{R}^{n \times \tilde{n}}$ with $\tilde{n} = \text{rank}(H)$, such that

$$(Mv)^T \cdot H \cdot (Mv) = 0$$

for all $v \in \mathbb{R}^{\tilde{n}-m}$ and the columns of M denoted as M_i also fulfill $(M_i)^T H M_j = 0$, for $i \neq j$. Further, they define the diagonal matrix $\Lambda = M^T H M$ and denote by $\Lambda^{-0.5}$ the diagonal matrix with entries $\lambda_1^{-0.5}, \dots, \lambda_{\tilde{n}-m}^{-0.5}$. The weightvectors can then be determined as

$$w_{m+1} = \frac{1}{\sqrt{s^T \Lambda^{-0.5} M^T M \Lambda^{-0.5} s}} \cdot M \Lambda^{-0.5} s$$

where s is the eigenvector of $\Lambda^{-0.5} M^T M \Lambda^{-0.5}$ which refers to the smallest eigenvalue.

2.6.4 Parameters for regulatory capital requirement

t	Risk-free interest rate $r_f(t)$	Relative change $s^{up}(t)$	Relative change $s^{down}(t)$
1	-0.00612	0.7	-0.75
2	-0.00594	0.7	-0.65
3	-0.00556	0.64	-0.56
4	-0.00513	0.59	-0.5
5	-0.00462	0.55	-0.46
6	-0.00353	0.52	-0.42
7	-0.00293	0.49	-0.39
8	-0.00232	0.47	-0.36
9	-0.00172	0.44	-0.33
10	-0.00114	0.43	-0.31
...

Table 2.7 Risk-free interest rate r_f structure provided by EIOPA. The data are from 08/2021. Additionally, upward and downward shocks for the interest rate module are presented, cf. European Commission (2015).

Duration (dur_i) in years	$stress_i$
$dur_i \leq 5$	$3\% \cdot dur_i$
$5 < dur_i \leq 10$	$15\% + 1.7\% \cdot (dur_i - 5)$
$10 < dur_i \leq 20$	$23.5\% + 1.2\% \cdot (dur_i - 10)$
$dur_i > 20$	$\min(35\% + 0.5\% \cdot (dur_i - 20), 1)$

Table 2.8 Parameters for the determination of $stress_i$ within the spread sub-module under Solvency II regulation for bonds unrated by nominated ECAI are reported.

Duration (dur_i) (in years)		Rating											
		AAA		AA		A		BBB		BB		B	
		a_i	b_i	a_i	b_i	a_i	b_i	a_i	b_i	a_i	b_i	a_i	b_i
$dur_i \leq 5$		$stress_i$											
$5 < dur_i \leq 10$		$b_i \cdot dur_i$											
$10 < dur_i \leq 15$		$a_i + b_i \cdot (dur_i - 5)$											
$15 < dur_i \leq 20$		$a_i + b_i \cdot (dur_i - 10)$											
$dur_i > 20$		$a_i + b_i \cdot (dur_i - 15)$											
		$\min(a_i + b_i \cdot (dur_i - 20), 1)$											
		-	0.9	-	1.1	-	1.4	-	2.5	-	4.5	-	7.5
		4.5	0.5	5.5	0.6	7.0	0.7	12.5	1.5	22.5	2.5	37.5	4.2
		7.0	0.5	8.4	0.5	10.5	0.5	20.0	1.0	35.0	1.8	58.5	0.5
		9.5	0.5	10.9	0.5	13.0	0.5	25	1.0	44.0	0.5	61.0	0.5
		12.0	0.5	13.4	0.5	15.5	0.5	30	0.5	46.5	0.5	63.5	0.5

Table 2.9 Parameters for the determination of $stress_i$ within the spread sub-module under Solvency II regulation for bonds rated by a nominated External Credit Assessment Institution (ECAI). All values for a_i and b_i are in percent.

2.6.5 Homogeneity of degree one of f^{SF}

We need to show that f^{SF} in (2.17) is homogeneous of degree one. Therefore, we let every figure as in section 2.3.2. We can calculate for $\lambda \in \mathbb{R}$ and $u = \left((u^B)^\top, (u^S)^\top \right)^\top \in \mathbb{R}^n$ as in section 2.3.2

$$\begin{aligned} f^{\text{SF}}(\lambda \cdot u) &= f^{\text{SF}}(\lambda \cdot \left((u^B)^\top, (u^S)^\top \right)) = \sqrt{x_\lambda^\top R_{\text{SF}} x_\lambda} \stackrel{(*)}{=} \sqrt{(\lambda \cdot x)^\top R_{\text{SF}} (\lambda \cdot x)} \\ &= \lambda \cdot \sqrt{x^\top R_{\text{SF}} x} = \lambda \cdot f^{\text{SF}}(u) \end{aligned}$$

with

$$\begin{aligned} x_\lambda &= (Mkt_{\text{int}}(\lambda \cdot u^B), Mkt_{\text{eq}}(\lambda \cdot u^S), Mkt_{\text{sp}}(\lambda \cdot u^B))^\top \\ x &= (Mkt_{\text{int}}(u^B), Mkt_{\text{eq}}(u^S), Mkt_{\text{sp}}(u^B))^\top \end{aligned}$$

The equality (*) holds if and only if Mkt_{int} , Mkt_{eq} and Mkt_{sp} are also homogeneous of degree one. Firstly, it is

$$\begin{aligned} Mkt_{\text{int}}(\lambda \cdot u^B) &= \max \left((PV^{\text{int}} - PV_{\text{int}}^{\text{up}})^\top (\lambda \cdot u^B), (PV_{\text{int}} - PV_{\text{int}}^{\text{down}})^\top (\lambda \cdot u^B) \right) \\ &= \lambda \cdot \max \left((PV^{\text{int}} - PV_{\text{int}}^{\text{up}})^\top u^B, (PV_{\text{int}} - PV_{\text{int}}^{\text{down}})^\top u^B \right) = \lambda Mkt_{\text{int}}(u^B) \end{aligned}$$

Secondly, it holds

$$Mkt_{\text{eq}}(\lambda \cdot u^S) = \sqrt{\tilde{x}_\lambda^\top R_{\text{eq}} \tilde{x}_\lambda} \stackrel{(**)}{=} \sqrt{(\lambda \cdot \tilde{x})^\top R_{\text{eq}} (\lambda \cdot \tilde{x})} = \lambda \cdot Mkt_{\text{eq}}(u^S)$$

for $\tilde{x}_\lambda = (Mkt_{\text{eq}, \text{global}}(\lambda \cdot u^S), Mkt_{\text{eq}, \text{other}}(\lambda \cdot u^S))^\top$ and

$\tilde{x} = (Mkt_{\text{eq}, \text{global}}(u^S), Mkt_{\text{eq}, \text{other}}(u^S))^\top$. To see (**), we have to observe that

$$\begin{aligned} Mkt_{\text{eq}, \text{global}}(\lambda \cdot u^S) &= \max \left(0.3 \cdot \lambda \cdot \sum_{i=1}^{k_{\text{global}}} u_i^S, 0 \right) = \lambda Mkt_{\text{eq}, \text{global}}(u^S) \\ Mkt_{\text{eq}, \text{other}}(\lambda \cdot u^S) &= \max \left(0.4 \cdot \lambda \cdot \sum_{i=k_{\text{global}}+1}^{n_S} u_i^S, 0 \right) = \lambda \cdot Mkt_{\text{eq}, \text{other}}(u^S) \end{aligned}$$

Thirdly, we can calculate

$$Mkt_{\text{sp}}(\lambda \cdot u^B) = \max (stress^\top (\lambda \cdot u_i^B), 0) = \lambda \cdot \max (stress^\top u^B, 0) = \lambda \cdot Mkt_{\text{sp}}(\lambda \cdot u^B)$$

f^{SF} thus is homogeneous of degree one.

2.6.6 Robustness check

In order to check the robustness of the presented approach to changes in the underlying f^{true} , the portfolio set-up is to be changed to coincide with the parameters presented in Eckert et al. (2016) and Gatzert and Martin (2012). On this basis, we can also consider an investment portfolio consisting of $n_B = 5$ bond investments, cf. Table 2.10, that are in line with Eckert et al. (2016) and $n_S = 2$ stocks, cf. Table 2.11. Here, the SCR employing the standard formula can be directly calculated. For the internal model, we

B_i	Type $_i$	rating $_i$	maturity $_i$	Coupon (in %) c_i
1	Corporate	AA	10	2.950
2	Corporate	A	10	4.550
3	Corporate	BBB	11	3.500
4	Government	A	15	3.000
5	Government	BB	11	5.125

Table 2.10 Specifications of the bonds that are taken into account. The parameters are taken from Eckert et al. (2016). B_1 : Colgate-Palmolive Company, B_2 : Woolworth LTD, B_3 : Areva SA, B_4 : Poland Republic of (Government) and B_5 : Turkey Republic of (Government).

again take into account correlated standard Wiener processes with correlation matrix R_{IM} as discussed in section 2.3.1. The entries of R_{IM} are presented in Table 2.12 and are again taken from Eckert et al. (2016). The stocks are then modeled as before following geometric Brownian motions with the parameters as in Table 2.11. Here, S_1 , namely MSCI World, represents the investment in a “global” asset and S_2 , India BSE 100, in an “other” asset. Again, we cover both potential classes in the equity risk sub-module. The parameters of the interest rate Vasicek (1977) process are given by $\kappa = 0.0953$,

S_i	Index $_i$	rating $_i$	μ_i	σ_i
1	MSCI World	Global	0.0509	0.1574
2	India BSE 100	Other	0.1043	0.3309

Table 2.11 The parameters for the specification of the geometric Brownian motions representing stock investments. The numbers are taken from Gatzert and Martin (2012) who estimated them based on monthly data from 01/1988 to 07/2011.

$\theta = 0.0437$ and $\zeta = 0.0069$, cf. Eckert et al. (2016).²¹ Furthermore, the initial value is set to $r(0) = \theta$. The specifications of bond investments are presented in Table 2.10. Eckert

²¹These are based on the monthly “EURIBOR” data from 01/1999 to 12/2008.

et al. (2016) follow then Liang et al. (2011), assuming that bonds in the same rating class have the same parameters for their hazard rate Vasicek (1977) process which are shown in Table 2.13. Additionally, the recovery rate is set constant to $\delta_R = 0.61$ as before.

We evaluate the goodness of the approximation of $f^{\text{true}}(u)$ by $f^{\text{SF}}(u) + g_m(u)$ as sug-

i	r	h_{AA}	h_A	h_{BBB}	h_{BB}	S_1	S_2
r	1						
h_{AA}	0.3	1					
h_A	0.3	0.3	1				
h_{BBB}	0.3	0.3	0.3	1			
h_{BB}	0.3	0.3	0.3	0.3	1		
S_1	-0.26	0	0	0	0	1	
S_2	-0.21	0	0	0	0	0.26	1

Table 2.12 The entries of correlation matrix R_{IM} . The values are taken from Gatzert and Martin (2012) and Eckert et al. (2016) who have estimated the correlation between stocks and interest rate r based on monthly data from 01/1988 to 07/2011. The correlations between bond classes h_i and interest rate r are originally from Liang et al. (2011).

Rating	χ	o	Γ
AA	0.9581	0.0072	0.0181
A	0.7553	0.0141	0.0126
BBB	0.5865	0.0258	0.0113
BB	0.4406	0.0781	0.0454

Table 2.13 Parameters for the Vasicek (1977) processes modeling the hazard rates depending on the bond rating. The values are again taken from Eckert et al. (2016).

gested in section 2.2 for investing seven units into an equally weighted portfolio specified as $u_{\text{initial}} = (1, \dots, 1)^T \in \mathbb{R}^n$. f^{true} is evaluated on the basis of a Monte Carlo simulation with 5,000,000 paths and it results in capital requirements of $f^{\text{true}}(u_{\text{initial}}) = 1.525$ and $f^{\text{SF}}(u_{\text{initial}}) = 1.309$ resulting in a relative error of -14.20% . Following the procedure described in section 2.2, seven scenarios can be identified which are presented in Table 2.14. Evaluating the goodness of the performance, we again take into account the shift presented in Eq. (2.18). Figure 2.4 presents the outcomes for $h \in [-1, 1]$. There, we obtain a similar result as in section 2.4: The standard formula is not capable of approximating the true risk reasonably underestimating the portfolio risk, and sensitivities are also not reflected correctly. An extension by $m = 1$ orthogonal convexity scenario overcomes one of these problems reflecting the true risk at u_{initial} and also first order sensitivities correctly.

i	Asset _i	x_{1i}^{OC}	x_{2i}^{OC}	x_{3i}^{OC}	x_{4i}^{OC}	x_{5i}^{OC}	x_{6i}^{OC}	x_{7i}^{OC}
1	B_1	0.0119	0.0115	-0.0147	0.0033	-0.0127	-0.0127	0.0056
2	B_2	-0.0044	0.0121	-0.0155	0.0021	-0.0137	-0.0137	0.0004
3	B_3	-0.0718	0.0174	-0.0239	-0.0010	-0.0213	-0.0213	0.0042
4	B_4	0.0557	0.0039	0.0009	0.0119	-0.0001	-0.0001	-0.0005
5	B_5	0.0534	0.0032	0.0018	-0.0163	-0.0072	-0.0072	-0.0005
6	S_1	-0.0100	0.0364	0.0424	0.0018	-0.0266	-0.0266	-0.0104
7	S_2	0.1814	-0.0845	0.0090	-0.0018	0.0815	0.0815	0.0013

Table 2.14 Scenarios for the definition of the approximation function $g_m(u)$ in the setting of Eckert et al. (2016).

Extending the regulatory risk calculation by $m = 2$ orthogonal convexity scenarios even allows for an inspection of non-marginal portfolio changes by reflecting the second order sensitivities of f^{true} at least in some subspace. With these observations, we have seen

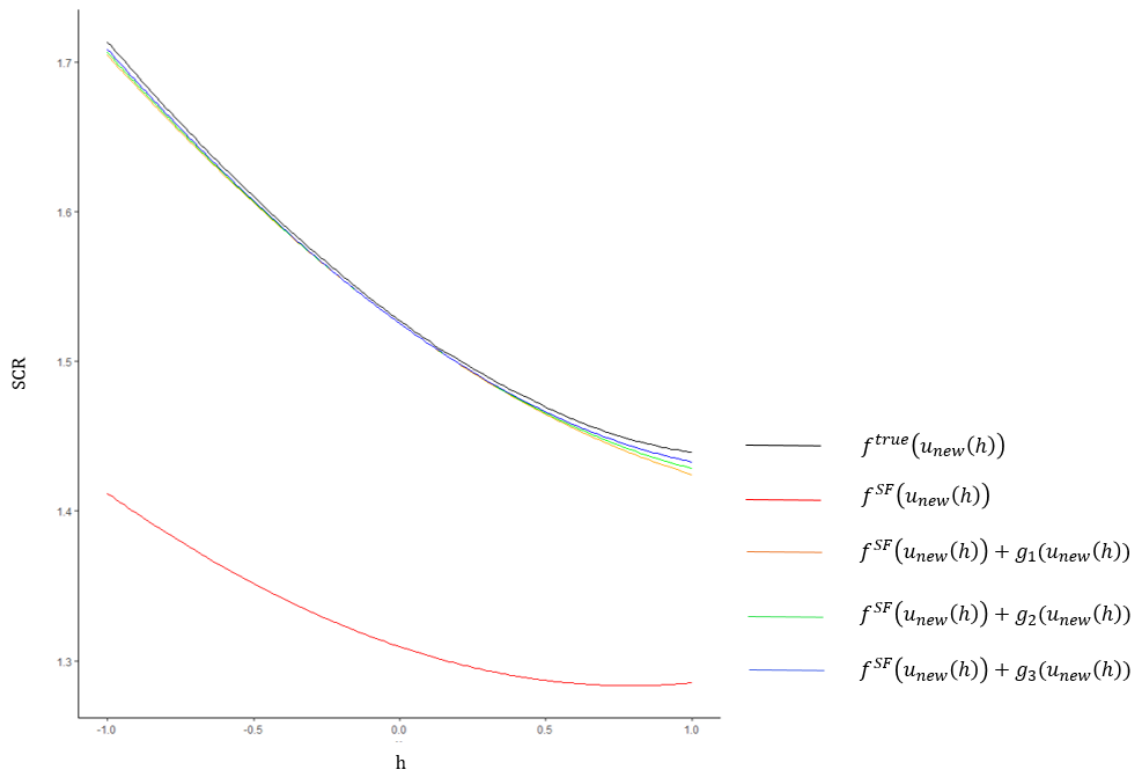


Figure 2.4 SCRs on the basis of the different risk measurement functions evaluating $u_{\text{new}}(h)$ as in Eq. (2.18) with the parameters in the internal model as reported in Eckert et al. (2016).

that the presented approach is robust to changes of the underlying true risk measurement function, making it applicable for a wide range of risk functions.

References

- Aigner, P., Schlütter, S., 2022. Enhancing gradient capital allocation with orthogonal convexity scenarios. Working Paper , 1–5.
- Albrecher, H., Bauer, D., Embrechts, P., Filipović, D., Koch-Medina, P., Korn, R., Loisel, S., Pelsser, A., Schiller, F., Schmeiser, H., et al., 2018. Asset-liability management for long-term insurance business. *European Actuarial Journal* 8, 9–25.
- Asadi, S., Al Janabi, M.A., 2020. Measuring market and credit risk under solvency ii: Evaluation of the standard technique versus internal models for stock and bond markets. *European Actuarial Journal* 10, 425–456.
- Becker, B., Ivashina, V., 2015. Reaching for yield in the bond market. *The Journal of Finance* 70, 1863–1902.
- Braun, A., Schmeiser, H., Schreiber, F., 2017. Portfolio optimization under Solvency II: Implicit constraints imposed by the market risk standard formula. *Journal of Risk and Insurance* 84, 177–207.
- Breuer, T., Csiszár, I., 2013. Systematic stress tests with entropic plausibility constraints. *Journal of Banking & Finance* 37, 1552–1559.
- Buch, A., Dorfleitner, G., Wimmer, M., 2011. Risk capital allocation for RORAC optimization. *Journal of Banking & Finance* 35, 3001–3009.
- Bundesanstalt für Finanzdienstleistungsaufsicht (BaFin), 2016. Governmentbonds: Treatment of risk under solvency ii. URL: <https://www.bafin.de/dok/8136732>.
- Casella, G., Berger, R., 2002. *Statistical Inference*, 2nd Edition. Duxbury.
- Chen, T., Goh, J.R., Kamiya, S., Lou, P., 2019. Marginal cost of risk-based capital and risk-taking. *Journal of Banking & Finance* 103, 130–145.
- Committee of European Insurance and Occupational Pensions Supervisors (CEIOPS), 2010. Quantitative impact study 5 - questions & answers. URL: <https://eiopa.europa.eu>.

- Duffie, D., Singleton, K.J., 1999. Modeling term structures of defaultable bonds. *The Review of Financial Studies* 12, 687–720.
- Eckert, J., Gatzert, N., Martin, M., 2016. Valuation and risk assessment of participating life insurance in the presence of credit risk. *Insurance: Mathematics and Economics* 71, 382–393.
- European Commission, 2015. Commission Delegated Regulation (EU) 2015/35 of 10 October 2014 supplementing Directive 2009/138/EC of the European Parliament and of the Council on the taking-up and pursuit of the business of Insurance and Reinsurance (Solvency II) .
- European Insurance and Occupational Pensions Authority (EIOPA), 2011. Report on the fifth Quantitative Impact Study (QIS5) for Solvency II. URL: https://www.eiopa.europa.eu/content/guidelines-own-risk-solvency-assessment-orsa_en.
- European Insurance and Occupational Pensions Authority (EIOPA), 2015. Guidelines on own risk and solvency assessment. URL: https://www.eiopa.europa.eu/document-library/guidelines/guidelines-own-risk-solvency-assessment-orsa_en_en.
- European Insurance and Occupational Pensions Authority (EIOPA), 2019. Insurance Statistics. URL: https://www.eiopa.europa.eu/tools-and-data/insurance-statistics_en.
- Fergusson, K., Platen, E., 2015. Application of maximum likelihood estimation to stochastic short rate models. *Annals of Financial Economics* 10, 1550009.
- Fischer, K., Schlütter, S., 2015. Optimal investment strategies for insurance companies when capital requirements are imposed by a standard formula. *Geneva Risk and Insurance Review* 40, 15–40.
- Gatzert, N., Martin, M., 2012. Quantifying credit and market risk under Solvency II: Standard approach versus internal model. *Insurance: Mathematics and Economics* 51, 649–666.
- Gourieroux, C., Laurent, J.P., Scaillet, O., 2000. Sensitivity analysis of values at risk. *Journal of Empirical Finance* 7, 225–245.

- Graf, S., Korn, R., 2020. A guide to monte carlo simulation concepts for assessment of risk-return profiles for regulatory purposes. *European Actuarial Journal* 10, 273–293.
- Guo, Q., Bauer, D., Zanjani, G., 2021. Capital allocation techniques: Review and comparison. *Variance* 14.
- Hull, J.C., 2018. *Risk Management and Financial Institutions*. Wiley Finance Series. 5th Edition.
- Islam, M.R., Nguyen, N., 2020. Comparison of financial models for stock price prediction. *Journal of Risk and Financial Management* 13, 181.
- Korn, R., Müller, L., 2021. Optimal portfolios in the presence of stress scenarios a worst-case approach. *Mathematics and Financial Economics* , 1–33.
- Liang, J., Ma, J.M., Wang, T., Ji, Q., 2011. Valuation of portfolio credit derivatives with default intensities using the vasicek model. *Asia-Pacific Financial Markets* 18, 33–54.
- Macaulay, F.R., 1938. Front matter to” some theoretical problems suggested by the movements of interest rates, bond yields and stock prices in the united states since 1856”, in: *Some Theoretical Problems Suggested by the Movements of Interest Rates, Bond Yields and Stock Prices in the United States since 1856*. NBER, pp. 15–6.
- Makam, V.D., Millossovich, P., Tsanakas, A., 2021. Sensitivity analysis with χ^2 -divergences. *Insurance: Mathematics and Economics* 100, 372–383.
- McNeil, A.J., Smith, A.D., 2012. Multivariate stress scenarios and solvency. *Insurance: Mathematics and Economics* 50, 299–308.
- Mitnik, S., 2014. VaR-implied tail-correlation matrices. *Economics Letters* 122, 69–73.
- Paulusch, J., 2017. The Solvency II standard formula, linear geometry, and diversification. *Journal of Risk and Financial Management* 10, 11.
- Paulusch, J., Schlütter, S., 2022. Sensitivity-implied tail-correlation matrices. *Journal of Banking & Finance* 134, 106333.
- Pesenti, S.M., Millossovich, P., Tsanakas, A., 2019. Reverse sensitivity testing: What does it take to break the model? *European Journal of Operational Research* 274, 654–670.

-
- Pfeifer, D., Strassburger, D., 2008. Solvency II: stability problems with the SCR aggregation formula. *Scandinavian Actuarial Journal* 1, 61–77.
- Scherer, M., Stahl, G., 2021. The standard formula of solvency ii: a critical discussion. *European Actuarial Journal* 11, 3–20.
- Schönbucher, P.J., 2003. *Credit derivatives pricing models: models, pricing and implementation*. John Wiley & Sons.
- Tasche, D., 2008. Capital allocation to business units and sub-portfolios: The Euler principle, in: Resti, A. (Ed.), *Pillar II in the New Basel Accord: The Challenge of Economic Capital*. Risk Books, London, pp. 423–453.
- Tasche, D., 2009. Capital allocation for credit portfolios with kernel estimators. *Quantitative Finance* 9, 581–595.
- Vasicek, O., 1977. An equilibrium characterization of the term structure. *Journal of Financial Economics* 5, 177–188.

Chapter 3

Scenarios of Systemic Risk*

Abstract

The so-called “systemic expected shortfall” (SES), introduced by Acharya et al. (2017), measures a financial institution’s contribution to systemic risk of the financial market. Acharya et al. propose taxing financial institutions based on their SES in order to internalize the social costs of systemic risk. The concept of SES leans on a well-known methodology of corporate risk management, namely the marginal expected shortfall, or Euler capital allocation principle. This paper shows that limitations known from the corporate risk management literature are also relevant for SES. The condition underlying the calculation of SES—the financial market being in distress—corresponds to a snapshot of the strategies currently chosen by financial institutions, disregarding potential reactions e.g. to a new tax. Introducing an SES-based tax therefore does not necessarily guide firms to a social optimum. We suggest measuring (firms’ contributions to) systemic risk by means of so-called orthogonal convexity scenarios (OCS). Our empirical investigation demonstrates that the traditional SES inappropriately reflects systemic risk induced by large insurance companies and Asian banks.

JEL classification: G28, G32, D62, H23

Keywords: Systemic risk, systemic expected shortfall, marginal expected shortfall, orthogonal convexity scenarios

*This versions of the paper was presented at the annual meeting of the DVfVW 2023.

3.1 Introduction

Systemic risks in financial markets pose a major threat to modern economies and societies. Financial institutions, i.e. banks and insurance companies, contribute to systemic risk by (i) holding insufficient capital and (ii) obtaining a risk profile which is associated with high losses when the whole market is under stress. Contributing to systemic risk is an externality, as it causes social costs such as potential governments bailouts. Measuring systemic risk is thus necessary from a regulatory perspective, cf. for instance Feinstein et al. (2017), in order to quantify the costs if such bailouts become necessary.

To mitigate systemic risks, a growing body of literature deals with the definition of appropriate capital requirements and the design of tax policies which internalize the associated social costs. In a much recognized recent paper, Acharya et al. (2017) derive a tax policy for financial institutions which aligns the firms' preferred risk management strategies with the social optimum. To this end, Acharya et al. measure systemic risks using the Expected Shortfall (ES) of assets minus capital for all firms in the financial system on aggregate. The tax of each firm i depends on its so-called Systemic Expected Shortfall (SES). The SES of firm i measures firm i 's contribution to systemic risk and is obtained as the expected assets minus capital of firm i conditioned on the whole system being in distress. Acharya et al.'s approach of using ES and SES in the context of a financial system is inspired by well-established corporate risk management theory. This theory tackles the question of how firms with several business segments should allocate their firm-wide capital needs back to business segments. A prominent method is the marginal (or Euler) capital allocation principle, which considers the impact of a marginal segment expansion on firm-wide capital.¹ The SES as proposed by Acharya et al. corresponds to a firm using ES to determine its firm-wide capital: here, the marginal allocation (or marginal ES) for a segment coincides with its expected losses conditioned on the firm being in distress (cf. Hong and Liu, 2009).

The corporate risk management literature has identified an important shortcoming of marginal capital allocation, which seems relevant for Acharya et al.'s usage of SES. Ex-

¹The marginal capital allocation principle has been applied in connection with homogeneous risk measures, such as Value-at-Risk or Expected Shortfall, cf. Gouriéroux et al. (2000), Tasche (2009), Hong and Liu (2009), Targino et al. (2015). It can also be used in connection with a firm's Default Put Option (DPO), which evaluates the losses of debtholders in the default case of the firm, cf. Myers and Read (2001) and Erel et al. (2015) in connection with Mildenhall (2004).

amples in Gründl and Schmeiser (2007, pp. 310 ff.) and Diers (2011, pp. 113 ff.) in the insurance context highlight that marginal capital allocations strongly depend on the firm's current portfolio composition. When segments are dropped or a group of segments is non-marginally expanded, natural hedges may vanish, and new risks can bring the firm into distress. To identify a firm's optimal mix of business segments, Buch et al. (2011) suggest using second-order derivatives of the diversified capital with respect to segment volumes, in addition to (first-order) marginal capital allocations. For the number of segments N being large, the complete Hesse matrix of ES becomes difficult to interpret, as it contains N^2 elements. Aigner and Schlütter (2022) propose so-called "Orthogonal Convexity Scenarios" (OCS). An OCS is a vector of size N containing realized losses for each segment. Aigner and Schlütter show that the marginal capital allocation (as the first scenario) in combination with a small number of OCS can reasonably reflect the nonlinear relationship between diversified capital and segment volumes.

Turning back to Acharya et al.'s measure for systemic risk, the strand of literature presented highlights that the SES depends on the composition of the financial market and can alter when firms change in size or strategy. The latter can occur, among other ways, by introducing the proposed tax policy based on SES,² as it is intended to induce changes in firms' strategies. The introduction of an SES-based tax would therefore need to happen in a sequence of rounds where firms adjust their strategy, the SES is determined based on the new strategies, firms adjust again, and so on. We also provide a stylized example which shows that such a sequence does not necessarily converge to the social optimum.

This paper proposes assessing the contribution of individual firms to systemic risk on a more robust basis by using the Systemic Expected Shortfall along with relevant Orthogonal Convexity Scenarios.

The empirical analysis included in this paper is based on data of "systemically important financial institutions" indicated each year by the Financial Stability Board (FSB). Firstly, we demonstrate how the SES in combination with OCS can be valuable for a regulator dealing with systemic risk. We find that extending the SES through additional OCS allows a proper reflection of changing sensitivities resulting from a change in market capitalizations. The necessity of several rounds implementing a tax for systemic risk can thereby be avoided. Additionally, we highlight that the resulting scenarios also allow

²Cf. Acharya et al. (2017), section 1.4.

for an economically useful interpretation depicting the interconnectedness between the evaluated institutions. Secondly, we illustrate scenarios for an investor distributing their portfolio in systemically relevant institutions. There, we especially find that insurance companies should play an important role for investment decisions. Notably, this is contrary to the fact that the FSB recently just designated banks as systemically important institutions and did not consider insurance companies.

The remainder of this article is structured as follows. Section 2 describes the model set-up and the systemic expected shortfall in line with Acharya et al. (2017). Section 3 introduces orthogonal convexity scenarios for measuring systemic risk. Section 4 explains the estimation methodology, data sets and results of our empirical analysis. Section 5 concludes.

3.2 Measuring systemic risk

We start with presenting the basic idea of Acharya et al. (2017, pp. 6-9) in order to measure the externality of systemic risk and internalize it into bank's decision making with an SES-based tax.

We consider a financial system of N banks³ Each bank $i \in \{1, \dots, N\}$ defines its strategy with k decision variables and its choices are collected in vector $u_i = (u_{i1}, \dots, u_{ik})^T \in \mathbb{R}^k$. Vector $u = (u_1^T, \dots, u_N^T)^T \in \mathbb{R}^{N \cdot k}$ lists the decision variables of all banks in the system. Variable u_{ij} can define, e.g., the amount of money that bank i invests into a specific asset class or the business volume of its segments.

Let random variable $LOSS_i(u_i)$ denote the loss or lack in capital of bank i depending on its strategy u_i . The stochastic event $COND(u)$ points out that the financial system is in a crisis. On this basis, the social cost of systemic risk is measured as in dependence of all banks' strategies as

$$\begin{aligned} \text{SYST} : \mathbb{R}^{N \cdot k} &\rightarrow \mathbb{R} \\ u &\mapsto \mathbb{E} \left[e \cdot \sum_{i=1}^N LOSS_i(u_i) \cdot \mathbb{1}_{COND(u)} \right] \end{aligned} \quad (3.1)$$

where e denotes a constant capturing the severity of externality costs if a crisis occurs.

³The term "bank" is used to simplify the wording and may represent other financial institutions, such as security providers or insurance companies, as well.

The Systemic Expected Shortfall of bank i is defined as

$$\begin{aligned} \text{SES}_i : \mathbb{R}^{N \cdot k} &\rightarrow \mathbb{R} \\ u &\mapsto \mathbb{E} [\text{LOSS}_i(u_i) | \text{COND}(u)] \end{aligned} \quad (3.2)$$

and measures the contribution of bank i to systemic risk. The SES-based tax, cf. Acharya et al. (2017, p. 12), reflects bank i 's contribution to systemic risk and is defined as

$$\begin{aligned} \text{TAX}_i(u) &= e \cdot P(\text{COND}(u)) \cdot \text{SES}_i(u) \\ &= \mathbb{E} [e \cdot \text{LOSS}_i(u_i) \cdot \mathbb{1}_{\text{COND}(u)}] \end{aligned}$$

Across all banks, the SES-based taxes sum up to the social costs of systemic risk, i.e.

$$\sum_{i=1}^N \text{TAX}_i(u_i) = \text{SYST}(u) \quad (3.3)$$

The objective of bank i is to maximize its post-tax profit which is defined as

$$\text{PROFIT}_i(u_i) = \text{PROFIT_PRE}_i(u_i) - \text{TAX}_i(u_i) \quad (3.4)$$

with $\text{PROFIT_PRE}_i(u_i)$ summarizing the bank's pre-tax profit.

The regulator's objective is maximizing social welfare, defined as

$$\text{SOCIAL}(u) = \sum_{i=1}^N \text{PROFIT_PRE}_i(u_i) - \text{SYST}(u) \quad (3.5)$$

Eq. (3.4) and (3.5) in connection with Eq. 3.3 imply that the sum of all banks' post-tax profits coincide with social welfare. Therefore, the first-order conditions of the banks' problems in terms of Eq. (3.4) coincide with the first-order conditions of maximizing social welfare in terms of Eq. (3.5), i.e.

$$\nabla_{u_i} \text{PROFIT}_i(u_i) = \nabla_{u_i} \text{SYST}(u) \text{ for all } i = 1, \dots, N \quad (3.6)$$

In other words, if $u^* = (u_1^*, \dots, u_N^*)^T$ is the social optimum in terms of (3.5), then u_i^* is also the optimal strategy of each bank i in terms of (3.4).

Our main concern is that banks' strategies in the financial system before the tax has been introduced, say $u^{\text{initial}} = (u_1^{\text{initial}}, \dots, u_N^{\text{initial}})^T$, may be far away from the social optimum u^* . Starting in the system pre taxation, the SES_i are calculated based on condition $\text{COND}(u^{\text{initial}})$ which reflects strategies u^{initial} . The SES-based tax penalizes bank

strategies which create losses in situations where condition $COND(u^{initial})$ applies. It does, however, not take into account that $COND(u^*)$ may apply in different states of the world than condition $COND(u^{initial})$. Hence, banks are not incentivized to reduce losses in those situations where the financial system is most distressed if strategies u^* were implemented. Appendix 3.6.1 provides a stylized example in order to substantiate this line of thought.

3.3 Orthogonal convexity scenarios (OCS)

In order to overcome the limitation of the SES-based tax as explained in section 3.2, we propose that the regulator should be in a good position to predict (i) how the social costs $SYST$ change in the strategies in the financial system u and (ii) how the banks' SES change in u . With these predictions, the regulator could early detect banks exposing to new risk clusters and could warn other banks that their SES-based tax will increase when they “follow the herd” in terms of the critical engagements.

If $COND(u)$ was fixed and unaffected by u , it would be sufficient for the regulator to monitor how each bank's strategy u_i impacts its SES, and then add up the SES to SYST. Banks with a large initial SES should be prioritized, i.e. their monitoring should be particularly close. Given that $COND(u)$ may in fact depend on u , a first challenge for the regulator is to identify potential changes in strategies which cause that major risks bringing the financial system into distress.

We start with an approach to make the relation $u \mapsto SYST(u)$ more tangible. A technical assumption allows us to employ procedures of the corporate risk management literature.⁴

Assumption (A): $SYST(u)$, as defined in (3.1), is positive homogeneous of degree one, i.e. for all $\lambda > 0$ we have $SYST(\lambda \cdot u) = \lambda \cdot SYST(u)$. Moreover, $SYST(u^{initial}) > 0$ and $SYST(u)$ is twice continuously differentiable at $u^{initial}$.

The assumption of positive homogeneity is not guaranteed in the generically formulated model of Acharya et al., but it seems justifiable, at least in approximation. In terms of the original specification from Acharya et al.,⁵ positive homogeneity means that if, for example, all banks increased all their investments by 5%, increase their debt by 5% and their equity endowment by 5%, then social costs in SYST also increase by 5%.

⁴Analogous assumptions about the relation between portfolio segment volumes and the aggregate portfolio risk can be found in the corporate risk management literature, e.g., in Tasche (2008), Buch et al. (2011), Aigner and Schlütter (2022).

⁵The original specification of Acharya et al. is explained in Appendix 3.6.3.

Under Assumption (A), Euler’s homogeneous function theorem allows to evaluate a firm’s risks by multiplying risk sensitivities with volumes (cf. Tasche, 2008, p. 429). In our context, we can rewrite the social costs of systemic risk as

$$SYST(u) = \sum_{i=1}^N \sum_{j=1}^k \frac{\partial SYST(u)}{\partial u_{ij}} \cdot u_{ij} \quad (3.7)$$

If u_{ij} reflects the business volume of bank i ’s segment j , then the sensitivity of systemic risk with respect to this segment, $\frac{\partial SYST}{\partial u_{ij}}$, multiplied with volume u_{ij} provides the contribution of this segment to the social costs of systemic risk.

The vector collecting all sensitivities,

$$x^{\text{grad}} = \left(\frac{\partial SYST}{\partial u_{11}}, \dots, \frac{\partial SYST}{\partial u_{nk}} \right)^{\text{T}}, \quad (3.8)$$

corresponds to the gradient (or Euler) capital allocation scheme.⁶ Considering the gradient vector as fixed, Eq. (3.7) states that

$$u \mapsto u^{\text{T}} \cdot x^{\text{grad}} \quad (3.9)$$

is a linear approximation of the relation $u \mapsto SYST(u)$. The goodness of this approximation is, however, limited since $SYST(u)$ is not linear when $COND(u)$ may vary in u . The approximation in (3.9) could theoretically be improved by including second-order derivatives in terms of the complete Hessian matrix of $SYST(u)$ and deriving a second-order Taylor polynomial.⁷ Given that the dimension of u , i.e. $N \cdot k$, might be large for a real financial system, the Hessian matrix, which includes $N^2 \cdot k^2$ elements, would be difficult to interpret.

To account for the nonlinearity of $SYST(u)$ with a better interpretable approach than the complete Hessian matrix, Aigner and Schlütter (2022) refer to $x_1 = x^{\text{grad}}$ as the “gradient scenario” and propose to consider a small set of further “orthogonal convexity scenarios” (OCS), x_2, \dots, x_m . With each of the m scenarios, a risk assessment is made analogous to

⁶Cf., e.g., Tasche (2008), Buch and Dorfleitner (2008) and McNeil and Smith (2012) for more details.

⁷In the corporate risk management literature, the corresponding Hessian matrix is used in Gouirieux et al. (2000) and Buch et al. (2011).

line (3.9) and these assessments are aggregated with the root sum of squares,

$$g_m : \mathbb{R}^{N \cdot k} \rightarrow \mathbb{R} \quad (3.10)$$

$$u \mapsto \sqrt{\sum_{l=1}^m u^T \cdot x_l}$$

Function $g_m(u)$ is able to reflect the curvature of $SYST(u)$ for strategies u in a subspace $\text{span}\{w_1, \dots, w_m\}$ of $\mathbb{R}^{N \cdot k}$. Aigner and Schlütter (2022) show that the vectors w_j which are most relevant in terms of convexity of the aggregate risk can be identified by an eigenvalue problem which is similar to a principal component analysis, but not restricted to elliptical distributions. Proposition 3.1, which is technically equivalent to Theorem 1 in Aigner and Schlütter (2022),⁸ summarizes to what extent function $g_m(u)$ reflects $SYST(u)$.

Proposition 3.1. *Let Assumption (A) be fulfilled and let H denote the Hessian matrix of $SYST^2(u)$ evaluated at $u^{initial}$. Consider vectors $w_1, \dots, w_m \in \mathbb{R}^{N \cdot k}$ with $w_1 = u^{initial}$ and $w_i^T \cdot H \cdot w_j = 0$ for all $1 \leq i < j \leq m$. Then function g_m as in Eq. (3.10) in connection with scenarios*

$$x_l = \frac{w_l^T H}{\sqrt{2 \cdot w_l^T H w_l}}, l = 1, \dots, m \quad (3.11)$$

satisfies

- i) $SYST(u^{initial}) = g_m(u^{initial})$
- ii) $\frac{\partial}{\partial h} SYST(u^{initial} + h \cdot v) |_{h=0} = \frac{\partial}{\partial h} g_m(u^{initial} + h \cdot v)$ for all $v \in \mathbb{R}^n$
- iii) $\frac{\partial^2}{\partial u} SYST(u^{initial} + h_1 \cdot v + h_2 \cdot w) |_{h_1=h_2=0} = \frac{\partial^2}{\partial u} g_m(u^{initial} + h_1 \cdot v + h_2 w) |_{h_1=h_2=0}$ for all $v, w \in \text{span}\{w_1, \dots, w_m\}$

We now turn to the relation between banks' strategies u and each bank's SES. To this end, our procedure requires another assumption, namely that banks' losses can be written as

$$LOSS_i(u_i) = \sum_{j=1}^k u_{ij} X_{ij} \text{ for all } i = 1, \dots, N \quad (3.12)$$

The random variables X_{ij} model losses at the level of bank i 's segments, divisions or asset classes, the volumes of which are assumed to be linearly scalable by u_{ij} . Lemma

⁸Therefore, a proof is omitted in this paper.

3.1 transfers the result of Hong and Liu (2009) about the sensitivity of the Expected Shortfall to the context of systemic risk. For notational simplicity, we summarize the overall losses as $LOSS(u) = \sum_{i=1}^N LOSS_i(u_i)$ for $u \in \mathbb{R}^{N \cdot k}$ and denote the Value-at-Risk to a certain α -level as $VaR_\alpha(u^T X)$ with X comprising all X_{ij} .

Lemma 3.1. *Let Assumption (A) be fulfilled, assume that the statement in line (3.12) is fulfilled and let $COND(u)$ be given as*

$$LOSS(u) > VaR_\alpha(u^T X)$$

We assume further that the following three general properties hold:

- i) *It exists a $N \cdot k$ -dimensional random vector K with $E(K) < \infty$ such that $|LOSS(u_1) - LOSS(u_2)| \leq K^T |u_1 - u_2|$ for all $u_1, u_2 \in \mathbb{R}^{N \cdot k}$.*
- ii) *$VaR_\alpha(u^T X)$ is differentiable for any $u \in \mathbb{R}^{N \cdot k}$.*
- iii) *For any $u \in \mathbb{R}^{N \cdot k}$, the probability of $LOSS(u) = VaR_\alpha(u^T X)$ is equal to 0.*

Then, we have

$$SES_i(u_i) = \sum_{j=1}^k \frac{\partial SYST(u)}{\partial u_{ij}} \cdot u_{ij} \quad (3.13)$$

for all $i \in \{1, \dots, N\}$.

With the specific definition of $COND(u)$ in this Lemma, Acharya et al. (2017) denote the SES_i as the Marginal Expected Shortfall, MES_i . On this basis, we will empirically study the systemic risk later on, cf. section 3.4.1 for more details. Notably, assumptions i) - iii) are more of technical use ensuring that $LOSS(u)$ is Lipschitz-continuous and that calculations can indeed be conducted, cf. Hong and Liu (2009, pp. 283-284) for more details.

Proposition 3.2 now provides a linear approximation of the SES_i based on OCS.

Proposition 3.2. *Let the assumptions from Lemma 3.1 be fulfilled. Let x_l^i denote elements $(i-1) \cdot k + 1, \dots, i \cdot k$ of vector x_l , i.e. those elements relating to decision variables of bank i . For all $u \in \text{span}\{w_1, \dots, w_m\}$, we have*

$$\begin{aligned} & SES_i(u^{\text{initial}}) + (\nabla_u SES_i)^T \cdot (u - u^{\text{initial}}) = \\ & = u_i^T \cdot x_1^i + (u - u^{\text{initial}})^T \cdot \frac{\sum_{l=2}^m x_l (x_l^i)^T}{SYST(u^{\text{initial}})} \cdot u_i^{\text{initial}} \end{aligned} \quad (3.14)$$

Whereas Proposition 3.1 has shown that the OCS allow for a second-order approximation of $SYST(u)$, Proposition 3.2 shows that OCS allow for a first-order approximation of the gradient of $SYST(u)$, with the latter directly relating to banks' SES, cf. Eq. (3.13). The left hand-side of Eq. (3.14) is the first-order Taylor polynomial of SES_i at u^{initial} , accounting for $COND(u)$ being adjusted to new strategies u . The first term on the right-hand side, $u_i^T \cdot x_1^i$, corresponds to the SES of bank i choosing strategy u_i , but with condition $COND(u)$ being fixed at strategies u^{initial} . The second-term on the right-hand side employs the OCS to forecast the change in SES_i resulting from the changes in the other banks' strategies.

3.4 Empirical calibration of OCS for systemic risk

3.4.1 Estimation methodology

To allow for an empirical estimation of the systemic risk measures from section 3.2, we consider the loss function for each financial institution $i = 1, \dots, N$ given as

$$LOSS_i(u_i) = \left(\frac{w_1}{w_0} \right)_i \cdot u_i \quad (3.15)$$

where the fraction $\left(\frac{w_1}{w_0} \right)_i$ expresses the overall returns of bank i after one time period comprising all respective decision variables.⁹ However, for our empirical analysis we will employ daily returns of the $N = 36$ financial institutions. u_i represents the market capitalization of the i th financial institute. Further, Acharya et al. (2017, p. 13 f.) then show based on power laws from extreme value theory that the SES_i from line (3.2) relates to the marginal expected shortfall,

$$MES_i^{5\%} = \mathbb{E} \left[\left(\frac{w_1}{w_0} \right)_i - 1 \middle| I_{5\%} \right], \quad (3.16)$$

where the condition $I_{5\%}$ identifies the “5% worst days for the market return”, cf. Acharya et al. (2017, p. 13). As outlined in section 3.2, changes in firms' strategies are likely to impact the condition $COND(u)$ and hence condition $I_{5\%}$. Specifically, changes in strategies can cause different sizes of firms and hence different weights in the composition of the market return.

Our empirical analysis focuses on potential changes in firm sizes measured by their mar-

⁹Appendix 3.6.3 shows in detail how Acharya et al. specify these returns.

ket capitalization. We therefore specify $u = (u_1, \dots, u_N)^T \in \mathbb{R}^N$ as the current market capitalizations in the financial system and

$$I_{5\%}(u) = \left\{ \text{states of world s.t. } \sum_{i=1}^N u_i \cdot \left(\frac{w_1}{w_0} \right)_i \leq q_{5\%} \left(\sum_{i=1}^N u_i \cdot \left(\frac{w_1}{w_0} \right)_i \right) \right\} \quad (3.17)$$

with $q_{5\%}$ being the 5% percentile. Moreover, we replace $\text{SYST}(u)$ from (3.1) by

$$ES(u) : \mathbb{R}^N \rightarrow \mathbb{R}, u \mapsto \mathbb{E} \left[\sum_{i=1}^N u_i \cdot \left(\left(\frac{w_1}{w_0} \right)_i - 1 \right) \middle| I_{5\%}(u) \right] \quad (3.18)$$

According to Lemma 3.1, we have

$$\frac{\partial}{\partial u_i} ES(u) = \mathbb{E} \left[\left(\frac{w_1}{w_0} \right)_i - 1 \middle| I_{5\%}(u) \right] = MES_i^{5\%}(u) \quad (3.19)$$

To determine OCS based on empirical data, we have to estimate H from Eq. (3.11), i.e. the Hessian matrix of $(ES(u))^2$. Recall that the OCS express systemic risk for strategies changing in directions of vectors w_2, \dots, w_m , which point out, for example, anticipated reactions to a new tax. To allow for a proper calibration of OCS, H needs to accurately reflect the curvature of the systemic risk measure specifically when strategies change in directions w_2, \dots, w_m . We therefore do not estimate H by varying u in the direction of the canonical unit vectors e_i ¹⁰, but in the direction of relevant vectors comprised in a matrix $M \in \mathbb{R}^{N \times N}$. Our procedure builds on a basic assertion from differential calculus which is summarized in Lemma 3.2.

Lemma 3.2. *Consider function*

$$f : U \mapsto \mathbb{R}, u \rightarrow f(u)$$

with $U \subset \mathbb{R}^n$ open and assume that f is twice continuously differentiable at $u^{initial} \in U$. Let $H \in \mathbb{R}^{n \times n}$ denote the Hesse matrix of $f(u)$ evaluated at $u^{initial}$. Let $M \in \mathbb{R}^{n \times n}$ be invertible and define $\tilde{H} = H \cdot M$. Then, it holds

$$\tilde{H}_{i,j} = \frac{\partial^2}{\partial h_1 \partial h_2} f(u^{initial} + h_1 \cdot e_i + h_2 \cdot M_{\cdot,j})$$

For the estimation of the Hesse matrix of $(ES(u))^2$, the columns of M will be set based

¹⁰Canonical unit vectors are vectors of dimension $N \cdot k$ (in our context) taking 1 on position i and 0 on all other positions.

on relevant vectors \tilde{w}_i .¹¹ We will determine the entries of matrix \tilde{H}

$$\begin{aligned}\tilde{H}_{i,j} &= \frac{\partial^2}{\partial h_1 \partial h_2} ES(u^{\text{initial}} + h_1 \cdot e_i + h_2 \cdot M_{\cdot,j}) \\ &= \frac{\partial}{\partial h_2} \mathbb{E} \left[\left(\frac{w_1}{w_0} \right)_i - 1 \middle| I_{5\%}(u^{\text{initial}} + h_2 \cdot M_{\cdot,j}) \right]\end{aligned}\quad (3.20)$$

and then derive $H = \tilde{H} \cdot M^{-1}$. The estimation of the interior term in (3.20), i.e.

$$\mathbb{E} \left[\left(\frac{w_1}{w_0} \right)_i - 1 \middle| I_{5\%}(u^{\text{initial}} + h_2 \cdot M_{\cdot,j}) \right], \quad (3.21)$$

is performed straightforward in line with Hong and Liu (2009, p. 284).¹²

3.4.2 Data

We consider $n_1 = 29$ banks and $n_2 = 7$ insurers, cf. Table 3.1. Notably, only banks have been indicated by the Financial Stability Board (FSB) to be “systemically important financial institution” lately. However, due to their high market capitalization it may be necessary to include insurers in the analysis as well. Therefore, we relied on the report of the FSB from 2019 also including the there listed insurance companies additional to the 29 banks indicated in the report from 2021. We consider the daily share prices from 7th October 2012 to 7th October 2022 which are all converted to US dollar using the respective daily exchange rates for company $i = 1, \dots, 36$ and which are denoted by $(s_t)_i$ for day t . Explicitly, we take the relative daily changes r_t as a measure for the stock return. It is given for each firm $i = 1, \dots, 36$ on each day $t > 1$ as¹³

$$(r_t)_i = \frac{(s_t)_i}{(s_{t-1})_i} - 1$$

Due to different public holidays in the countries where the companies are located, different observation days are available. To address this problem, we merge the shares data by date, dropping days in which not all shares are available.¹⁴ Finally, we weight the returns by the market capitalizations at the 7th of October 2022, cf. Table 3.1.

¹¹Cf. the next section for details on the identification of these directions.

¹²As proposed by Hong and Liu (2009, p. 284), we use a strongly consistent estimator for the 5% percentile in (3.17) based on the order statistic. Based on those points in time (i.e. days) from our historical data which are within $I_{5\%}(u)$, we take the average of $\frac{w_1}{w_0} - 1$ for each bank i . Alternative estimation approaches for (3.21) can be found in Gribkova et al. (2022) and referenced literature.

¹³In the sense of Acharya et al. (2017), we set $\left(\frac{w_1}{w_0} \right)_i = \frac{(s_t)_i}{(s_{t-1})_i}$.

¹⁴Addressing this problem differently by, for instance, setting the shares constant if data points are not available does not lead to different results in the latter analysis.

Company	Country	Market cap (in Bn. USD)	Bucket
Bank of America Corp	US	274.08	2
Bank of New York Mellon Corp	US	31.90	1
Citigroup Inc	US	81.71	3
Goldman Sachs Group Inc	US	102.77	2
JPMorgan Chase & Co	US	310.79	4
MetLife Inc	US	50.45	Insurance
Morgan Stanley	US	135.51	1
State Street Corp	US	22.83	1
Wells Fargo & Co	US	158.512	1
Agricultural Bank of China Ltd	CN	139.23	1
Ping An Insurance Group Co of China Ltd	CN	102.19	Insurance
Industrial and Commercial Bank of China Ltd	CN	207.61	2
China Construction Bank Corp	CN	151.32	2
Bank of China Ltd	CN	121.04	2
Mitsubishi UFJ Financial Group Inc	JP	55.48	2
Mizuho Financial Group Inc	JP	28.11	1
Sumitomo Mitsui Financial Group Inc	JP	39.66	1
Aegon NV	NL	8.07	Insurance
Allianz SE	DE	65.06	Insurance
AXA SA	FR	51.67	Insurance
BNP Paribas SA	FR	52.19	3
UniCredit SpA	IT	21.00	1
Deutsche Bank AG	DE	15.43	2
Societe Generale SA	FR	17.02	1
Banco Santander SA	ES	41.16	1
Groupe Cr�dit Agricole	FR	24.96	1
ING Bank	NL	33.63	1
Aviva PLC	UK	12.47	Insurance
Barclays PLC	UK	25.25	2
HSBC Holdings PLC	UK	103.51	3
Prudential PLC	UK	27.80	Insurance
Standard Chartered PLC	UK	18.55	1
Royal Bank of Canada	CA	122.94	1
Toronto-Dominion Bank	CA	108.85	1
Credit Suisse Group AG	CH	11.60	1
UBS Group AG	CH	51.74	1

Table 3.1 The financial institutions indicated by the Financial Stability Board contributing to systemic risk are reported with including the respective buckets, their countries and market capitalizations. The grey cells highlight the ones with the highest market capitalization.

3.4.3 Results

3.4.3.1 Taking a regulator's perspective

As stated before, we are interested in changes in the current market capitalizations in the financial system. Technically, this is given by a vector $u = (u_1, \dots, u_{36})^T \in \mathbb{R}^{36}$ in our set-up. As starting composition, we choose u^{initial} to be the market capitalizations from 3.1.¹⁵ Further, we assume the Expected Shortfall to an α -level of 5% as risk measure, cf. line (3.18).

In order to estimate the Hessian matrix which is necessary for the identification of the OCS in line (3.11), we have to determine relevant directions $\tilde{w}_1, \dots, \tilde{w}_m$ as outlined in section 3.4.1. We set $\tilde{w}_1 = u^{\text{initial}}$ ensuring that we analyze changes in an environment of u^{initial} . The weights $\tilde{w}_2, \dots, \tilde{w}_m$ are then determined successively. For the sake of simplicity, we restrict our analysis to $m = 3$ scenarios to be included. For the estimation of \tilde{w}_2 we run the following steps:

- 1) Set arbitrarily ten of the u_i in u^{initial} to zero and denote the outcome as u_{new}
- 2) Determine the new resulting ES based on u_{new}
- 3) Determine the estimation error $\sqrt{\sum_{i=1}^{36} (MES_i(u_{\text{new}}) - MES_i(MES_i(u^{\text{initial}})))^2}$

We then repeat 1) – 3) for 10000 times and select \tilde{w}_2 as the u_{new} that leads to the biggest estimation error. Thereby, it can be ensured that the selected direction reflects the one that provides the highest error when relying only on the first scenario x_1^{OCS} . By choosing ten companies arbitrarily to be set to zero in 1), we consider various different shifts away from the starting portfolio u^{initial} capturing the directions leading to the strongest convexity. Similarly, we determine \tilde{w}_3 :

- 1) Set arbitrarily ten of the u_i in u^{initial} to zero and denote the outcome as u_{new}
- 2) Determine the new resulting ES based on u_{new}
- 3) Determine the estimation error as $\sum_{i=1}^{36} \varepsilon_i^2$

The ε_i in 3) represent the residuals of regressing $MES_i(u_{\text{new}})$ by $MES_i(\tilde{w}_1)$ and $MES_i(\tilde{w}_2)$ for all $i = 1, \dots, 36$. Again, we repeat 1) – 3) for 10000 times and select \tilde{w}_3 as the direction leading to the highest accumulated error $\sum_{i=1}^{36} \varepsilon_i$. Thereby, we again ensure that

¹⁵Notably, u^{initial} can be set freely and the choice is just made for the sake of illustration.

the most relevant direction not reflected by \tilde{w}_1 and \tilde{w}_2 is chosen. Since we do not want to determine more directions here, we fill up the columns of M , cf. section 3.4.1, with unit vectors $e_i \in \mathbb{R}^{36}$ such that the matrix has full rank. This property is necessary for it to be invertible such that we can proceed as suggested in section 3.4.1.

Afterwards, we can obtain the Hessian matrix H as outlined by lines (3.20) and (3.21) following the estimation process by Hong and Liu (2009).¹⁶ The OCS are then derived as presented in line (3.11) in connection with weightvectors w_1, \dots, w_m as suggested by Aigner and Schlütter (2022, Appendix I).

The resulting scenarios are presented in Table 3.2. We observe that the first scenario — which coincides with the *SES* and the Euler allocation as shown in Lemma 3.1 and Proposition 3.1 — distributes the highest risk to the financial institutions with the highest market capitalizations since these companies have the most severe impact on the financial system. The second scenario provides evidence for the importance of Asian companies assigning the highest losses to exactly those one. Since HSBC Holdings PLC is closely linked to the Asian market due to its history, it is not surprising that it also faces a strong interconnectedness with them. The third scenario additionally highlights some interconnectedness between single companies.

To numerically demonstrate that additional scenarios extending the SES are indeed helpful, we consider the following error measure introduced by Aigner and Schlütter (2022)

$$\text{Error} = \frac{|g_{\text{Taylor}}(u_{m+1}) - g_m(u_{m+1})|}{g_{\text{Taylor}}(u_{m+1})} \quad (3.22)$$

Therein, we employ the observation of Paulusch and Schlütter (2022) that for a positive homogeneous risk measure of degree one the second order polynomial of f can be written as¹⁷

$$g_{\text{Taylor}}(u) := \sqrt{0.5 \cdot u^T H u}$$

Further, it is

$$u_{m+1} = \operatorname{argmax}\{g_{\text{Taylor}}^2(u) - g_m^2(u) \text{ such that } \|u - u^{\text{initial}}\| = 1\}$$

¹⁶It is to note that the estimation process is quite sensitive to the selection of step size. We choose $h = -0.2$ such that even non marginal changes in the market capitalizations can be captured.

¹⁷Notably, this is a rather weak assumption, since the typical risk measures as the Value-at-Risk and the Expected Shortfall fulfill this property, cf. Artzner et al. (1999).

Company	1st OCS	2nd OCS	3rd OCS
Bank of America Corp	12.125	-0.227	1.420
Bank of New York Mellon Corp	1.137	0.077	0.251
Citigroup Inc	3.521	-0.900	-0.183
Goldman Sachs Group Inc	3.728	-0.278	0.204
JPMorgan Chase & Co	11.473	-3.495	-0.014
MetLife Inc	2.112	0.119	0.479
Morgan Stanley	5.565	-0.871	0.152
State Street Corp	0.914	-0.205	0.032
Wells Fargo & Co	6.499	-0.390	1.078
Agricultural Bank of China Ltd	2.270	1.902	-0.246
Ping An Insurance Group Co of China Ltd	1.876	0.670	-0.685
Industrial and Commercial Bank of China Ltd	3.481	8.812	0.923
China Construction Bank Corp	2.519	1.810	-0.344
Bank of China Ltd	1.791	1.113	-0.818
Mitsubishi UFJ Financial Group Inc	0.795	0.358	-0.977
Mizuho Financial Group Inc	0.306	0.044	-0.343
Sumitomo Mitsui Financial Group Inc	0.513	0.179	-0.518
Aegon NV	0.299	-0.235	-0.117
Allianz SE	1.883	-0.259	-0.371
AXA SA	1.698	-0.238	-0.316
BNP Paribas SA	1.988	-1.315	-0.376
UniCredit SpA	0.816	-2.516	2.966
Deutsche Bank AG	0.614	-0.158	-0.094
Societe Generale SA	0.754	-0.537	-0.260
Banco Santander SA	1.654	-0.461	0.112
Groupe Cr�dit Agricole	0.923	-0.408	-0.184
ING Bank	1.441	-0.742	-0.041
Aviva PLC	0.311	-0.009	-0.089
Barclays PLC	1.043	-0.168	-0.182
HSBC Holdings PLC	1.887	-0.823	-1.611
Prudential PLC	1.115	-0.336	-0.363
Standard Chartered PLC	0.467	-0.242	-0.273
Royal Bank of Canada	3.525	0.499	0.941
Toronto-Dominion Bank	3.023	-0.467	0.284
Credit Suisse Group AG	0.468	-0.032	-0.050
UBS Group AG	1.743	-0.269	-0.389
Error	80.81 %	23.69%	0%

Table 3.2 The OCS for systemic risk are reported. The gray cells represent the highest contributions for each scenario. Also the error introduced in line (3.22) is reported for each scenario.

$\hat{u}(h)$	$ES(\hat{u}(h))$	$g_1(\hat{u}(h))$	$g_2(\hat{u}(h))$	$g_3(\hat{u}(h))$
$\hat{u}(1)$	82.04	73.23 (-10.74%)	80.60 (-1.76 %)	80.65 (-1.70%)
$\hat{u}(1.5)$	88.43	66.71 (-24.56%)	83.66 (-5.40%)	83.77 (-5.27%)
$\hat{u}(2)$	111.94	60.19 (-46.23 %)	90.30 (-19.33 %)	90.48 (-19.18%)

Table 3.3 Overall systemic risk for $\hat{u}(h)$ as in line (3.23) based on the expected shortfall and 1-3 OCS. In brackets the relative error compared to the ES is shown

maximizing the error between the Taylor approximation and the scenario based result on the sphere around u^{initial} with a radius one. The results for all three scenarios are reported in the last line in Table 3.1. We observe that including additional scenarios can reduce the error drastically from 80.81% (one scenario) to 0% (three scenarios).

To further demonstrate the advantage of additional scenarios, we inspect how the risk measurement process can be improved inspecting single potential changes in the sizes of market capitalizations. Therefore, we investigate a change in market capitalizations starting from u^{initial} in the sense of

$$\hat{u}(h) = u^{\text{initial}} - h \cdot u_{\text{change}} \quad (3.23)$$

Therein, $u_{\text{change}} \in \mathbb{R}^{36}$ is set such that all entries referring to institutions with a registered office in Asia and, additionally, the entries reflecting the Royal Bank of Canada, MetLife and Bank of New York Mellon are equal to 1.5. All other entries are set to -0.66 . Thereby, we model a change in the sense of the second OCS from Table 3.1. It is to note that for u_{change} it holds $\sum_{i=1}^{36} (u_{\text{change}})_i = 0$. Thus, it does only reflect reallocations in market capitalizations but no increase or decrease in the overall capitalizations. Table 3.3 reports the outcomes and the relative errors for this new composition based on the SES, including additional OCS and the “true” measurement. We observe that including additional scenarios to the SES can reduce the relative error compared to the results based on the expected shortfall. Notably, the situation $h = 2$ reflects that all companies except the above highlighted one become bankrupt. This is for sure a quite unrealistic example, but for illustration it allows us to observe that there is a certain convexity in the systemic risk not captured by the SES. Further, it is to note that the third scenario does not improve the measurement by a lot. This is due to the selection of $\tilde{u}(h)$ which is mostly reflected by the second OCS already.

In terms of changing sensitivities, we inspect Figure 3.1. There, we compare the marginal expected shortfall evaluated at the starting portfolio u^{initial} and evaluated for \tilde{w}_2 and \tilde{w}_3 as identified before. If the sensitivities would not change, we would expect the marginals to lie on a angle-bisecting line. As we note, this is not the case. In the left part of the figure we can see that the sensitivities with respect to the companies highlighted in red, differ. Namely, these institutions are the Asian companies taken into account in our sample. Technically, the OCS allow to meet not just first order but also second-order sensitivities of the expected shortfall, cf. Proposition 3.1. Thereby, also the effect of changing sensitivities can be captured. A similar, but less severe effect can be observed in the right part of the figure inspecting the marginals at \tilde{w}_3 . Notably, there other companies face changing sensitivities. Per construction these are exactly the ones highlighted by the third OCS.

3.4.3.2 Taking an investor's perspective

Let us now put ourselves now in the situation of an investor — instead of the regulator as before — who wants to invest in an equally weighted portfolio comprising all systemically relevant companies. Instead of seeing the portfolio u as vector of market capitalizations, we can also assume it to be the weights of investment decisions. Therefore, we only investigate potential returns and do not multiply them with the market capitalizations. Let us assume, an investor has 36 units to invest and decides to put it in an equally weighted portfolio $u^{\text{initial}} = \mathbb{1}_{36}$.¹⁸ We can then derive OCS as before and obtain the results provided in Table 3.4. Therein, we observe *return* scenarios. We have to interpret the entries as returns in percent and positive values are set to reflect losses. It is to note that the scenarios look very different compared to Table 3.2 since we do no longer deal with systemic risk in general but just implicitly. The first scenario again coincides with the Euler-allocation principle and assigns the highest losses to the European companies. The second OCS highlights the importance of insurance companies to be considered distributing losses to them. Overall, it is to note that insurance companies should play a relevant role in the decision making of an investor since they are assigned high losses.

¹⁸Benartzi and Thaler (2001) find evidence that the so-called naive strategy is widely used. This may be viewed critically due to more sophisticated investment rules available such as the mean-variance optimal portfolio by Markowitz (1952). However, DeMiguel et al. (2009) point out that investing in an equally weighted portfolio can still be a reasonable choice since it does not need any parameter estimation.

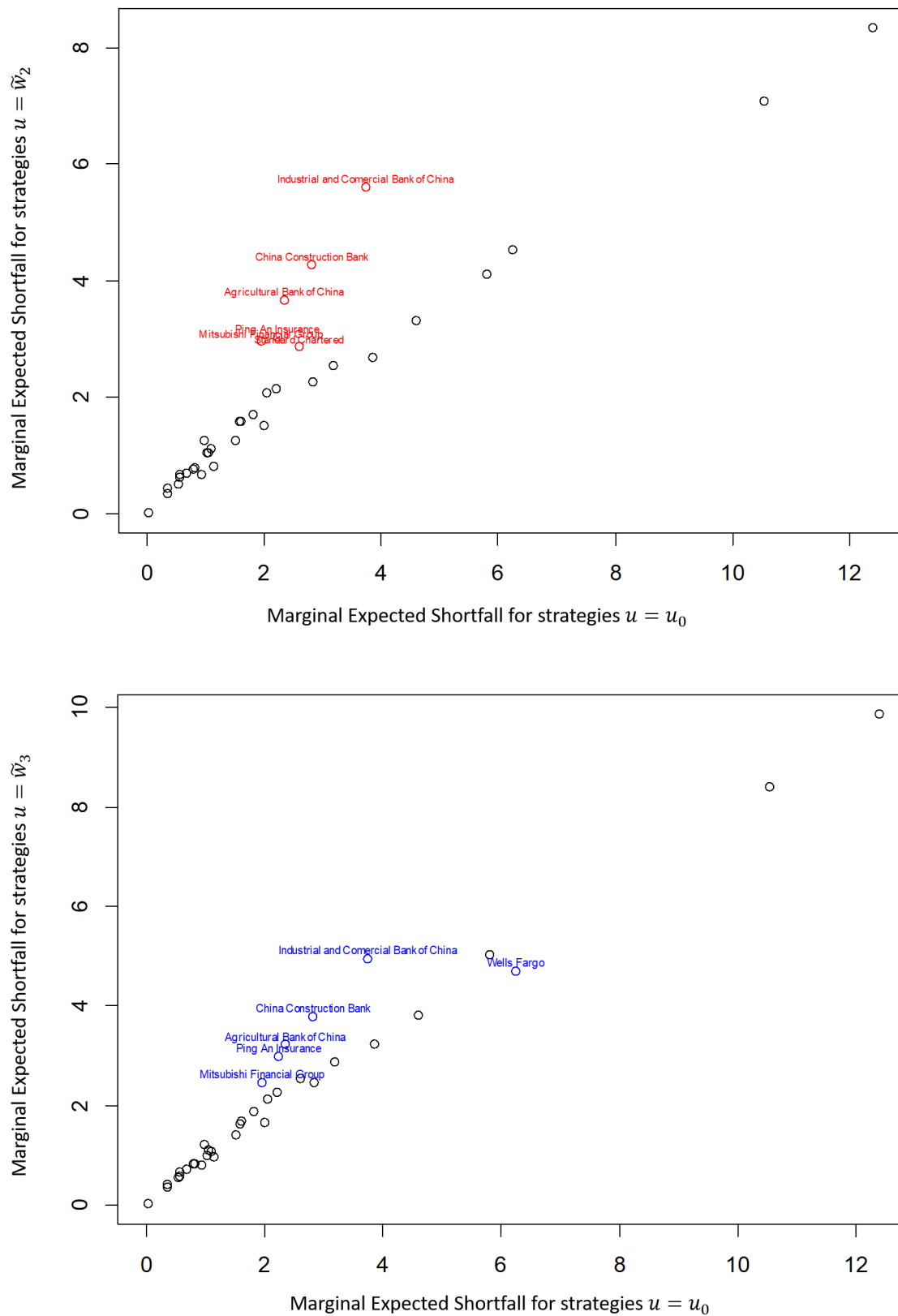


Figure 3.1 Changing sensitivities for new portfolio compositions are shown. The left part compares the marginal expected shortfall at the starting portfolio u^{initial} with the marginals at \tilde{w}_2 . The right part does the same for \tilde{w}_3 .

Company	1st OCS	2nd OCS	3rd OCS
Bank of America Corp	3.82	-1.41	-0.48
Bank of New York Mellon Corp	3.03	0.24	-0.38
Citigroup Inc	4.07	-1.03	-0.56
Goldman Sachs Group Inc	3.18	-1.02	-0.47
JPMorgan Chase & Co	3.26	-0.56	-0.42
MetLife Inc	3.78	-0.57	-0.33
Morgan Stanley	3.8	-0.64	-0.29
State Street Corp	3.47	-0.42	0.25
Wells Fargo & Co	3.39	-0.93	-0.51
Agricultural Bank of China Ltd	1.49	-0.14	-0.04
Ping An Insurance Group Co of China Ltd	1.88	0.78	0.37
Industrial and Commercial Bank of China Ltd	1.5	0.37	-0.02
China Construction Bank Corp	1.63	0.53	0.04
Bank of China Ltd	1.48	0.16	0.01
Mitsubishi UFJ Financial Group Inc	1.82	1.05	-0.4
Mizuho Financial Group Inc	1.49	4.83	-2.04
Sumitomo Mitsui Financial Group Inc	1.63	1.06	0.04
Aegon NV	4.61	0.36	0.2
Allianz SE	3.36	3.51	2.74
AXA SA	3.87	0.79	-0.13
BNP Paribas SA	4.46	-0.22	0.89
UniCredit SpA	4.59	-2.17	1.05
Deutsche Bank AG	4.33	-0.73	1
Societe Generale SA	5.31	0.11	1.01
Banco Santander SA	4.27	-0.72	0.9
Groupe Cr�dit Agricole	4.42	0.02	0.66
ING Bank	4.52	-0.51	-0.01
Aviva PLC	3.09	0.4	0.15
Barclays PLC	3.51	-1.19	-0.39
HSBC Holdings PLC	2.19	0.24	-1.17
Prudential PLC	3.63	0.59	-0.37
Standard Chartered PLC	2.95	-0.02	-1.19
Royal Bank of Canada	2.27	-1.63	-0.4
Toronto-Dominion Bank	2.4	-1.38	-0.46
Credit Suisse Group AG	3.99	0.04	0.28
UBS Group AG	3.49	0.19	0.49

Table 3.4 We provide the resulting scenarios for the investor’s perspective. Notably, we have to interpret positive values as losses. The gray cells highlight the 25% highest losses per scenario.

3.5 Conclusion

This paper demonstrates how Orthogonal Convexity Scenarios can extend the Systemic Expected Shortfall introduced by Acharya et al. (2017) in order to measure systemic risk.

We demonstrate how changes in the current portfolio composition can lead to non-optimal results with respect to the social welfare by including the tax suggested by Acharya et al.. We also demonstrate that, by including OCS into the analysis, the potential convexity in systemic risk can be captured. This allows to evaluate systemic risk even if the market capitalizations of the relevant companies change. We highlight this effect by employing returns data of the financial institutions designated as “systemically important financial institution” by the Financial Stability Board (FSB) (status 2022). We explicitly include insurance companies in our analysis which are often not considered in the discussion about systemic risk. However, they are quite important due to their high market capitalization in the system and our analysis shows that they contribute to the overall systemic risk.

3.6 Appendix

3.6.1 Example: SES-based tax does not induce social optimum

To create an example as simple as possible, we build on the set-up from section 3.4.1. There are $N = 2$ banks in the financial system. The distribution of $\left(\frac{w_1}{w_0}\right)_i$ is governed through a regime-switching model, similar to, e.g., Ang and Chen (2002, p. 447 f.). The random variable Y is uniformly distributed on the interval $[a_{\min}, a_{\max}] = [-0.5, 2.5]$. At time 1, one of the regimes s_1 or s_2 will occur each with a 0.5 probability. Conditioned on regime s_j , the distribution of bank i 's return is given by

$$\left(\frac{w_1}{w_0}\right)_i \Big|_{s_j} = \beta_i(s_j) \cdot Y \quad (3.24)$$

For regime 1, we set $\beta_1(s_1) = 1.5$ and $\beta_2(s_1) = 1$; for regime 2, we set $\beta_1(s_2) = -0.25$ and $\beta_2(s_2) = 1.5$. Banks decide on their market capitalizations u_1 and u_2 . Bank i 's utility is modelled with an exponential utility (EUT) function, exhibiting constant absolute risk aversion (CARA). The risk preference parameter is $\lambda_1 = 1.5$ for bank 1 and $\lambda_2 = 5.5$ for bank 2. Bank i 's expected utility is therefore

$$\begin{aligned} EUT_i(u_i) &= 1 - 0.5 \cdot \sum_{j=1}^2 \int_{x=a_{\min}}^{a_{\max}} \frac{\exp(-\lambda_i \cdot u_i \cdot \beta_j(s_i) \cdot x)}{a_{\max} - a_{\min}} dx \\ &= 1 - 0.5 \cdot \sum_{j=1}^2 \frac{\exp(-\lambda_i \cdot u_i \cdot \beta_j(s_i) \cdot a_{\min}) - \exp(-\lambda_i \cdot u_i \cdot \beta_j(s_i) \cdot a_{\max})}{(a_{\max} - a_{\min}) \cdot \lambda_i \cdot u_i \cdot \beta_j(s_i)} \end{aligned} \quad (3.25)$$

We measure the pre-tax profit of bank i with the certainty equivalent (CE) relating to line (3.25), i.e.

$$\begin{aligned} 1 - \exp(-\lambda_i \cdot CE_i(u_i)) &= EUT_i(u_i) \\ \Leftrightarrow CE_i(u_i) &= -\frac{1}{\lambda_i} \log(1 - EUT_i(u_i)) \end{aligned} \quad (3.26)$$

In the absence of a tax on systemic risk, banks choose strategies which maximize $CE_i(u_i)$. We find that the optimal strategies are $u^{\text{NO TAX}} = (u_1^{\text{NO TAX}}, u_2^{\text{NO TAX}})^T = (0.397, 0.284)^T$.

Social costs from systemic risk are measured with $ES(u)$, as defined in line (3.18), and social welfare with¹⁹

$$SOCIAL(u) = CE_1(u_1) + CE_2(u_2) - ES(u) \quad (3.27)$$

The regulator's objective in line (3.27) is maximized by $u_1^{SOCIAL} = 0.0964$ and $u_2^{SOCIAL} = 0.1347$.

We study the effects of introducing an SES-based tax. The objective of bank i becomes

$$CE_i(u_i) - TAX^i(u_i) = CE_i(u_i) - u_i \cdot MES_i^{5\%}(u) \quad (3.28)$$

As shown in line (3.16), $MES_i^{5\%}(u)$ depends on $I_{5\%}(u)$, which in turn depends on the banks' strategies. For $I_{5\%}(u)$ being determined based on $u^{NO TAX}$, the tax is

$$TAX_1(u_1) = 0.525 \cdot u_1 \text{ and } TAX_2(u_2) = 0.35 \cdot u_2 \quad (3.29)$$

For $I_{5\%}(u)$ being determined based on u^{SOCIAL} , the tax is

$$TAX_1(u_1) = 0.411 \cdot u_1 \text{ and } TAX_2(u_2) = 0.461 \cdot u_2 \quad (3.30)$$

Being confronted with the tax in (3.30), banks' post tax profit is maximal for strategy u^{SOCIAL} ; this result is in line with Proposition 1 from Acharya et al. (2017). Realistically, however, the starting point of the system pre-taxation is $u^{NO TAX}$. Being confronted with the tax corresponding to $u^{NO TAX}$ in (3.29), banks adjust their strategies to $u_1 = 0.045$ and $u_2 = 0.162$. According to these strategies, $MES_i^{5\%}(u)$ is 0.256 for bank 1 and 0.534 for bank 2. Considering a multistage process, Table 3.5 presents banks' strategies at the beginning of the stage, and the $MES_i^{5\%}(u)$ corresponding to these strategies. From stage to stage, $MES_i^{5\%}(u)$ varies between two pairs of value, which alternately assign a relatively heavy contribution to one bank and a light contribution to the other bank; the MES therefore always deviates from the rather balanced MES in (3.30). In consequence, banks react to taxation by taking strategies that too much concentrated either on bank 1 or bank 2. After stage 3, the strategies and MES repeat alternately and hence, the system never converges to the social optimum.

¹⁹For simplicity, we disregard here costs of debt insurance, i.e. component P^2 in Acharya et al. (2017, p. 9). Note, however, that Acharya et al. allow for two parameters c and e which weight the utility of bank owners and the social costs of systemic risk. If these parameters are large, costs of debt insurance are negligible.

Stage	u_1	u_2	MES_1	MES_2
1 (pre taxation)	0.397	0.284	0.525	0.350
2	0.043	0.162	0.256	0.534
3	0.184	0.119	0.525	0.350
4	0.043	0.162	0.256	0.534
5	0.184	0.119	0.525	0.350

Table 3.5 The strategies maximizing banks' profits in the presence of an SES-based tax are reported.

3.6.2 Proof of Lemma 3.1

With the assumptions i) - iii) it follows from Hong and Liu (Theorem 3.1 2009) that

$$\begin{aligned} \frac{\partial}{\partial u_{ij}} SYST(u) &= \frac{\partial}{\partial u_{ij}} \mathbb{E} [LOSS(u) \mid LOSS(u) \geq VaR_\alpha(u^T X)] = \\ &= \mathbb{E} \left[\frac{\partial}{\partial u_{ij}} LOSS(u) \mid LOSS(u) \geq VaR_\alpha(u^T X) \right] \end{aligned}$$

Writing $LOSS_i(u_i)$ as in Eq. (3.12), it is $\frac{\partial}{\partial u_{ij}} LOSS(u) = X_{ij}$. Then, it is

$$\sum_{j=1}^k \frac{\partial}{\partial u_{ij}} SYST(u) \cdot u_{ij} = \sum_{j=1}^k \mathbb{E} [X_{ij} \mid LOSS(u) \geq VaR_\alpha(u^T X)] \cdot u_{ij} = SES_i(u)$$

3.6.3 Specification of $LOSS_i$ and $COND$ in line with Acharya et al. (2017)

We start from the model set-up as defined in Acharya et al. (2017, pp. 6-9) including the following decision variables for each bank $i = 1, \dots, N$. First, $(x_j)_i$ reflects the amount of investments in assets $j = 1, \dots, k$ and are comprised in the total assets as

$$a_i = \sum_{j=1}^k (x_j)_i$$

To finance these investments, a bank can use equity endowment, denoted by $(w_0)_i$, at time $t = 0$ or by taking debt b_i such that it amounts

$$(w_0)_i + b_i = a_i$$

At time $t = 1$, $(r_j)_i$ reflects the per dollar pay-off of asset j invested by bank i .²⁰ The total market value of each bank is then denoted by

$$y_i = \hat{y}_i - \phi_i$$

where ϕ_i are the costs of financial distress and

$$\hat{y}_i = \sum_{j=1}^J (r_j)_i (x_j)_i$$

reflects the pre-distress income. The costs of distress are assumed to depend on the market value of bank assets and the facial value f^i of the outstanding debt

$$\phi_i = \Phi(\hat{y}_i, f_i).$$

In especial, the face value of debt is set, such that it holds

$$b_i = \alpha_i f_i + (1 - \alpha_i) \mathbb{E}[\min(f_i, y_i)]$$

where α_i is a fraction of debt that is assumed to be guaranteed by the government. Overall, these decision variables of bank i are then subsumed by the vector $u_i = ((x_1)_i, \dots, (x_k)_i, b_i, (w_0)_i)$. Moreover, the vector $u = \left((u_1)^\top, \dots, (u_N)^\top \right)^\top \in \mathbb{R}^{N \cdot (J+2)}$ contains the decision variables of all banks in the system.

At time $t = 1$ the net worth of a bank is given as

$$(w_1)_i = \hat{y}_i - \phi_i - f_i$$

In terms of the total system, we denote the aggregate assets and the aggregate debt at time $t = 1$ as

$$A = \sum_{i=1}^N a_i \text{ and}$$

$$W_1 = \sum_{i=1}^N (w_1)_i$$

In such a set-up a financial crisis occurs if the aggregate capital W_1 falls below a fraction z of the assets A .

²⁰Notably, Acharya et al. (2017) allow for assets to be bank-specific reflecting differences in investment opportunities.

3.6.4 Proof of Proposition 3.2

Let $H_{\text{SYST}}(u)$, $H_{g_m}(u)$ and $H_{g_m^2}(u) = 2 \sum_{l=1}^m x_l x_l^\top$ denote the Hessian of functions $\text{SYST}(u)$, $g_m(u)$ and $g_m^2(u)$ evaluated at u . We rewrite Eq. (3.13) as

$$SES_i(u) = (\nabla_{u_i} \text{SYST})^\top \cdot u_i \quad (3.31)$$

and hence, we have

$$\nabla_u SES_i(u^{\text{initial}}) = (H_{\text{SYST}}(u^{\text{initial}}))_{\cdot, \text{dec}(i)} \cdot u_i^{\text{initial}} + \overline{\nabla_{u_i} \text{SYST}} \quad (3.32)$$

with $\text{dec}(i) = \{(i-1) \cdot k + 1, \dots, i \cdot k\}$ denoting the positions of the decision variables of bank i in u , and $\overline{\nabla_{u_i} \text{SYST}}$ being an $(N \cdot k)$ -dimensional column vector which includes $\nabla_{u_i} \text{SYST}(u^{\text{initial}})$ in entries $\text{dec}(i)$ and 0 in all other entries. Note that

$$\begin{aligned} \nabla_u g^2(u) &= 2g(u) \cdot \nabla_u g(u) \\ H_{g^2}(u) &= 2g(u) \cdot H_g(u) + 2\nabla_u g(u) (\nabla_u g(u))^\top \\ \Rightarrow H_g(u^{\text{initial}}) &= \frac{1}{g(u^{\text{initial}})} \left(\sum_{l=1}^m x_l x_l^\top - x_1 x_1^\top \right) = \frac{\sum_{l=2}^m x_l x_l^\top}{\text{SYST}(u^{\text{initial}})} \end{aligned} \quad (3.33)$$

For all $u_1, u_2 \in \text{span}\{w_1, \dots, w_m\}$, the last assertion of Proposition 3.1 implies $u_1^\top H_{\text{SYST}}(u^{\text{initial}}) \cdot u_2 = u_1^\top H_g(u^{\text{initial}}) \cdot u_2$. Therefore,

$$\begin{aligned} & SES_i(u^{\text{initial}}) + (\nabla_u SES_i)^\top \cdot (u - u^{\text{initial}}) \\ \stackrel{\text{Eq. (3.32)}}{=} & SES_i(u^{\text{initial}}) + (u - u^{\text{initial}})^\top \cdot (H_{\text{SYST}}(u^{\text{initial}}))_{\cdot, \text{dec}(i)} \cdot u_i^{\text{initial}} \\ & + (u - u^{\text{initial}})^\top \cdot \overline{\nabla_{u_i} \text{SYST}} \\ \stackrel{\text{Eq. (3.33)}}{=} & SES_i(u^{\text{initial}}) + (u - u^{\text{initial}})^\top \cdot \frac{\sum_{l=2}^m x_l (x_l^i)^\top}{\text{SYST}(u^{\text{initial}})} \cdot u_i^{\text{initial}} \\ & + u_i^\top \cdot x_1^i - (u_i^{\text{initial}})^\top \cdot x_1^i \\ = & u_i^\top \cdot x_1^i + (u - u^{\text{initial}})^\top \cdot \frac{\sum_{l=2}^m x_l (x_l^i)^\top}{\text{SYST}(u^{\text{initial}})} \cdot u_i^{\text{initial}} \end{aligned}$$

3.6.5 Proof of Lemma 3.2

Let D_v denote the first order directional derivative in the direction $v \in \mathbb{R}^n$, such that

$$\frac{\partial}{\partial h_1} f(u^{\text{initial}} + h_1 \cdot v) = D_v f(u^{\text{initial}})$$

It is now a result from basic Analysis that

$$D_v f(u^{\text{initial}}) = \langle v, \nabla_u f(u^{\text{initial}}) \rangle = v^T \cdot \nabla_u f(u^{\text{initial}})$$

where $\langle \cdot, \cdot \rangle$ denotes the euclidean dot product and ∇ the gradient of f . To obtain the second order directional derivative in the direction $v, w \in \mathbb{R}^n$, denoted as $D_w D_v f(u^{\text{initial}}) = \frac{\partial^2}{\partial h_1 \partial h_2} f(u^{\text{initial}} + h_1 \cdot v + h_2 \cdot w)$, we employ the chain rule and write

$$D_w D_v f(u^{\text{initial}}) = \langle w, \nabla(D_v f(u^{\text{initial}})) \rangle = \langle w, \langle v, \frac{\partial^2}{\partial^2 u} f(u^{\text{initial}}) \rangle \rangle = \langle w, \langle v, H \rangle \rangle = w^T H v$$

In summary, we obtain

$$\frac{\partial^2}{\partial h_1 \partial h_2} f(u^{\text{initial}} + h_1 \cdot v + h_2 \cdot w) = w^T H v$$

Setting $w = e_i$ iteratively and $v = M_{.,j}$ shows then Lemma 3.2.

3.6.6 Derivation of MES in the example from Appendix 3.6.1

Per definition, it is $Y \in [-0.5, 2.5]$ and

$$\beta_i(s_j) = \begin{cases} 1.5, & \text{if } i=j=1 \\ 1, & \text{if } i=2, j=1 \\ -0.25, & \text{if } i=1, j=2 \\ 1.5, & \text{if } i=j=2 \end{cases}$$

Overall, we are interested in the expected shortfall of the combined portfolio depending on exposures $u = (u_1, u_2)^T$

$$Z(u) := \begin{pmatrix} w_0 \\ w_1 \end{pmatrix}_1 \cdot u_1 + \begin{pmatrix} w_0 \\ w_1 \end{pmatrix}_2 \cdot u_2 \stackrel{\text{Eq.(3.24)}}{=} (\beta_1(s_j) \cdot u_1 + \beta_2(s_j) \cdot u_2) \cdot Y \quad (3.34)$$

differentiating between regime $j = 1$ and $j = 2$. Notably, the calculations are only done for $j = 1$ and could be analogously derived for $j = 2$

With the specification of Y to lie in a certain interval $[a_{\min}, a_{\max}]$, we can define breaks as shown in Figure 3.2 which distinguish between the respective regimes and depend on

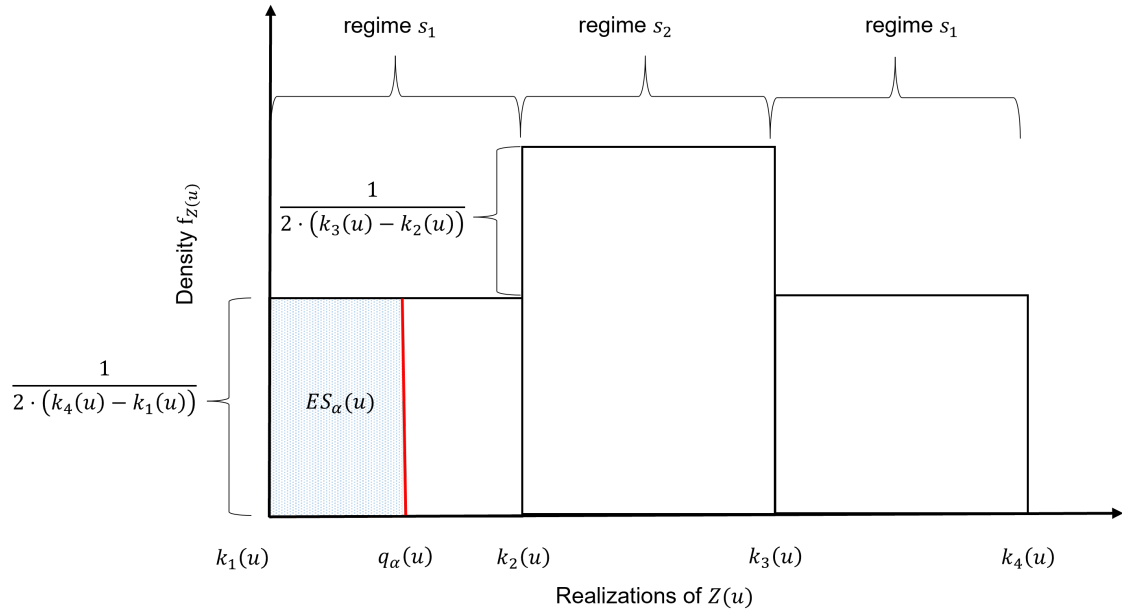


Figure 3.2 We report the density function of $Z(u)$ as in Eq. (3.34) graphically. Notably, the intervals depend on the selection of portfolio u and are not necessarily equidistant.

the exposure $u = (u_1, u_2)^T$

$$k_1(u) = \min(a_{\min} \cdot \beta_1(s_1) \cdot u_1 + a_{\min} \cdot \beta_2(s_1) \cdot u_2, a_{\min} \cdot \beta_1(s_2) \cdot u_1 + a_{\min} \cdot \beta_2(s_2) \cdot u_2)$$

$$k_2(u) = \max(a_{\min} \cdot \beta_1(s_1) \cdot u_1 + a_{\min} \cdot \beta_2(s_1) \cdot u_2, a_{\min} \cdot \beta_1(s_2) \cdot u_1 + a_{\min} \cdot \beta_2(s_2) \cdot u_2)$$

$$k_3(u) = \min(a_{\max} \cdot \beta_1(s_1) \cdot u_1 + a_{\max} \cdot \beta_2(s_1) \cdot u_2, a_{\max} \cdot \beta_1(s_2) \cdot u_1 + a_{\max} \cdot \beta_2(s_2) \cdot u_2)$$

$$k_4(u) = \max(a_{\max} \cdot \beta_1(s_1) \cdot u_1 + a_{\max} \cdot \beta_2(s_1) \cdot u_2, a_{\max} \cdot \beta_1(s_2) \cdot u_1 + a_{\max} \cdot \beta_2(s_2) \cdot u_2)$$

In especial, $k_1(u)$ is the lowest and $k_4(u)$ the highest possible value, which the random variable in Eq. (3.34) can take. The respective quantile function $q_\alpha(u)$ of the random variable, depending on the confidence level α and the exposure vector u , is then given by solving

$$\int_{k_1(u)}^{q_\alpha(u)} f_{Z(u)}(x) dx = \alpha$$

and results in

$$q_\alpha(u) = \begin{cases} k_1(u) + 2\alpha(k_4(u) - k_1(u)), & \text{if } \frac{k_2(u) - k_1(u)}{k_4(u) - k_1(u)} > 2\alpha \\ \frac{(2\alpha \cdot (k_3(u) - k_2(u)) + k_2(u) + \frac{k_1(u) \cdot (k_3(u) - k_2(u))}{k_4(u) - k_1(u)})}{(1 + \frac{k_3(u) - k_2(u)}{k_4(u) - k_1(u)})}, & \text{else} \end{cases}$$

only differentiating between state 1 and state 2. We can then derive the expected shortfall

by solving

$$ES_\alpha(u) = -\frac{1}{\alpha} \int_0^\alpha q_\gamma(u) d\gamma$$

resulting in

$$ES_\alpha(u) = -\frac{q_\alpha(u) + k_1(u)}{2} \quad (3.35)$$

if $\frac{k_2(u)-k_1(u)}{k_4(u)-k_1(u)} > 2\alpha$ and

$$ES_\alpha(u) = - \left(0.25 \cdot \frac{k_2(u) - k_1(u)}{k_4(u) - k_1(u)} \cdot (k_1(u) + k_2(u)) \right) \cdot \alpha^{-1} \quad (3.36)$$

$$+ \left(\left(\alpha - \frac{k_2(u) - k_1(u)}{k_4(u) - k_1(u)} \cdot \alpha \right) \cdot 0.5 \cdot (q_\alpha(u) + k_2(u)) \right) \cdot \alpha^{-1}$$

otherwise. Taking then the derivative of Eq. (3.35) and (3.36) with respect to u then allows to determine the $MES_i^{5\%}(u)$

References

- Acharya, V.V., Pedersen, L.H., Philippon, T., Richardson, M., 2017. Measuring systemic risk. *The Review of Financial Studies* 30, 2–47.
- Aigner, P., Schlütter, S., 2022. Enhancing gradient capital allocation with orthogonal convexity scenarios. Working Paper , 1–5.
- Ang, A., Chen, J., 2002. Asymmetric correlations of equity portfolios. *Journal of Financial Economics* 63, 443–494.
- Artzner, P., Delbaen, F., Eber, J.M., Heath, D., 1999. Coherent measures of risk. *Mathematical Finance* 9, 203–228.
- Benartzi, S., Thaler, R.H., 2001. Naive diversification strategies in defined contribution saving plans. *American Economic Review* 91, 79–98.
- Buch, A., Dorfleitner, G., 2008. Coherent risk measures, coherent capital allocations and the gradient allocation principle. *Insurance: Mathematics and Economics* 42, 235–242.
- Buch, A., Dorfleitner, G., Wimmer, M., 2011. Risk capital allocation for RORAC optimization. *Journal of Banking & Finance* 35, 3001–3009.
- DeMiguel, V., Garlappi, L., Uppal, R., 2009. Optimal versus naive diversification: How inefficient is the $1/n$ portfolio strategy? *The Review of Financial Studies* 22, 1915–1953.
- Diers, D., 2011. Management strategies in multi-year enterprise risk management. *The Geneva Papers on Risk and Insurance - Issues and Practice* 36, 107–125.
- Erel, I., Myers, S.C., Read Jr, J.A., 2015. A theory of risk capital. *Journal of Financial Economics* 118, 620–635.
- Feinstein, Z., Rudloff, B., Weber, S., 2017. Measures of systemic risk. *SIAM Journal on Financial Mathematics* 8, 672–708.
- Gourieroux, C., Laurent, J.P., Scaillet, O., 2000. Sensitivity analysis of values at risk. *Journal of Empirical Finance* 7, 225–245.

- Gribkova, N., Su, J., Zitikis, R., 2022. Inference for the tail conditional allocation: large sample properties, insurance risk assessment, and compound sums of concomitants. *Insurance: Mathematics and Economics* 107, 199–222.
- Gründl, H., Schmeiser, H., 2007. Capital allocation for insurance companies—what good is it? *Journal of Risk and Insurance* 74, 301–317.
- Hong, L.J., Liu, G., 2009. Simulating sensitivities of conditional value at risk. *Management Science* 55, 281–293.
- Markowitz, H., 1952. The utility of wealth. *Journal of Political Economy* 60, 151–158.
- McNeil, A.J., Smith, A.D., 2012. Multivariate stress scenarios and solvency. *Insurance: Mathematics and Economics* 50, 299–308.
- Mildenhall, S.J., 2004. A note on the myers and read capital allocation formula. *North American Actuarial Journal* 8, 32–44.
- Myers, S.C., Read, J.A., 2001. Capital allocation for insurance companies. *Journal of Risk and Insurance* 68, 545–580.
- Paulusch, J., Schlütter, S., 2022. Sensitivity-implied tail-correlation matrices. *Journal of Banking & Finance* 134, 106333.
- Targino, R.S., Peters, G.W., Shevchenko, P.V., 2015. Sequential monte carlo samplers for capital allocation under copula-dependent risk models. *Insurance: Mathematics and Economics* 61, 206–226.
- Tasche, D., 2008. Capital allocation to business units and sub-portfolios: The Euler principle, in: Resti, A. (Ed.), *Pillar II in the New Basel Accord: The Challenge of Economic Capital*. Risk Books, London, pp. 423–453.
- Tasche, D., 2009. Capital allocation for credit portfolios with kernel estimators. *Quantitative Finance* 9, 581–595.

Conclusion

This work provides and deeply evaluates a newly developed methodology for a scenario-based risk measurement. We theoretically develop so-called “orthogonal convexity scenarios” in chapter 1, where we demonstrate that they allow the translation of portfolio risk into several multivariate scenarios concerning profits or losses of portfolio components. Aggregating the outcomes resulting from the scenarios then allows the proper depiction of the overall risk of the evaluated portfolio. In particular, due to the selection of multiple scenarios, the scenario-based measurement even allows the capturing of new risk situations when the exposures to the single risk factors change.²¹ This property allows the overcoming of the deficiencies faced by the gradient capital allocation, cf. Tasche (2009) or McNeil and Smith (2012). We can thus gain a more detailed insight into the composition of a risk portfolio in a simple, deterministic manner, thereby directly addressing the first problem mentioned at the beginning of this work, namely the lack of communicability of risk measurement. Technically, we determine scenarios in a similar way to the well-studied “Principal Component Analysis” (PCA). The PCA may be a useful tool but is limited to multivariate elliptically distributed risk vectors and to linear dependencies, since it is based on the covariance matrix. Instead we employ a more sophisticated methodology – the so-called “sensitivity-implied tail-correlation matrix” – by Paulusch and Schlütter (2022). Here, no distributional assumption to the evaluated risk vector is necessary and nonlinear dependencies can also be captured. This opens a wide field of applications for our scenarios. Some of them are already sketched in chapter 1, and two are evaluated in detail in chapters 2 and 3 of this work.

The first general application studied addresses the limitations of regulatory approaches that do not necessarily meet the true risk. As outlined in the literature, cf. for instance Gatzert and Martin (2012) or Eckert et al. (2016), there may be a gap between the risk measurement results based on a standardized approach, such as regulatory approaches, and the “true” portfolio risk faced by a financial institution. We show that approximating the residual between the two approaches based on the OCS allows the identification of risks that are not captured by the regulatory calculations. We namely observe that the assumption made under Solvency of government bonds being spread-risk free, is not

²¹For instance, a company may decide to reallocate their capital among the risk drivers.

valid.²² Moreover, we demonstrate empirically by considering stock and bond investments in the context of insurance companies and market risk that the scenario-based measurement indeed allows the closing of the gap between the two approaches. The OCS provide a tool in this case adjusting the standard formula to meet the true risk of an insurance company. A regulatory authority may then, for instance, derive the OCS for an exemplary insurer and provide the outcome to the insurance companies supervised in addition to the standard formula.

The second application of the OCS that is demonstrated in detail refers to systemic risk. This type of risk imposes a significant threat to modern economies in general by potentially leading to social costs such as bailout payments by governments. By holding insufficient capital or setting up a portfolio that faces high losses when the whole market is under stress, individual companies contribute to systemic risk. In order to internalize systemic risk into capital requirements placed on financial institutions, there is some literature that designs tax policies to buffer the associated social costs. We show that the OCS can extend and improve the taxing methodology provided by Acharya et al. (2017). The approach relies on the so-called “Systemic Expected Shortfall” (SES), which shows several similarities to the gradient capital allocation. However, the gradient capital allocation is shown to be of limited use by the examples in Gründl and Schmeiser (p. 310 ff. 2007) and Diers (pp. 113 ff. 2011). We show that the OCS extend the approach by including additional scenarios such that changes in the contribution of single companies to the overall systemic risk are reflected. We thereby provide the regulator with a tool to quantify and adjust taxing and capital requirements for systemic risk.

Overall, this work can help to answer the central questions remaining open to risk management nowadays that we posed at the beginning: we provide a simple but reliable risk measurement methodology that is easy to communicate but can depict the risk profile of a company in a broader sense than competing approaches. We also provide suggestions of how to directly implement the recommendations in terms of regulatory requirements, addressing the problem of potentially misleading risk steering based on standardized approaches. Finally, we show the effectiveness of the OCS-based risk measurement in several settings and based on theoretical and empirical considerations.

²²This observation is in line with Gatzert and Martin (2012).

References

- Acharya, V.V., Pedersen, L.H., Philippon, T., Richardson, M., 2017. Measuring systemic risk. *The Review of Financial Studies* 30, 2–47.
- Aebi, V., Sabato, G., Schmid, M., 2012. Risk management, corporate governance, and bank performance in the financial crisis. *Journal of Banking & Finance* 36, 3213–3226.
- Aigner, P., Schlütter, S., 2022. Enhancing gradient capital allocation with orthogonal convexity scenarios. Working Paper , 1–5.
- Albrecher, H., Bauer, D., Embrechts, P., Filipović, D., Koch-Medina, P., Korn, R., Loisel, S., Pelsser, A., Schiller, F., Schmeiser, H., et al., 2018. Asset-liability management for long-term insurance business. *European Actuarial Journal* 8, 9–25.
- Ang, A., Chen, J., 2002. Asymmetric correlations of equity portfolios. *Journal of Financial Economics* 63, 443–494.
- Artzner, P., Delbaen, F., Eber, J.M., Heath, D., 1999. Coherent measures of risk. *Mathematical Finance* 9, 203–228.
- Asadi, S., Al Janabi, M.A., 2020. Measuring market and credit risk under solvency ii: Evaluation of the standard technique versus internal models for stock and bond markets. *European Actuarial Journal* 10, 425–456.
- Aven, T., 2016. Risk assessment and risk management: Review of recent advances on their foundation. *European Journal of Operational Research* 253, 1–13.
- Becker, B., Ivashina, V., 2015. Reaching for yield in the bond market. *The Journal of Finance* 70, 1863–1902.
- Benartzi, S., Thaler, R.H., 2001. Naive diversification strategies in defined contribution saving plans. *American Economic Review* 91, 79–98.
- Braun, A., Schmeiser, H., Schreiber, F., 2017. Portfolio optimization under Solvency II: Implicit constraints imposed by the market risk standard formula. *Journal of Risk and Insurance* 84, 177–207.

- Breuer, T., Csiszár, I., 2013a. Systematic stress tests with entropic plausibility constraints. *Journal of Banking & Finance* 37, 1552–1559.
- Breuer, T., Csiszár, I., 2013b. Systematic stress tests with entropic plausibility constraints. *Journal of Banking & Finance* 37, 1552–1559.
- Buch, A., Dorfleitner, G., 2008. Coherent risk measures, coherent capital allocations and the gradient allocation principle. *Insurance: Mathematics and Economics* 42, 235–242.
- Buch, A., Dorfleitner, G., Wimmer, M., 2011. Risk capital allocation for RORAC optimization. *Journal of Banking & Finance* 35, 3001–3009.
- Bundesanstalt für Finanzdienstleistungsaufsicht (BaFin), 2016. Governmentbonds: Treatment of risk under solvency ii. URL: <https://www.bafin.de/dok/8136732>.
- Bundesanstalt für Finanzdienstleistungsaufsicht (BaFin), 2017. Annotated text of the minimum requirements for risk management (marisk). URL: https://www.bafin.de/SharedDocs/Downloads/EN/Rundschreiben/dl_rs0917_marisk_Endfassung_2017_pdf_ba_en.html;jsessionid=44EC3F74F3FAE78875982C06B6B937A1.2_cid503?nn=9866146.
- Casella, G., Berger, R., 2002. *Statistical Inference*, 2nd Edition. Duxbury.
- Chen, T., Goh, J.R., Kamiya, S., Lou, P., 2019. Marginal cost of risk-based capital and risk-taking. *Journal of Banking & Finance* 103, 130–145.
- Christensen, J.H., Rudebusch, G.D., 2015. Estimating shadow-rate term structure models with near-zero yields. *Journal of Financial Econometrics* 13, 226–259.
- Clay, D., Lay, S.R., McDonald, J.J., 2015. *Linear Algebra and Its Applications*, 5th Edition. Pearson.
- Committee of European Insurance and Occupational Pensions Supervisors (CEIOPS), 2010. Quantitative impact study 5 - questions & answers. URL: <https://eiopa.europa.eu>.
- Cramér, H., 1946. A contribution to the theory of statistical estimation. *Scandinavian Actuarial Journal* 1946, 85–94.

- Darmois, G., 1945. Sur les limites de la dispersion de certaines estimations. *Revue de l'Institut International de Statistique*, 9–15.
- DeMiguel, V., Garlappi, L., Uppal, R., 2009. Optimal versus naive diversification: How inefficient is the 1/n portfolio strategy? *The Review of Financial Studies* 22, 1915–1953.
- Diers, D., 2011. Management strategies in multi-year enterprise risk management. *The Geneva Papers on Risk and Insurance - Issues and Practice* 36, 107–125.
- Doff, R., 2016. The final solvency ii framework: will it be effective? *The Geneva Papers on Risk and Insurance-Issues and Practice* 41, 587–607.
- Duffie, D., Singleton, K.J., 1999. Modeling term structures of defaultable bonds. *The Review of Financial Studies* 12, 687–720.
- Eckert, J., Gatzert, N., Martin, M., 2016. Valuation and risk assessment of participating life insurance in the presence of credit risk. *Insurance: Mathematics and Economics* 71, 382–393.
- Eling, M., Schmeiser, H., 2010. Insurance and the credit crisis: Impact and ten consequences for risk management and supervision. *The Geneva Papers on Risk and Insurance–Issues and Practice* 35, 9–34.
- Erel, I., Myers, S.C., Read Jr, J.A., 2015. A theory of risk capital. *Journal of Financial Economics* 118, 620–635.
- European Commission, 2015. Commission Delegated Regulation (EU) 2015/35 of 10 October 2014 supplementing Directive 2009/138/EC of the European Parliament and of the Council on the taking-up and pursuit of the business of Insurance and Reinsurance (Solvency II) .
- European Insurance and Occupational Pensions Authority (EIOPA), 2011. Report on the fifth Quantitative Impact Study (QIS5) for Solvency II. URL: https://www.eiopa.europa.eu/content/guidelines-own-risk-solvency-assessment-orsa_en.
- European Insurance and Occupational Pensions Authority (EIOPA), 2015. Guidelines on own risk and solvency assessment. URL:

https://www.eiopa.europa.eu/document-library/guidelines/guidelines-own-risk-solvency-assessment-orsa_en_en.

European Insurance and Occupational Pensions Authority (EIOPA), 2019. Insurance Statistics. URL: https://www.eiopa.europa.eu/tools-and-data/insurance-statistics_en.

Feinstein, Z., Rudloff, B., Weber, S., 2017. Measures of systemic risk. *SIAM Journal on Financial Mathematics* 8, 672–708.

Fergusson, K., Platen, E., 2015. Application of maximum likelihood estimation to stochastic short rate models. *Annals of Financial Economics* 10, 1550009.

Financial Stability Board, 2013. Principles for an effective risk appetite framework. Consultative Document .

Fischer, K., Schlütter, S., 2015. Optimal investment strategies for insurance companies when capital requirements are imposed by a standard formula. *Geneva Risk and Insurance Review* 40, 15–40.

Frye, J., 1997. Principals of risk: Finding var through factor-based interest rate scenarios, in: *VAR: Understanding and Applying Value at Risk*. Risk Publications, London, pp. 275–288.

Gatzert, N., Martin, M., 2012. Quantifying credit and market risk under Solvency II: Standard approach versus internal model. *Insurance: Mathematics and Economics* 51, 649–666.

Golub, B.W., Tilman, L.M., 1997. Measuring yield curve risk using principal components analysis, value at risk, and key rate durations. *Journal of Portfolio Management* 23, 72.

Gómez, F., Tang, Q., Tong, Z., 2022. The gradient allocation principle based on the higher moment risk measure. *Journal of Banking & Finance* 143, 106544.

Gourieroux, C., Laurent, J.P., Scaillet, O., 2000. Sensitivity analysis of values at risk. *Journal of Empirical Finance* 7, 225–245.

- Graf, S., Korn, R., 2020. A guide to monte carlo simulation concepts for assessment of risk-return profiles for regulatory purposes. *European Actuarial Journal* 10, 273–293.
- Gribkova, N., Su, J., Zitikis, R., 2022. Inference for the tail conditional allocation: large sample properties, insurance risk assessment, and compound sums of concomitants. *Insurance: Mathematics and Economics* 107, 199–222.
- Gründl, H., Schmeiser, H., 2007. Capital allocation for insurance companies—what good is it? *Journal of Risk and Insurance* 74, 301–317.
- Guo, Q., Bauer, D., Zanjani, G., 2021. Capital allocation techniques: Review and comparison. *Variance* 14.
- Hong, L.J., Liu, G., 2009. Simulating sensitivities of conditional value at risk. *Management Science* 55, 281–293.
- Huber, C., Scheytt, T., 2013. The dispositif of risk management: Reconstructing risk management after the financial crisis. *Management Accounting Research* 24, 88–99.
- Hull, J.C., 2018. *Risk Management and Financial Institutions*. Wiley Finance Series. 5th Edition.
- Islam, M.R., Nguyen, N., 2020. Comparison of financial models for stock price prediction. *Journal of Risk and Financial Management* 13, 181.
- Jorion, P., 2006. *Value at risk: The new benchmark for managing financial risk*. New York: McGraw–Hill .
- Korn, R., Müller, L., 2021. Optimal portfolios in the presence of stress scenarios a worst-case approach. *Mathematics and Financial Economics* , 1–33.
- Liang, J., Ma, J.M., Wang, T., Ji, Q., 2011. Valuation of portfolio credit derivatives with default intensities using the vasicek model. *Asia-Pacific Financial Markets* 18, 33–54.
- Lintner, J., 1965. Security prices, risk, and maximal gains from diversification. *The Journal of Finance* 20, 587–615.
- Macaulay, F.R., 1938. Front matter to” some theoretical problems suggested by the movements of interest rates, bond yields and stock prices in the united states since

- 1856”, in: Some Theoretical Problems Suggested by the Movements of Interest Rates, Bond Yields and Stock Prices in the United States since 1856. NBER, pp. 15–6.
- Makam, V.D., Millossovich, P., Tsanakas, A., 2021. Sensitivity analysis with χ^2 -divergences. *Insurance: Mathematics and Economics* 100, 372–383.
- Markowitz, H., 1952. The utility of wealth. *Journal of Political Economy* 60, 151–158.
- McNeil, A.J., Frey, R., Embrechts, P., 2015. *Quantitative Risk Management: Concepts, Techniques and Tools - Revised Edition*. Princeton Series in Finance.
- McNeil, A.J., Smith, A.D., 2012. Multivariate stress scenarios and solvency. *Insurance: Mathematics and Economics* 50, 299–308.
- Mildenhall, S.J., 2004. A note on the myers and read capital allocation formula. *North American Actuarial Journal* 8, 32–44.
- Mitnik, S., 2014. VaR-implied tail-correlation matrices. *Economics Letters* 122, 69–73.
- Mossin, J., 1966. Equilibrium in a capital asset market. *Econometrica: Journal of the Econometric Society* , 768–783.
- Myers, S.C., Read, J.A., 2001. Capital allocation for insurance companies. *Journal of Risk and Insurance* 68, 545–580.
- Nordström, K., 1991. The concentration ellipsoid of a random vector revisited. *Econometric Theory* 7, 397–403.
- Packham, N., Woebbecking, C., 2019. A factor-model approach for correlation scenarios and correlation stress testing. *Journal of Banking & Finance* 101, 92–103.
- Panjer, H.H., 2002. Measurement of risk, solvency requirements and allocation of capital within financial conglomerates. Institute of Insurance and Pension Research, University of Waterloo, Research Report , 01–15.
- Paulusch, J., 2017. The Solvency II standard formula, linear geometry, and diversification. *Journal of Risk and Financial Management* 10, 11.
- Paulusch, J., Schlütter, S., 2022. Sensitivity-implied tail-correlation matrices. *Journal of Banking & Finance* 134, 106333.

- Pesenti, S.M., Millossovich, P., Tsanakas, A., 2019. Reverse sensitivity testing: What does it take to break the model? *European Journal of Operational Research* 274, 654–670.
- Pfeifer, D., Strassburger, D., 2008. Solvency II: stability problems with the SCR aggregation formula. *Scandinavian Actuarial Journal* 1, 61–77.
- Rockafellar, R.T., Uryasev, S., et al., 2000. Optimization of conditional value-at-risk. *Journal of Risk* 2, 21–42.
- Rosenberg, J.V., Schuermann, T., 2006. A general approach to integrated risk management with skewed, fat-tailed risks. *Journal of Financial Economics* 79, 569–614.
- Scherer, M., Stahl, G., 2021. The standard formula of solvency ii: a critical discussion. *European Actuarial Journal* 11, 3–20.
- Schilling, K., Bauer, D., Christiansen, M.C., Kling, A., 2020. Decomposing dynamic risks into risk components. *Management Science* 66, 5738–5756.
- Schlütter, S., 2021. Scenario-based measurement of interest rate risks. *The Journal of Risk Finance* 22 No. 1, 56–77.
- Schönbucher, P.J., 2003. *Credit derivatives pricing models: models, pricing and implementation*. John Wiley & Sons.
- Sharpe, W.F., 1964. Capital asset prices: A theory of market equilibrium under conditions of risk. *The Journal of Finance* 19, 425–442.
- Stulz, R.M., 2008. Risk management failures: What are they and when do they happen? *Journal of Applied Corporate Finance* 20, 39–48.
- Targino, R.S., Peters, G.W., Shevchenko, P.V., 2015. Sequential monte carlo samplers for capital allocation under copula-dependent risk models. *Insurance: Mathematics and Economics* 61, 206–226.
- Tasche, D., 2008. Capital allocation to business units and sub-portfolios: The Euler principle, in: Resti, A. (Ed.), *Pillar II in the New Basel Accord: The Challenge of Economic Capital*. Risk Books, London, pp. 423–453.

-
- Tasche, D., 2009. Capital allocation for credit portfolios with kernel estimators. *Quantitative Finance* 9, 581–595.
- Vasicek, O., 1977. An equilibrium characterization of the term structure. *Journal of Financial Economics* 5, 177–188.
- Wilson, T.C., 2015. *Value and Capital Management: A Handbook for the Finance and Risk Functions of Financial Institutions*, 1st Edition. Wiley.
- Zanjani, G., 2002. Pricing and capital allocation in catastrophe insurance. *Journal of Financial Economics* 65, 283–305.

Curriculum Vitae

Personal Details

Name	Philipp Aigner
Home Address	Ceciliengärten 4 12159 Berlin
Date of Birth	April 19, 1996
Citizenship	German

Education

May 2019	Master of Science Mathematics, Regensburg University
Sep 2017	Bachelor of Science Mathematics, Regensburg University

Positions

Jul 2019 - Sep 2022	Research Assistant and Doctoral Student, School of Business, Mainz University of Applied Sciences
---------------------	---